BAYERISCHE JULIUS-MAXIMILIANS-UNIVERSITÄT WÜRZBURG

FAKULTÄT FÜR MEDIZIN

INSTITUT FÜR MEDIZINISCHE STRAHLENKUNDE UND ZELLFORSCHUNG

Tumour development in Raf-driven cancer mouse models

Tumor-Entwicklung in Raf-transgenen Mausmodellen

Dissertation
zur Erlangung des naturwissenschaftlichen Doktorgrades
der Bayerischen Julius-Maximilians-Universität Würzburg

vorgelegt von
Katharina Lütkenhaus
geboren in Regensburg

Würzburg 2010

Eingereicht am:

Mitglieder der Prüfungskommission:

1. Gutachter: Prof. Dr. U.R.Rapp

2. Gutachter: Prof. Dr. T.Rudel

Tag des Prüfungskolloqiums:

Doktorurkunde ausgehändigt am:

Ich versichere, dass die vorliegende Arbeit nur unter Verwendung der angegebenen Hilfsmittel angefertigt und von mir selbständig durchgeführt und verfasst wurde.

Diese Dissertation hat weder in gleicher noch in ähnlicher Form in einem anderen Prüfungsverfahren vorgelegen.

Neben dem akademischen Grad „Diplom-Biologin Univ." habe ich keine weiteren akademischen Grade erworben oder zu erwerben versucht.

Würzburg,

Katharina Lütkenhaus

ACKNOWLEDGEMENTS

Abstract

Metastasis is the cause of death in 90% of cancer-related deaths in men. Melanoma and Non-Small-Cell Lung Cancer (NSCLC) are both tumour types with poor prognosis, lacking appropriate therapeutic possibilities, not least because of their high rate of metastasis. Thus understanding the process of metastasis might unravel therapeutic targets for developing further therapeutic strategies.

The generation of a transgenic mouse model expressing B-Raf^{V600E} in melanocytes, a mutation that is found in about 60% of all melanoma, would result in an ideal tool to study melanoma progression and metastasis. In this work, a doxycycline-inducible system was constructed for expression of B-Raf^{V600E} and transgenic animals were generated, but the expression system has to be improved, since this strategy didn't give rise to any viable, transgene carrying mice.

Furthermore, since it was shown in the work of others that the metastatic behavior of tumour cell lines could be reversed by an embryonic microenvironment and the influence of a tumourigenic microenvironment on melanocytes lead to the acquisition of tumour cell-like characteristics, the question arose, whether B-Raf is as important in melanocyte development as it is in melanoma progression. In this work, the embryonal melanocyte development in B-Raf-deficient and wildtype mouse embryos was examined and there were no differences observed in the localization and number of neural crest stem cells as well as in the localization of the dopachrome-tautomerase positive melanoblasts in the embryos and in cultured neural tube explants.

The expression of oncogenic C-Raf in lung epithelial cells has yielded a model for NSCLC giving rise to adenomas lacking spontaneous progression or metastasis. The co-expression of c-Myc in the same cells accelerates the tumour development and gives rise to liver and lymphnode metastases. The expression of c-Myc alone in lung epithelial cells leads to late tumour development with incomplete penetrance. A mutation screen in this work resulted in the observation that a secondary mutation in *KRas* or *LKB1* is necessary for tumour formation in the c-Myc single transgenic animals and suggested metastasis as an early event, since the corresponding metastases of the mutation-prone primary lung tumours were negative for the observed mutations. Furthermore, in this work it was shown that the expression of chicken c-Myc in a non-metastatic NSCLC cell line leads to metastatic clones, showing that c-Myc is sufficient to induce metastasis. Additionally a panel of metastasis markers was identified, that might serve as diagnostic markers in the future.

Zusammenfassung

In 90% der Todesfälle aufgrund von Krebserkrankungen sind Metastasen für den Tod des Patienten verantwortlich. Sowohl Melanom, als auch nicht-kleinzelliges Lungenkarzinom (Non-Small Cell Lung Cancer, NSCLC) sind beides Tumortypen, die eine schlechte Prognose haben und für die sich wenige Therapiemöglichkeiten bieten, nicht zuletzt aufgrund ihrer häufigen Metastasierung. Somit würde ein besseres Verständnis des Metastasierungsprozesses neue therapeutische Angriffspunkte aufdecken und damit die Möglichkeit zur Entwicklung neuer Therapieansätze bieten.

Die Entwicklung eines transgenen Mausmodells, in dem B-Raf^{V600E}, eine Mutation die man in 60% der Melanompatienten findet, melanocyten-spezifisch exprimiert wird, würde ein geeignetes Werkzeug ergeben, um die Entstehung und die Metastasierung von Melanom zu untersuchen. Im Rahmen dieser Arbeit wurde ein Konstrukt zur Doxycyclin-abhängingen Expression von B-Raf^{V600E} erzeugt und mit diesem wurden transgene Tiere generiert. Da dieser Ansatz nicht zu lebensfähigen, das Transgen tragenden Linien führte, muss das Expressionssystem weiter verbessert werden.

Da in der Arbeit von anderen gezeigt wurde, dass das metastasierende Verhalten von Tumor-Zelllinien durch eine embryonale Mikroumgebung aufgehoben werden konnte, und dass der Einfluss einer tumorähnlichen Mikroumgebung in Melanocyten zur Erlangung von Tumorzell-Charakteristika führte, kam die Frage auf, ob B-Raf eine ähnlich wichtige Rolle in der Entwicklung von Melanocyten wie in der Entstehung von Melanomen spielt. Im Rahmen dieser Arbeit wurde die embryonale Melanocytenentwicklung in B-Raf-defizienten sowie in wildtypischen Mausembryonen untersucht. Es konnten keine Unterschiede in der Lokalisation und Anzahl von Stammzellen des Neuralrohres und in der Lokalisation von Dopachrome-tautomerase positiven Melanoblasten in den Embryonen und in kultivierten Explantaten des Neuralrohres festgestellt werden.

Die Expression von oncogenem C-Raf in Lungenepithelzellen von Mäusen ist ein Modell für NSCLC und führt zur Ausbildung von Adenomen ohne spontane Weiterentwicklung oder Metastasen. Die Koexpression von C-Raf mit c-Myc in denselben Zellen beschleunigt die Entwicklung von Tumoren und führt zu Metastasen in Leber und Lymphknoten. Die Expression von c-Myc alleine in Lungenepithelzellen führt zu einer verspäteten Entwicklung von Tumoren mit nicht vollständiger Penetranz. Ein Screening für Mutation im Rahmen dieser Arbeit führte zu der Beobachtung, dass Sekundärmutationen in *KRas* oder *LKB1* für die Tumorentwicklung in den c-Myc

transgenen Tieren notwendig sind und dass die Metastasierung ein frühes Ereignis zu seien scheint, da die zugehörigen Metastasen in Leber und Lymphknoten im Gegensatz zum Primärtumor in der Lunge keine Mutationen in diesen Genen trugen. Desweiteren wurde in dieser Arbeit gezeigt, dass die Expression von avianem c-Myc in einer nicht-metastasierenden NSCLC Zelllinie zu metastasierenden Klonen führte, was zeigt, dass c-Myc ausreichend ist um Metastasierung auszulösen. Zusätzlich wurde eine Reihe von Markern für Metastasen identifiziert, die in Zukunft als diagnostische Marker Verwendung finden könnten.

TABLE OF CONTENTS

1   Introduction

Right next to cardiovascular diseases, cancer is on the list of the most common causes of death in western countries. Lung cancer accounts for most of the cancer-related death in both men and women. The American Cancer Society estimates the rate of melanoma increasing 2.5-4% per year. Both tumour types have a poor prognosis not least because of their high rate of metastasis, which is the cause of death in the vast majority of cancer patients.

1.1   Melanoma

Melanoma is a tumour that originates in the melanocytes, specialised pigment-producing cells, which are predominantly found in the skin and eyes. They originate from highly motile neural-crest progenitors that migrate to the skin during embryonal development and reside in the basal layer of the epidermis, where their homeostasis is regulated by the keratinocytes (Slominski et al., 2004). Although melanoma accounts for only 4% of all dermatologic cancers, it is the most dangerous form and is responsible for 80% of skin cancer related deaths (Miller and Mihm, 2006). The reason for this is a rather small, often undetected primary tumour with a high frequency of metastasis. Metastatic melanoma holds an extraordinary resistance to chemotherapy, radiotherapy and immunotherapy and patients have a median survival rate of 6 months and the 5-year survival rate is less than 5% (Cummins et al., 2006). The first step in melanoma development is the formation of a nevus upon disruption of the growth control of the melanocytes, often induced by a mutation in the mitogenic cascade. These nevi can stay dormant for decades and rarely progress to malignancy, probably because of oncogene-induced senescence (Braig and Schmitt, 2006). Upon an additional mutation of a tumour suppressor like p16^{INK4a} or PTEN, dysplastic nevi are formed, which carry abnormalities in genes responsible for cell growth, DNA repair and susceptibility to cell death (Thompson et al., 2005). The next stage in melanoma development is the radial-growth-phase, during which the cells acquire the ability to grow intraepidermally. Invasive characteristics of

the developing melanoma occur in the vertical-growth-phase, when the melanoma cells not only penetrate the basement membrane, but also grow intradermally as an expanding nodule. Once the tumour cells dissociate from the primary tumour, migrate through the surrounding stroma and invade blood and lymph vessels to form secondary lesions at distant sites, the disease has reached its metastatic stage (Haass et al., 2005).

1.1.1   Molecular Biology of Melanoma

Melanoma is a complex genetic disease and for improvement of its poor prognosis, it is necessary to understand the molecular biology of melanoma. As already described a mutation in the mitogenic cascade is often involved in nevi formation. In 15% of the patients this is a mutation in N-RAS and in about 60% it is an activating mutation of B-Raf. These mutations, which occur exclusively of each other cause a constitutive activation of the serine-threonine specific kinases in the ERK-MAPK cascade (Albino et al., 1989; Davies et al., 2002).

The fact that B-Raf mutations occur in a similar frequency in nevi, primary tumours and metastatic cancer suggests that nevi must acquire additional mutations to free themselves of growth restraints and progress to malignancy (Pollock et al., 2003). This second mutation is often found in familial melanoma in the *CDKN2A* locus, a single gene that encodes two tumour suppressor proteins, p16^{INK4A} and p19^{ARF} (Albino et al., 1989). p16^{INK4A} is a protein that blocks the cell cycle at the G1-S checkpoint by inhibiting cyclin-dependent kinases, while p19^{ARF} functions as a tumour suppressor by arresting the cell cycle or inducing cell death after DNA damage or upon oncogene-induced aberrant cell proliferation (Sharpless and Chin, 2003). In contrast to familial melanoma, in non-familial cases with a frequency of 25-50% the predominant mutation is found in a different tumour suppressor, *PTEN* (Wu et al., 2003). *PTEN* encodes a phosphatase that attenuates signalling by a variety of growth factors that use phosphatidylinositol phosphate (PIP$_3$) as an intracellular signal. In absence of PTEN, PIP$_3$ levels increase and by this activate the protein kinase AKT, which phosphorylates and by this

inactivates proteins that suppress the cell cycle or stimulate apoptosis (Wu et al., 2003). In murine models for melanoma the inactivation of one, either the *CDKN2A* or the *PTEN* locus is not sufficient to induce melanoma, only the combination of both or of one with mutations in other genes leads to the development of melanoma (You et al., 2002).

Since the failure of differentiation is necessary for dysplasia, many nevi regress through differentiation (Clark et al., 1984). During normal melanocyte development differentiation requires exit from the cell cycle and the expression of melanogenic enzymes, like dopachrome-tautomerase (DCT) or Tyrosinase, which are involved in the melanin synthesis. The microphthalmia-associated transcription factor (Mitf), the according gene of which has been shown to be amplified in 10-20% of malignant melanoma metastases (Garraway et al., 2005), is involved in both processes during melanocyte development (Hodgkinson et al., 1993). During development Mitf appears to contribute to melanocyte survival by upregulating the expression of the Bcl-2 gene, which is a key antiapoptotic factor (McGill et al., 2002). Additionally, Mitf induces cell cycle arrest by induction of *INK4A* expression during melanocyte differentiation (Loercher et al., 2005). Mitf is present in nearly all melanomas, although it causes differentiation and cell cycle arrest in normal melanocytes.

1.1.2   Melanocyte Development

For an in-depth understanding of the disease melanoma, a broad knowledge in the physiological melanocyte biology might improve the insights into melanoma progression.

Melanocytes are pigmented cells that derive from the neural crest, which is a unique population of cells that emigrate from the dorsal neural tube during early embryonal development. During development these neural crest cells migrate extensively along defined pathways to specific sites in the embryo, where they differentiate and form bone, cartilage and adipose tissue, endocrine cells, several types of neurones and glia, as well as melanocytes (Thomas and Erickson, 2008). The specification of the cells depends on their axial level,

neural crest cells from the trunk give rise to neurons and glia of the sensory, autonomic and enteric nervous system, to chromaffin cells of the adrenal gland and to pigment cells (Harris and Erickson, 2007). These cells are divided into two populations, the neurogenic and the
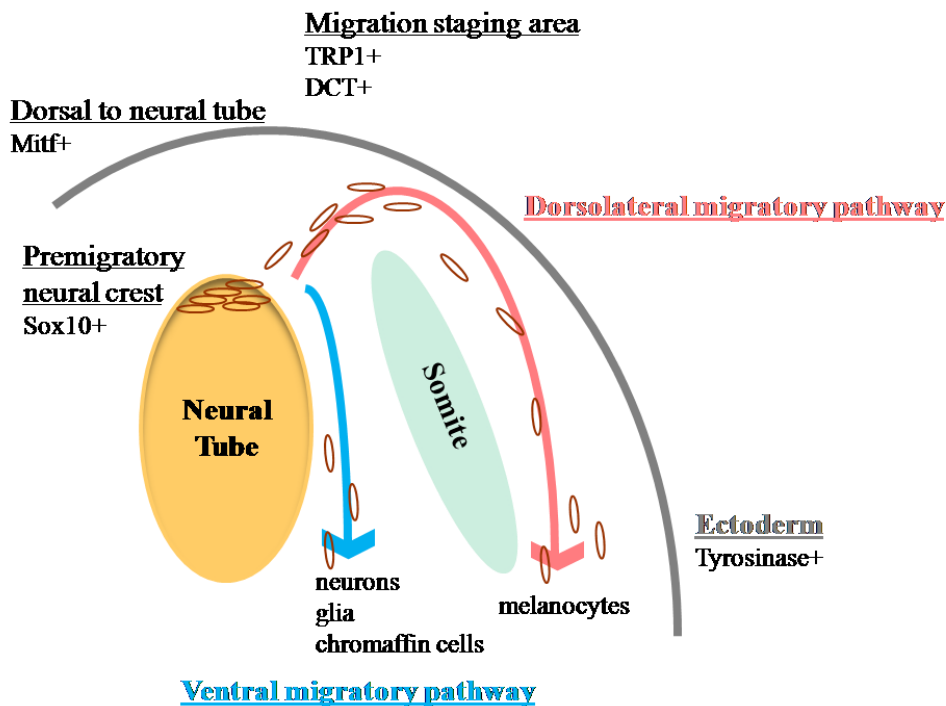
Figure 1-1 Migratory pathways of trunk neural crest cells (Thomas and Erickson, 2008). Neural crest cells migrate along the ventral and the dorsolateral migratory pathways after emerging the premigratory neural crest. Premigratory neural crest cells are positive for Sox10, while emerging the neural tube, they start to express Mitf and once they reached the migration staging area they are positive for the melanoblast markers TRP1 and DCT. When the melanoblasts invade the ectoderm they fully differentiate to mature melanocytes and express the melanogenic enzyme Tyrosinase.

melanogenic population, and have distinct migratory properties (Henion and Weston, 1997).

While neurogenic neural crest cells migrate ventrally along the neural tube, the melanoblasts migrate dorsolaterally between the somites and ectoderm and later invade the ectoderm, where they differentiate to mature melanocytes (Thomas and Erickson, 2008) (Figure 1-1).

1.2 *Non Small Cell Lung Cancer (NSCLC)*

Lung cancer is categorized into two main types, depending on the size and appearance of the malignant cells, the non-small cell lung cancer (NSCLC), which comprises 80% of all lung cancers, and the small cell lung cancer (SCLC), which comprises 20% of all lung cancers.

SCLC is a tumour of neural crest origin, while NSCLC is thought to originate in the lung epithelial cells and is divided in several histological subtypes, like adenocarcinoma, bronchioalveolar, squamous cell carcinoma and large cell lung cancer (Sharma et al., 2007). Adenocarcinoma is the most common subtype of NSCLC, accounting for 25-35% of lung cancers. Although there are advances in early detection and standard treatment, NSCLC is in about 75% of the patients detected at an advanced stage of the disease, which usually is in line with a poor prognosis (Borczuk and Powell, 2007). SCLC and NSCLC show major differences in histopathologic characteristics that can correlate with the distinct patterns of genetic lesions found in both tumour classes (Zochbauer-Muller et al., 2002). Although other markers have prognostic significance, none are more significant than the clinicopathological stage (Mountain, 1997). Therefore the identification of novel markers is an urgent need.

In NSCLC tumour onset and progression proceed via morphologically distinct lesions, hyperplasia, metaplasia, dysplasia, carcinoma in situ and fully invasive tumours (Meuwissen and Berns, 2005). A fundamental step in the progression of a dormant, local tumour to a malignant stage cancer is the attraction of blood supply and the growth of new vessels from pre-existing ones, the process of angiogenesis (Horn and Sandler, 2009).

1.2.1 Molecular Biology of NSCLC

Many genetic and epigenetic aberrations have been identified in human lung cancer. Significant progress has been made in identifying genetic lesions in lung cancer by sequencing-based mutation screenings (Futreal et al., 2004) and characterizing copy-number alterations (Weir et al., 2007). The most frequent genetic aberrations in NSCLC are shown in Table 1-1. These genetic aberrations do not only occur on the chromosomal level as large deletions resulting in the loss of heterozygosity (LOH) or as amplifications of genes like *Myc*-family genes. Genetic changes also occur through nucleotide exchange mutations like alterations in the DNA sequence of the *KRas* gene and epigenetic changes in the promoter

methylation, i.e. of the *CDH1* promoter, which drives the expression of E-cadherin, a cell adhesion molecule expressed in epithelial tissue (Angst et al., 2001).

Gene	Aberration	Frequency
Myc	Amplifications	5%-20%
KRas	Mutations	15%-20%
EGFR	Mutations	20%
INK4a	LOH	70%
p16 INK4a	Mutations	20%-50%
p14 ARF	Mutations	20%
TP53	LOH	60%
TP53	Mutations	50%
RB	LOH	30%
RB	Mutations	15%-30%
FHIT	Mutations	40%
DMBT1	Mutations	40%-50%
LOH in various regions	*3p* *4p* *4q* *8p*	10%-100%
INK4a	Promoter hm	8%-40%
RARß	Promoter hm	40%
CDH1	Promoter hm	55%
TIMP-3	Promoter hm	25%

Table 1-1 Major genetic aberrations in NSCLC. LOH: loss of heterozygosity. Modified from (Meuwissen and Berns, 2005)

One of the early events in NSCLC is a mutation in one of the *Ras*-genes resulting in persistent signaling. *Ras*-mutations are not found in SCLC and the presence of *KRas* mutations marks a poor prognosis in early- as well as late-stage NSCLC (Meuwissen and Berns, 2005). Another alteration that is frequently found in NSCLC is an amplification and by this overexpression of genes of the *Myc*-gene-family. While in SCLC *L-*, *N-* and *c-Myc* are often amplified, in NSCLC it is exclusively *c-Myc* (Angst et al., 2001).

1.2.2 Lung development

During embryonal development, the cells present in the lung bud of the ventral foregut endoderm form the epithelial lining of the conducting airways and the distal sak-like structures, which form the gas-exchange surface. The postnatal maturation of the lung involves the formation of septa in the terminal sacs leading to the expansion of the gas-exchange surface (Cardoso and Lu, 2006). In the adult lung different types of epithelial cells

line the trachea, bronchi, bronchioli (Clara cells and bronchio-alveolar stem cells (BASCs))
and alveoli (Type I and Type II pneumocytes). The alveolar Type II pneumocytes secrete
surfactant proteins (SP), like SP-C, and are the precursors of the Type I pneumocytes, which
form the thin diffusion barrier, important for gas exchanges in the alveoli (Cardoso and Lu,
2006). SP-C is not only expressed in the Type II cells of the murine lung, but also by a rare
cell population located at the bronchio-alveolar duct-junction, which also express the Clara-
cell antigen CC10, a marker for Clara cells, which line the bronchi and bronchioles
(Giangreco et al., 2002). These cells have been shown to be capable of self-renewal and
differentiation *in vitro* and are called bronchio-alveolar stem cells (BASCs) (Kim et al.,
2005). More recent lineage tracing experiments raise the question about the role of BASCs in
regeneration of the distal lung (Rawlins et al., 2009).

1.2.3 The Neuroendocrine Cell Population in the lung

Pulmonary neuroendocrine cells (PNECs) are part of the diffuse endocrine system (DES)
distributed throughout the body (Linnoila, 2006). Other parts of the DES include cell
populations in the hypothalamus and adenohypophysis, pineal gland, paraganglia, cell
populations in the thymus, pancreatic islets, thyroid C cells, parathyroid glands, endocrine
cells of the breast, gastrointestinal and genitourinary tracts, melanocytes and Merkel cells of
the skin (Baylin, 1990). The PNEC system is located in the bronchial epithelium and consists
of solitary PNECs and neuroepithelial bodies (NEBs). In 1972, Lauweryns and Peuskens
introduced the term neuroepithelial body. By definition, NEBs are corpuscular, organoid
structures composed of PNECs, which are heavily innervated and reach from the basement
membrane to the airway lumen (Lauweryns and Peuskens, 1972). Perl et al., 2002 showed
that there is an early spatial restriction of progenitor cells forming the proximal conducting
airways, compared with the peripheral lung during development. PNECs were shown to be
derived from a different group of precursors than those forming the peripheral subset of

respiratory epithelial cells (Perl et al., 2002b). PNECs are thought to regulate branching morphogenesis and cellular growth and maturation in fetal and newborn lung development (King et al., 1995). NEBs emerge as foci of growth by secreting neuropeptides and growth factors in a paracrine fashion. Although PNECs are only a minor component of normal lung epithelium, one third of human lung cancers display features of neuroendocrine differentiation. Clinicopathologically, the most important NE carcinoma is the SCLC, which accounts for 15-20% of all lung cancers; others include NSCLC with neuroendocrine features (NSCLC-NE), carcinoid and Large Cell NE Carcinoma (LCNEC) (Travis et al., 2004). Approximately 10-15% of all NSCLCs may show differentiation towards the NE phenotype by immunohistochemical characterization (Linnoila et al., 1988).

1.3   Metastasis

Metastasis causes 90% of death from solid tumours and the risk of metastatic recurrence can sometimes be predicted from certain features of the primary tumour (Nguyen and Massague, 2007). Metastasis is a complex, multistep process, for which the tumour cells have to fulfil certain tumourigenic prerequisites, like unlimited proliferation, evasion of cell-intrinsic and environmental constraints, attraction of blood supply and the capacity to detach and move away from the primary tumour (Nguyen and Massague, 2007). When aggressive tumour cells become invasive and start to enter the bloodstream, dissemination starts. Intravasation is promoted by processes like epithelio-mesenchymal transition (EMT), and the fact, that pathologically leaky vasculature is common for many tumours. Once the tumour cells have survived the stresses of the bloodstream due to acquired features like evasion from anoikis, they have to enter the parenchyma of a target organ either by vascular-remodelling events or as a result of mechanical disruption of capillaries by expanding tumour emboli. On entry the tumour cells have to survive a different microenvironment and can then either immediately or after a prolonged, micrometastatic dormancy grow to full metastatic lesions (Nguyen and

Massague, 2007). These functions are acquired during tumour initiation and local development, but must remain active during malignant progression. The metastatic dissemination has stereotypical patterns of organ tropism that reflects the heterogeneity of the tumour cells and depends on the cancer type (Weiss, 2000).

1.4 The mitogenic cascade

In a variety of human tumours one can find a deregulation of the mitogenic cascade on different levels. Going through the list of hallmarks of cancer defined by Hanahan and Weinberg in 2000 (Hanahan and Weinberg, 2000), the Ras/Raf-signaling can contribute to any individual of these criteria (Table 1-2). The growth factor receptor that triggers the consecutive signalling pathway, the EGF-receptor (EGFR), was found to be mutated in various epithelial tumours (Gschwind et al., 2004), i.e. in 20% of NSCLC a mutation in the *EGFR* can be observed (Meuwissen and Berns, 2005). Furthermore, the Ras proteins, the transceiver of the receptor signals, are also popular targets for mutations in approximately 30% of human cancers (Karreth and Tuveson, 2009), as for example in 15-20% of NSCLC activating *KRas*–mutations are found (Meuwissen and Berns, 2005). Other important targets for mutations in the mitogenic cascade are the Raf-kinases, which are the central players of the mitogenic cascade, i.e. *B-Raf* is mutated in 66% of the melanoma patients (Schreck and Rapp, 2006).

Hallmarks of a cancer cell	Corresponding effect of the Ras/Raf-signalling pathway
Immortalisation	Telomerase induction
Growth-factor-independent growth	Cell-cycle activation
Insensitivity to growth-inhibitory signals	Inactivation of tumour suppressors
Ability to invade and metastasise	Stimulation of motility and extracellular matrix remodelling
Ability to secure nutrients by stimulating angiogenesis	Stimulation of the production of pro-angiogenetic factors
Avoidance of apoptosis	BAD inactivation; caspase inhibition
Resistance to therapeutical measures	Induction of radiation resistance; induction of the multidrug-resistance protein MDR1

Table 1-2 The Ras/Raf-signaling impacts on all hallmarks of cancer defined by Hanahan and Weinberg (modified from (Kolch et al., 2002)).

1.4.1 Raf-isoforms

In multicellular organisms the Raf-family consists of three members, A-, B- and C-Raf, which are serine/threonine specific kinases and have all the same structural organization. All Raf-family proteins have three highly conserved regions, two in the N-terminus (CR1 and CR2) and the third (CR3), which contains the kinase activity, in the C-terminal part of the protein (Figure 1-2). All three isoforms can be activated via phosphorylation of the activation segment (Chong et al., 2001), but while there are further phosphorylations of serine and threonine residues in the kinase domain necessary for full activation of A- and C-Raf, B-Raf is fully activated by this single phosphorylation event. Not least for this reason B-Raf has a higher basal kinase activity than the other two isoforms (Wan et al., 2004). There are three different functional *Raf*-genes, which are located on different chromosomes, encoding the three isoforms. While C-Raf is expressed ubiquitously, the expression pattern for A- and B-Raf is more restricted. Urogenital organs show elevated expression levels of A-Raf and B-Raf is expressed on high levels in neuronal tissue and testis (Luckett et al., 2000; Storm et al., 1990). The generation of transgenic and knock-out mice has shown the crucial role of all three isoforms in embryonal development. While A-Raf deficient mice survive until birth, but die 7-21 days later due to neurological and gastrointestinal defects (Pritchard et al., 1996), the *b-raf$^{-/-}$* and *c-raf$^{-/-}$* embryos die *in utero* 10.5 to 12.5 days postcoitum due to growth retardation, vascular and neuronal defects and massive liver apoptosis, respectively (Wojnowski et al., 1998; Wojnowski et al., 1997). Although there is clearly a functional overlap in the three Raf-isoforms in the activation of the mitogenic cascade, the differences in structure and tissue distribution suggest additional specific roles of the different isoforms (Hagemann and Rapp,

1999).
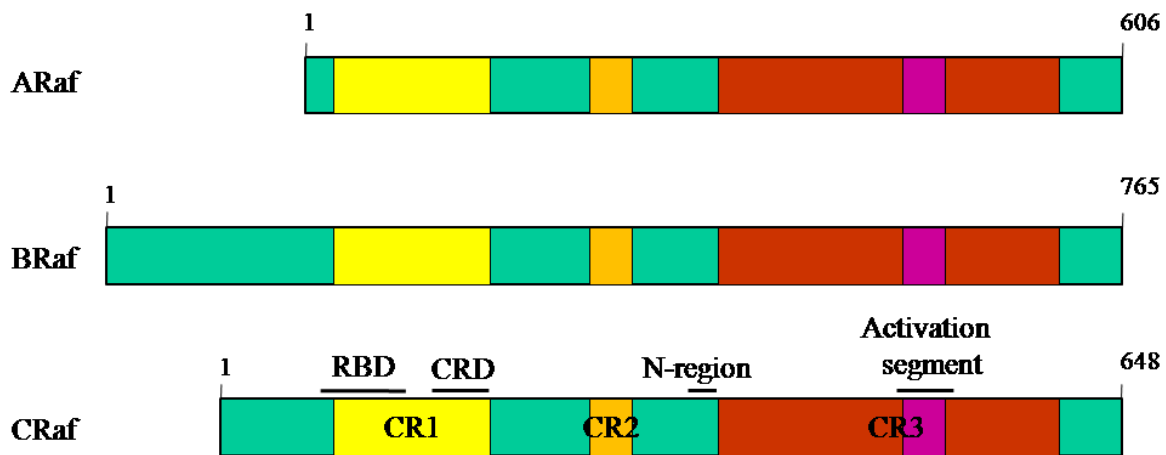
Figure 1-2 Structure of the Raf-family proteins (modified from (Wellbrock et al., 2004)). Proteins of the Raf-family share three highly conserved domains. The CR1 domain (yellow) contains the two regions required for Ras-binding and membrane recruitment, the Ras-binding domain and the cysteine rich domain. Displayed in orange is the CR2 domain and in red the CR3 domain, which is the catalytic region containing the activation segment (highlighted in purple).

1.5 Ras/Raf-signalling

Raf proteins are part of a highly conserved signalling module, the mitogenic cascade, which transduces signals from the cell surface to the nucleus (Figure 1-3). The upstream regulators of the Raf-proteins are members of the Ras-family of small G-proteins (Robbins et al., 1994). Ras is activated by extracellular ligands such as growth factors, cytokines or hormones binding to their receptor leading to the exchange of GDP with GTP, which converts Ras into its active conformation (McCormick, 1993). Activated Ras directly interacts with high affinity with Raf and recruits it to the cytoplasm membrane, where Raf activation via phosphorylation takes place (Avruch et al., 1994). Activated Raf phosphorylates and by this activates the kinases MEK1 and MEK2 on two serine residues in their activation segment. These kinases phosphorylate and activate the mitogen-activated protein kinases (MAPK) ERK1 and ERK2 (extracellular signalling related kinase) on threonine and tyrosine residues within their activation segment. ERK1/2 have both cytosolic (kinases and cytoskeletal proteins) and nuclear (transcription factors) substrates (Flory et al., 1996; Marshall, 1999). The activation of this cascade leads to transcriptional activation of proteins possessing cell

cycle stimulating, pro-survival and anti-apoptotic properties (Rapp et al., 2003). In addition to the Raf-kinases, Ras also regulates other proteins, for example the
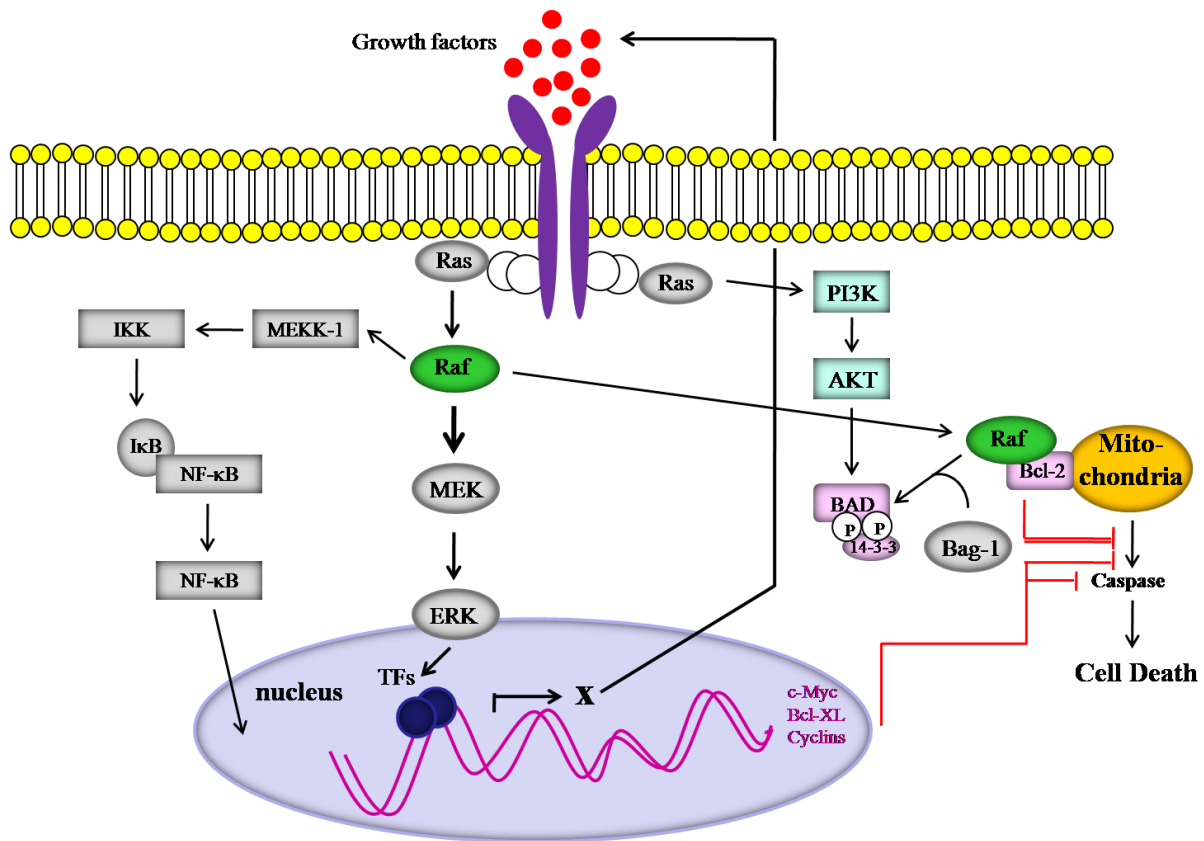
Figure 1-3 Raf signaling pathway regulating cell growth, differentiation, proliferation and survival (modified from (Rapp et al., 2003)). The induction of the mitogenic cascade via growth factor binding to a receptor leads to the transcriptional onset of a variety of genes including the induction of autocrine loops of the growth factors themselves.

phosphatidylinositol-3 (PI3) kinases, which activates the serine/threonine-specific protein kinase Akt (PKK) via phosphorylation leading to phosphorylation and inactivation of the proapoptotic protein Bad (Downward, 1998). Raf-kinases not only phosphorylate and by this activate MEK1/2, but also interact with the antiapoptotic protein Bcl-2 and by this block the mitochondrial apoptotic pathway. Furthermore they phosphorylate and thereby inactivate the proapoptotic Bcl-2 family protein BAD (Troppmair and Rapp, 2003).

1.6   *Myc-family proteins*

c-Myc has been one of the first oncogenes identified and has subsequently been linked with a wide spectrum of human cancers, i.e. it is amplified in 5-20% of NSCLC (Meuwissen and

Berns, 2005). The family of Myc genes consists of three members, c-*Myc*, N-*Myc* and L-*Myc*, which all have been implicated in the genesis of specific human tumours (Patel et al., 2004). *In vivo* Myc proteins are not occurring as monomers, but are always bound to a partner molecule, most commonly Max, through a C-terminal domain (Blackwood et al., 1992) (Figure 1-4). To regulate the transcription of the target genes, this complex binds directly to a

Figure 1-4 Structure of Myc-family proteins (modified from (Adhikary and Eilers, 2005)). The C-terminus of Myc contains a basic-region/helix-loop-helix/leucine zipper (BR/HLH/LZ) domain, where Max is binding (Max binding domain (BD), red). In the N-terminal part of the protein are three highly conserved regions located, which are called Myc-boxes I-III (yellow).

specific DNA sequence, which is a subset of the general E-box sequence (Blackwell et al., 1990) or is recruited by other DNA binding factors to the corresponding binding sites (Mao et al., 2003). The study of *in vivo* binding sites of Myc-proteins has yielded in as many as ~25,000 sites in the human genome, which by far exceeds the number of Myc molecules that are present in one cell, leading to the suspicion that a relatively brief binding of Myc leads to longer-lasting changes in the chromatin organization (Adhikary and Eilers, 2005). The N-terminal part of Myc proteins contains three highly conserved elements, the Myc-boxes I, II and III (Figure 1-4). While Myc-box I is implicated in the turnover of the protein (Bahram et al., 2000), Myc-box III is required for full transactivation and transrepression of the target genes (Herbst et al., 2005). Myc-box II is not required for DNA or Max binding, but is known to be necessary for all known biological functions of Myc (Stone et al., 1987). It has been shown in the last decades that the elevated expression of Myc contributes in many different ways to tumour development, i.e. by driving unrestricted cell proliferation and inhibiting differentiation (Rapp et al., 1985), by its ability to drive cell growth (Johnston et al., 1999) and angiogenesis (Baudino et al., 2002), by reducing cell adhesion (Arnold and Watt, 2001), and by promoting metastasis (Rapp et al., 2009) and genomic instability (Felsher and Bishop, 1999). But although *Myc* is overexpressed in many human and rodent tumours, it is not

sufficient to convert human and rodent cells into tumour cells alone. Tumours that arise from *Myc* transgenic mice are clonal and have a long latency, which implies that additional mutations are required for tumour formation (Rapp et al., 2009). Cooperation of Myc with oncogenes that function i.e. in the Ras/Raf-pathway results in cellular transformation and tumourigenesis (Rapp et al., 2009). Downstream kinases of the Ras/Raf-pathway phosphorylate and thereby stabilize Myc. Furthermore, Ras inhibits the glycogen synthase kinase-3 (GSK3), which targets Myc for ubiquitylation (Sears et al., 2000). Additionally several Myc target genes are co-regulated by members of the FoxO protein family. Unphosphorylated these transcription factors bind to and by this repress many Myc target genes until they are phosphorylated and activated by the Akt kinase, which is a downstream kinase of the Ras/Raf-signalling (Bouchard et al., 2004). Another reason for the incapability of Myc alone to transform cells is its ability to induce apoptosis (Askew et al., 1993; Evan et al., 1992) by two distinct mechanisms. It induces the expression of p19[Arf] leading to the stabilization of the tumour-suppressor protein p53 (Eischen et al., 1999) and it represses the anti-apoptotic proteins Bcl-2 and Bcl-X_L (Eischen et al., 2001). The effects of Myc are dose-dependent. Low levels of Myc promote ectopic proliferation of somatic cells and oncogenesis, while its overexpression leads to apoptosis (Murphy et al., 2008).

1.6.1 Cooperation of Raf with other oncogenes

Myc and Raf are oncogenes that go well together, not only because they complement each other in their limitations in the ability of fully transforming a cell by cancelling out each other's deleterious oncogene effects, but also because coexpressing cells fulfil both key elements of carcinogenesis, tumour initiation and promotion, via induction of genomic instability by Myc (Prochownik and Li, 2007) and assurance of survival and genomic stability by Raf (Rapp, 2007). To result in proliferation and survival of progenitor cells, Raf and Myc oncogenic effects have to be in equilibrium. While the predominance of Myc induces

genomic instability in early progenitor cells and a differentiation block, leading to dedifferentiation and apoptosis, the prevalence of Raf results in differentiation, G1-arrest and survival in late progenitor cells and differentiated cells leading to oncogene-induced senescence. Additionally, the predominance of Raf promotes an overall genomic stability (Rapp, 2007). Furthermore, several publications of the group of Rapp showed the ability of Raf and Myc in combination to induce cellular plasticity (Principato et al., 1988; Rapp et al., 2009).

Another example for the cooperation of Raf with another oncogene is the cooperation of Raf and Mitf in melanoma. The protein-levels of Mitf must be carefully controlled, because critically high levels of Mitf result in cell cycle arrest and differentiation and reduce melanoma cell tumourigenicity, while low levels lead to cell cycle arrest and apoptosis. Only at intermediate levels proliferation is favoured. A constitutive active signalling of the mitogenic cascade, i.e. as a result of B-Raf^{V600E}, in this context not only provides essential survival functions and contributes to proliferation, but also keeps the Mitf protein doses on an intermediate level by targeting Mitf for degradation after its phosphorylation by ERK (Gray-Schopfer et al., 2007).

1.7 *Experimental design and aim of the project*

1.7.1 Melanoma

Constitutive active B-Raf was shown to play an important role in melanoma development as it seems to lead to the first step in melanoma development, the nevi formation. But B-Raf is not sufficient to induce full malignancy, as already described, additional mutational events are necessary for malignant progression. Mouse models for human disease offer the opportunity that the effects of oncogenes can be studied and their roles in the stages of the disease and disease progression can be identified. Thus a mouse model expressing the oncogenic B-Raf^{V600E}, which accounts for most of the oncogenic B-Raf mutations with just one amino acid

substitution leading to a constitutive kinase activity (Pollock and Meltzer, 2002), in melanocytes would be a powerful tool to gain more insights in melanoma progression and the secondary events that are necessary for full malignancy and to develop new therapeutic approaches. Since the constitutive expression of oncogenic C-Raf (Rapp et al, unpublished data) and for B-Raf even the tissue-specific expression under the control of the Tyrosinase-promoter was embryonal lethal (Marais et al, unpublished data), in this work a tetracycline-regulatable vector for the B-Raf^{V600E} expression was designed (Figure 1-5). In this tetracycline-regulatable system, several repeats of the TetO DNA sequence are fused to a minimal CMV promoter forming a compound tetracycline-responsive promoter (Gossen and Bujard, 1992). The tetracycline-controlled transcriptional activator (tTA) protein binds in the absence of Dox to the TetO DNA sequence, which results in the expression of the adjacent gene. Binding of Dox to the tTA protein leads to a conformational change of the protein causing the protein to detach from the TetO DNA sequence leading to silencing of the
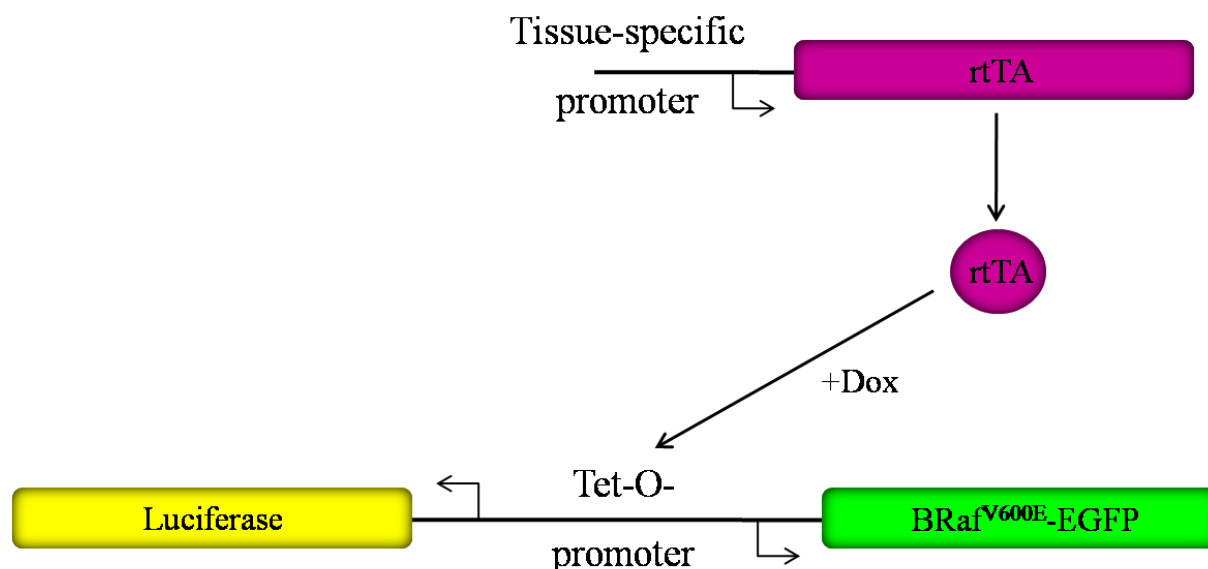
Figure 1-5 Tetracycline-inducible gene expression system. A tissue-specific promoter drives the expression of the reverse tetracycline-controlled transcriptional activator (rtTA). In the presence of the tetracycline-analogue doxycycline (Dox) the rtTA can bind to and by this activate the expression activity of the tetracycline-inducible promoter element (Tet-O).

corresponding gene expression (Furth et al., 1994). The usefulness of this system is limited, because to turn off the system the administration of Dox during a long period of time would

be necessary. Four mutations in the tTA sequence reverse the behavior of the protein in interacting with the TetO DNA sequence in response to presence or absence of Dox. This mutant reverse tTA (rtTA) protein stays soluble in the absence of Dox and binds to the TetO DNA sequence in the presence of Dox inducing its promoter activity (Gossen et al., 1995). In this work a vector for tetracycline-inducible expression of B-Raf^{V600E} was designed to generate transgenic mice that can be combined with animals expressing the rtTA tissue-specific, in the case of a melanoma model for example under the control of the DCT- or the Tyrosinase-promoter.

Multipotent tumour cells and many embryonic progenitor cells share common characteristics of cell fate plasticity and invasiveness. Furthermore, growing evidence suggests that cancer might arise from aberrant activation of normally carefully controlled developmental pathways. Understanding of the processes during embryonal development as they relate to tumour development and progression might lead to new therapeutic approaches for cancer. Exciting studies have recently shown that signals derived from the embryonic microenvironment can influence multipotent tumour cells to behave like their embryonal progenitors (Kulesa et al., 2006). To gain more insights into the role of B-Raf in melanocyte development, in this work the previously established B-Raf knock-out mouse was used (Wojnowski et al., 1997). For the generation of this mouse, a neo-cassette was introduced into the exon3 of B-Raf, which is common for all splice isoforms and contains the Ras-binding domain. While in heterozygous animals no phenotype was observed, homozygous animals die *in utero* between day E10.5 and E12.5 during embryonal development probably due to vascular and placental defects (Wojnowski et al., 1997). In this work the melanocyte development in E9.5 B-Raf$^{-/-}$-embryos was examined to get an idea about the role of B-Raf during melanocyte development.

1.7.2   Non-small-cell lung cancer

During the past three decades, many genes have been identified for which gain or loss of function results in autonomous proliferative activity, resistance to cell death, angiogenesis and altered cell adhesion and motility. These processes are involved in the initiation and the local progression of the primary tumour and are prerequisites for metastasis. However, the genetic determinants of metastases, that mediate tumour cell invasion, intravasation, survival in circulation, scattering to distant tissues, extravasation and colonization of vital organs, are just in the beginning of being unraveled. To gain more information about the process of metastasis, in this work a previously established mouse model for metastasis in NSCLC was used for mutation and gene expression analyses (Rapp et al., 2009). In this model single transgenic SpC-C-Raf-BxB mice, which express oncogenic C-Raf-BxB just containing the C-terminal part of the protein including the kinase domain, but lacking the N-terminal regulatory parts in the alveolar type II cells under control of the SpC-promoter, were combined with single transgenic SpC-c-Myc animals overexpressing c-Myc in the type II pneumocytes under the control of the same promoter. The SpC-C-Raf-BxB single transgenic animals develop premalignant adenoma lacking spontaneous progression, but show complete tumour penetrance at an age of two weeks (Kerkhoff et al., 2000). In contrast, in SpC-c-Myc single transgenic mice pleomorphic clusters could be observed, but these were often diminished or completely absent in long term survivors. Only in a fraction of late SpC-c-Myc animals rapidly expanding tumour foci containing columnar cells could be detected. Cells in these tumour foci carried mutations in *KRas* or *LKB1*, indicating that secondary genetic events were required to rescue premalignant c-Myc foci. Combining these two transgenes in compound SpC-C-Raf-BxB/SpC-c-Myc animals resulted in accelerated tumour development and a phenotypic switch of the in the SpC-C-Raf-BxB mice observed cuboidal to columnar shape tumour cells. Furthermore, multiple macroscopic liver- and lymphnode- metastases were observed in the compound SpC-C-Raf-BxB/SpC-c-Myc animals as early as ten months of age

and in late SpC-c-Myc single transgenic mice. Although the incidence of metastasis was higher and the development was earlier in the SpC-C-Raf-BxB/SpC-c-Myc compound animals, macroscopic metastases could also be observed in the SpC-c-Myc single transgenic animals (Rapp et al., 2009).

Furthermore, since a mouse model for a disease not always completely phenocopies the full human disease, in this work a cell culture model was established by the introduction of chicken c-Myc into a non-metastatic human NSCLC cell line and this cell line was analyzed in comparison to the data obtained from the mouse model.

2 Materials and Methods

2.1 Materials

2.1.1 Instruments

Hardware	Manufacturer
Berthold Luminator	BioRad
Blotting Chamber	BioRad
Cell Culture Hud	Heraeus Instruments
Cell Culture Incubator	Heraeus Instruments
Cryo microtome	Leica
Developing machine	Agfa
Electrophoresis power supply	BioRad
Electrophoresis unit for Agarose Gels	BioRad
Electrophoresis unit for SDS Gels	BioRad
Fluorescence Microscope	Keyence, Leica
Glass plates for SDS Gels	BioRad
Heat Block	Liebisch, Type 2099-DA
Homogenizer	Ultra-Turrax
Incubator	Heraeus Instruments
Megacentrifuge	Beckman
Minicentrifuge	Eppendorf
Microtome	Leitz, Wetzlar
Neubauer Chamber	Hartenstein
Paraffin Embedding Machine	Leica
pH meter	Microprocessor, WTW
Roto-Gene 2000	Corbett Research
Shaker	New Brunswick Scientific
Sonicator	Sono Plus HD70
Spectrophotometer	Ultraspec 3000, Pharmacia Bio.
Thermocycler	Eppendorf
Ultracentrifuge	Beckmann
Vortex	Scientific Industries
Waterbath	Amersham-Buchler

2.1.2 General Material

Material	Purchased from
1.2/2ml reaction tubes	Eppendorf
15/50ml tubes	Sarstedt
100/40/20 µm cell strainer	BD Falcon
Beckmann Quickseal Tubes	Beckmann
Cell culture flasks	Sarstedt
Cell culture plates	Sarstedt
Cryotubes	Sarstedt
Earmarks	Harlan
Glass coverslips	Leica

Material	Purchased from
Glass slides	Leica
Hybond-N Membrane	Amersham
Pasteur Pipette	Hartenstein
Petridish	Roth
Scalpel	Hartenstein
SuperFrost Slides	Menzel-Gläser
Whatman-paper	Hartenstein
X-Ray films	Agfa

All used materials not listed was ordered with Noras or Hartenstein.

2.1.3 Chemicals

Reagent	Purchased from
1kb DNA ladder	Fermentas
100bp DNA ladder	Fermentas
Acetone	Hartenstein
Acrylamide(30%)/Bisacrylamide(0.8%)	Roth
Agarose, ultra pure	Invitrogen
Ammoniumpersulfate (APS)	Sigma
Ampicillin	Sigma
Bacto-Agar	Roth
Bacto-Tryptone	Roth
β-Mercaptoethanol	Roth
BCP	Molecular Research Center Inc.
BCIP-T	Fermentas
Blocking reagent	Roche
Bovine serum albumin (BSA)	Sigma
Bromphenol blue	Sigma
CHAPS	Sigma
Chloroform	Roth
Citric acid	Roth
CsCl	Sigma
DAPI	Sigma
DEPC	Roth
Diaminobenzidine (DAB)	Sigma
Dimethylforamide	Roth
Dimethylsulfoxide (DMSO)	Sigma
Doxycycline	Sigma
dNTPs	Fermentas
ECL-solutions	Amersham
EDTA	Sigma
Endothelin-3	Sigma
Entellan	Merck
Eosin	Merck
Ethanol	Roth
Ethidiumbromide	Invitrogen
Fetal Calf Serum (FCS)	Invitrogen
Fibronectin	Sigma
Ficoll	Hartenstein

Reagent	Purchased from
Formaldehyde	Roth
Formamide	Roth
Glacical acetic acid	Roth
Glucose	Sigma
Glycerol	Sigma
HCl	Roth
Hematoxilin	Merck
Heparin	Roth
HEPES	Roth
Hydrogenperoxide (30%)	Hartenstein
Isopropanol	Merck
Kalimacetate	Sigma
Ketanest	Pfizer
Levamisol	Sigma
LiCl	Sigma
Lipofectamine	Invitrogen
Low-melting agarose	Biozyme
Luciferin	Promega
Methanol	Hartenstein
$MgCl_2$	Sigma
Mowiol	Calbiochem
Na_2EDTA	Sigma
NaCl	Roth
NaOH	Sigma
NBT	Fermentas
n-butanol	Roth
Paraformaldehyde (PFA)	Sigma
Paraffin wax	Merck
Phenol	Roth
Phosphate-buffered saline (PBS)	Roth
Prestained protein ladder	Fermentas
Polybrene	Sigma
Polyvinil Pyrolidine (PVP-40)	Roth
Ponceau S	Sigma
riboseATP	Fermentas
Rompum	Bayer
Sea Plaque Agarose	Biozym
Serum (rabbit, goat, donkey)	Chemicon
Sodiumchloride	Roth
Sodiumdodecylsulfat (SDS)	Roth
TEMED	Roth
Tissue TEK (OCT)	Chemicon
Tris	Roth
triSodium dihyrdrate	Roth
Triton X-100	Sigma
Trizol reagent	Invitrogen
Tween-20	Roth
Whatman 3MM Paper	Schleicher & Schüll
X-ray film	Amersham
Yeast-extract	Invitrogen

Reagent	Purchased from
Yeast tRNA	Invitrogen

All used chemicals not listed were ordered with Roth, Sigma, Invitrogen or Fermentas.

2.1.4 Antibodies

Primary Antibody	Cat. or Clone number	Purchased from
Anti-β-actin (rabbit)	I-19	Santa Cruz
Anti-B-Raf (rabbit)	C-19	Santa Cruz
Anti-chicken Myc (rabbit)		Klaus Bister
Anti-Cytokeration7	M7018	Dako
Anti-Digoxigenin-AP	11093274910	Roche
Anti-Gata4 (goat)	C-20	Santa Cruz
Anti-Gata6 (rabbit)	H-92	Santa Cruz
Anti-p75 (mouse)		Abcam
Anti-pERK1/2 (rabbit)	4094	Cell signalling
Anti-Sox10		Michael Wegener
Anti-VEGF (rabbit)	sc-507	Santa Cruz

Secondary Antibody	Purchased from
Anti-rabbit IgG conjugated Peroxidase	Amersham
Anti-mouse-biotinylated (rabbit)	Dako
Streptavidin-Alexa555	Molecular Probes
Anti-rabbit-Cy5 (donkey)	Jackson Immuno Research
Anti-rabbit-Alexa488 (goat)	Molecular Probes
Anti-goat-Alexa647 (donkey)	Molecular Probes
Anti-rabbit-Cy3 (donkey)	Jackson Immuno Research

2.1.5 Enzymes

Enzyme	Purchased from
Agarase	Biozym
Calf Intestine Alkaline Phosphatase	Fermentas
DNaseI	Fermentas
Proteinase K	Roth
Restrictionendonucleases	Fermentas
RNaseA	Fermentas
T4 Ligase	Fermentas
Taq Polymerase	Genecraft

2.1.6 Kits

Kit	Purchased from
BCA-Kit	Thermo Scientific Pierce
DIG RNA labeling kit	Roche
DyNAMO HS SYBR Green qPCR Kit	New England Biolabs
ECL Western blotting detection reagents	Amersham
First strand synthesis Kit	Fermentas
Luciferase assay kit	Promega
QIAGEN DNeasy tissue kit	Qiagen

Kit	Purchased from
QIAGEN GelExtraction Kit	Qiagen
QIAGEN PCR Purification Kit	Qiagen
QIAGEN Plasmid Maxi Kit	Qiagen
QIAGEN Plasmid Midi Kit	Qiagen
QIAGEN Plasmid Mini Kit	Qiagen
QIAGEN RNeasy Kit	Qiagen

2.1.7 Plasmids

Plasmid-Name	Source
J5	Prof. Dr. U.R.Rapp
pcDNA3	Invitrogen
pBi5-B-Raf^{V600E}	PD Dr. R.Götz
B-Raf-EGFP	Dr. C. Xiang
pBi5-B-Raf^{V600E}-EGFP	this work
pLKO.1-puro-shGATA4-24	Sigma Mission® shRNA Bacterial Glycerol stocks
pLKO.1-puro-shGATA4-25	Sigma Mission® shRNA Bacterial Glycerol stocks
pLKO.1-puro-shGATA4-26	Sigma Mission® shRNA Bacterial Glycerol stocks
pLKO.1-puro-shGATA4-27	Sigma Mission® shRNA Bacterial Glycerol stocks
pLKO.1-puro-shGATA4-28	Sigma Mission® shRNA Bacterial Glycerol stocks

2.1.8 Oligonucleotides

For Genotyping

Mouse-line	Sequence	ANN. TEMP.
B-Raf-KO	mB3-1 (WT/KO) 5'-GCCTATGAAGAGTACACCAGCAAGCTAGATGCCC-3' mBdel (WT) 5'-TAGGTTTCTGTGGTGACTTGGGGGTTGTTCCGTGA-3' NeoL (KO) 5'-AGTGCCAGCGGGGCTGCTAAA -3'	60°C
SpC-c-Myc	SpC_S1 5'GAGGAGAGGAGAGCATAGCACC-3' SpC-cMyc 5'AAGGACTTGGCTGGCAGACAGG-3'	60°C
SpC-C-Raf-BxB	as 5'-GCTGGTGTTCATGCACTGCAG-3' s 5'-AAAGACTCAATGCATGCCACG-3'	60°C
SpC-rtTA	as 5'-TCCTGGCTGTAGAGTCCCTG-3' s 5'-CTCCAGGAACCCACTCTCTG-3'	60°C
Tet-O-B-RafV600E-EGFP	B-Raf*_end_for 5'-TCAGAACCCTCCTTGAATCG-3' B-Raf*_EGFP_rev 5'-GCTGAACTTGTGGCCGTTTA-3'	56°C

For Cloning

Name	Sequence	ANN. TEMP.
DCT-RT-for	5'-GTGCTGAACAAGGAATGCTG-3'	54°C
DCT-RT-rev	5'-CAAGCTGTCGCACACAATCT-3'	
Mitf-RT-for	5'-TGAGTGCCCAGGTATGAACA-3'	54°C
Mitf-RT-rev	5'-AAGTTGGAGCCCATCTTCCT-3'	
Sox10-RT-for	5'CTGCTGCTATTCAGGCTCACT-3'	55°C
Sox10-RT-rev	5'-AGGGCCCCATGTAAGAAAAG-3'	
Tyrosinase-NotI-for	5'-GCCCAAAGCGGCCGCGCACCATCTGGACCTCAGTT-3'	54°C
Tyrosinase-XbaI-rev	5'-CGTTGGGTCTAGAGCTTCATGGGCAAAATCAAT-3'	

For Expression analysis

Primers used for expression analysis. All primers were designed using the program AIO (Karreman, 2002).

Gene	Sequence	PRODUCT SIZE	ANN. TEMP.
57578	s 5'-ACGCAGTCAATAAGTGATACCA-3'	177	56°C
	as 5'-GGATGTTTCCTGGTCAGCCT-3'		
β-actin	s1 5'-GTCGTACCACAGGCATTGTGATGG-3'	500	56°C
	as1 5'-GCAATGCCTGGGTACATGGTGG-3'		
AFP	s 5'-TGCAGAAACACATCGAGGAGAG-3'	474	56°C
	as 5'- GCTTCACCAGGTTAAGAGAAGCT-3'		
APQ5	s 5'- AATCCGGCCATTACTCTGGC-3'	583	56°C
	as 5'-TCAGCTCGATGGTCTTCTTC-3'		
ASCI	s 5'-TCGCCCACCATCTCCCCCAA-3'	205	56°C
	as 5'-GATGCAGGATCTGCTGCCAT-3'		
Axud1	s 5'-ACCAGGTGGTCAGGCACCCC-3'	195	56°C
	as 5'-GCCATGCCCAGGGTACAGCC-3'		
B-Raf	Braf ex1s 5'-GACCCGGCCATTCCTGAAG-3'		54°C
	Braf ex4as 5'-CTGTCTCGAACTGTAACACCACAT-3'		
CCL19	s 5'-TTCCCAGCCCCAACTCTGGG-3'	196	56°C
	as 5'-CCACCCAGGGCTGGTCTGGA-3'		
CCR7	s 5'-GCCAGAGAGGGCTAGCTGGA-3'	196	56°C
	as 5'-CACCGTGGTATTCTCGCCGA-3'		
CD44	s 5'-TATCCGGAGCACCTTGGCCA-3'		56°C
	as 5'-CCAGTGCCAGGAGAGATGCC-3'		
CDCA7L	s 5'-ACTCTGCTTCTGATGCCGAG-3'	201	56°C
	as 5'-AGAAGGCCCGTCGTGGTGTT-3'		
CLECSF8	s 5'-CAGTGGGTGGACAAGACGCC-3'	203	56°C
	as 5'-GATCACTTCGAGGGCTTCCAA-3'		
DBPHT2	s 5'-TGCCAGACCTGGGGGCATGA-3'	200	56°C
	as 5'-CCTTTCCGGACCTGCTCTGT-3'		

Gene	Sequence	PRODUCT SIZE	ANN. TEMP.
DCT	Ex7 5'-AACAACCCTTCCACAGATGC-3' Ex8 5'-TTGAAGAAAAGCCAGCAACC-3'	249	56°C
Enol	s 5'-CTCCCAGTGGGTGCTGAGAG-3' as 5'-GTGTAGCCAGCCTTGTCGAT-3'	200	56°C
ERAF	s 5'-GGCGGGCTCAGCACCATTAG-3' as 5'-TCCCCATGCACGAGCTTCTT-3'	204	56°C
ERFI	s 5'-TATGAAGTCCTGCTGGGGCA-3' as 5'-GGGGCAAGCTTGACCTTGGA-3'	194	56°C
FoxD3	s 5'-CCAGCGATATGTCCGGCCAG-3' as 5'-GGCTTGCGGTTGAGACTGGC-3'	200	56°C
Fzd10	s 5'-AAGTGCCAGCCGGTGGAGAT-3' as 5'-ACCTGCTCGGTGCACATGGG-3'	200	56°C
Gadd45a	s 5'-CTCCTGCTCTTGGAGACCGA-3' as 5'-TCATTCAGATGCCATCACCG-3'	212	56°C
Gadd45b	s 5'-ACGAGTCGGCCAAGTTGATG-3' as 5'-CGCACGATGTTGATGTCGTT-3'	151	56°C
Gadd45g	s 5'-GTGCTGAGCTCTGGCTGTCA-3' as 5'-AGCAACTCATGCAGCGCTTT-3'	175	56°C
GATA4	s 5'-CTACATGGCCGACGTGGGAG-3' as 5'-CTCGCCTCCAGAGTGGGGTG-3'	132	56°C
GATA6	s 5'-TCCATGGGGTGCCTCGACCA-3' as 5'-CCCTGAGGTGGTCGCTTGTG-3'	200	56°C
HBBB1	s 5'-AAGGGCACCTTTGCCAGCCT-3' as 5'-CTTGTGAGCCAGGGCAGCAG-3'	189	56°C
Ifi202b	s 5'-AGGCTGGTTGATGGAGAGTT-3' as 5'-TCAGAAACCACTCATCTGCA-3'	196	56°C
Jagged	s 5'-CGGGATGGAAACAGCTCAC-3' as 5'-CACCAAGCAACAGACCCAAG-3'	135	56°C
Klf4	s 5'-CTCATGCCACCGGGTTCCTG-3' as 5'-CCACAGCCGTCCCAGTCACA-3'	110	56°C
Lats	s 5'-CAGCAAATGAGAGCCACCCC-3' as 5'- CTCCTACTGCCCGTCTGCTT-3'	200	56°C
Malat1	s 5'-ACTTGAGAGGCCCTGGGCTT-3' as 5'-CATGGTGGCGATGTGGCAGA-3'	195	56°C
Mucin2	s 5'-CGACTAACAACTTCGCCTCCG-3' as 5'-CGCGGGAGTAGACTTTGGTG-3'	246	56°C
Myc (MM)	s 5'-TCTCTCCTTCCTCGGACTCG-3' as 5'-GAGATGAGCCCGACTCCGAC-3'	198	56°C
Myc (GG)	s 5'-CGGCCTCTACCTGCACGACC-3' as 5'-GACCAGCGGACTGTGGTGGG-3'	298	56°C
Mitf	Mitf-RT-for 5'-TGAGTGCCCAGGTATGAACA-3' Mitf-RT-rev 5'-AAGTTGGAGCCCATCTTCCT-3'	822	56°C
NeuroD1	s 5'-CCCACGCAGAAGGCAAGGTG-3' as 5'-GTCTGCCTCGTGTTCCTCGT-3'	196	56°C
Notch1	s 5'-TCAATGCCGTGGATGACCTA-3' as 5'-CCTTGTTGGCTCCGTTCTTC-3'	102	56°C
Notch2	s 5'-TGGCGCCTTCCACTGTGAGT-3' as 5'-CACACGGGTTGCTCTGGCAT-3'	200	56°

Gene	Sequence	PRODUCT SIZE	ANN. TEMP.
Notch3	s 5'-CACTCCCTGCCGGAATGGTG-3' as 5'-TCTCACAGCGTATGCCCGTA-3'	204	56°C
Notch4	s 5'-TTCCCAAAAGGAGCCTCTGC-3' as 5'-TCTACACAACACCCGGCACA-3'	88	56°C
ODC	s 5'-GGTTCCAGAGGCCAAACATCT-3' as 5'-GCTCTCCTGGGCACAAGACA-3'	140	56°C
p53	s 5'-GCACATGACGGAGGTTGTGA-3' as 5'-ATGATGGTGAGGATGGGCCT-3'	264	56°C
p63	s 5'-CCTCCAACACCGACTACCCA-3' as 5'-TCACCTTGATCTGGATGGGG-3'	150	56°C
p73	s 5'-CGCGTGGAAGGCAATAATCT-3' as 5'-GTTCATGCCCCCTACACAGC-3'	156	56°C
PBK	s 5'-AGCCAGCCCGTCACTTTCAC-3' as 5'-GCTGACCCCAGTCCCAAAGC-3'	197	56°C
PGP9.5	s 5' ATTCCTGTGGCACAATCGGA-3' as 5'-GACATTGGCCTTCCTGTGCC -3'	195	56°C
RSAD2	s 5'-CTAGCCCTGCCCTCTGTGAG-3' as 5'-CCTGCACCACCTCCTCAGCT-3'	198	56°C
SHMT1	s 5'-GAAGGACCAGGGGCTCCACG-3' as 5'-TCTGAGCTGGTAGAGGCCGC-3'	198	56°C
SNCA	s 5'-GGAGGGAGTTGTGGCTGCTG-3' as 5'-GCGACTGCTGTCACACCAGT-3'	198	56°C
SNCG	s 5'-ACATCGTGGTCACCACCGGG-3' as 5'-GCAGGGCATTCAGTGTGCCA-3'	419	56°C
Sox2	s 5'-TCAAGAGGCCCATGAACGCC-3' as 5'-GGGTGCTCCTTCATGTGCAG-3'	196	56°C
Sox9	s 5'- TGAAGAAGGAGAGCGAGGAAGATAA-3' as 5'- GGTGGCAAGTATTGGTCAAACTCA-3'	721	56°C
Sox10	Sox10-RT-for 5'-CTGCTGCTATTCAGGCTCACT-3' Sox10-RT-rev 5'-AGGGCCCCATGTAAGAAAAG-3'	693	56°C
SYB	s 5'-TGCAGGCCGGAGCATCACAA-3' as 5'-GGCAGGGCTGGGAGAAGTCT-3'	196	56°C
SYK	s 5'-TCAGCGGGTGGAATAATCTC-3' as 5'-TGTGCACAAAATTGCTCTCC-3'	625	56°C
tert	s 5'-GCACTGGCTGATGAGTGTGT-3' as 5'-CTCGGCCCTCTTTTCTCTG-3'	322	56°C
Tiam2	s 5'-TGTGTGCCCGCGCTGTATGA-3' as 5'-CGTATGCCAGGCTGTCAGGG-3'	202	56°C
TMP4	s 5'-GAGGAGGAACTGGACCGGGC-3' as 5'-ACTTGCGGTCGGCTTCGTCA-3'	199	56°C
Tyrosinase	Ex1 5'-GGGATTGGAGAGATGCAGAA-3' Ex2 5'-TCAGGTGTTCCATCGCATAA-3'	175	58°C

2.1.9 Media and Additives

Media and Additives for bacterial culture

LB (Luria-Bertani)-Medium	**g for 1 liter H_2O**
Bacto-tryptone	10g
NaCl	10g
Yeast extract	5g

After the substances were dissolved, the pH was adjusted to 7.5 using NaOH.

For production of plates, 15 g/l bacto-agar was added. All media were autoclaved for 20 min at 120°C. Antibiotics for the production of selective plates were added after cooling of the autoclaved liquids to about 45°C. The plates were stored at 4°C.

Additive	**Stock-solution**	**Final concentration**
Ampicillin	100 mg/ml in H_2O	100 µg/ml
Kanamycin	20 mg/ml in H_2O	20 µg/ml

Media and Additives for Eukaryotic cell culture

Medium	**Source**
D-MEM	Invitrogen

Additive	**Source**	**Final concentration**
Doxycycline	Sigma	100nM
Fetal Calf Serum (FCS)	Invitrogen	10x stock
Penicillin/Streptomycin	Invitrogen	10x stock
Trypsin-EDTA	Invitrogen	

2.1.10 Bacterial strains, Cell lines, Mouse lines

Cell lines

Cell lines	**Source**
3041	Mouse lung adenocarcinoma cell line (MSZ)
A-549	Human lung adenocarcinoma cell line (MSZ)
B16	Murine melanoma cell line (Dermatology, University of Würzburg)
NIH3T3-tTA	Murine fibroblast cell line (MSZ)
Phoenix ampho	MSZ

Mouse strains

Mouse lines	**Source**
B-Raf-KO	MSZ

Mouse lines	Source
C57Bl6	All were obtained from Harlan Winkelmann GmbH
NMRI	All were obtained from Harlan Winkelmann GmbH
FvB/N	All were obtained from Harlan Winkelmann GmbH
Rag1$^{-/-}$	All were obtained from Harlan Winkelmann GmbH
SpC-c-Myc	Gift from Roland Halter
SpC-C-Raf-BxB	MSZ

Bacterial strains

Bacterial strain	Source
E.coli DH5α	MSZ
E.coli XL1-Blue	Stratagene

2.1.11 Solutions and buffers

General Solutions

Solution	Ingredients	
Blotting buffer	25mM Tris	
	192mM Glycine	
	10% Methanol	
6x DNA loading dye	Glycerol	1.2ml
	0.5mM Na$_2$EDTA	1.2ml
	20% SDS	300μl
	bromphenol blue	
	water	up to 10ml
Injectionbuffer	5mM Tris-HCl (pH7.4)	in water
	0.1mM EDTA	
ProteinaseK buffer	10mM Tris-HCl (pH8.0)	
	1mM EDTA	
	1% Tween	
Running buffer (for SDS-PAGE)	25mM Tris	
	250mM Glycine	
	0.1 % SDS	
5x SDS loading buffer	50mM Tris-HCl (pH 6.8)	
	10% Glycerol	
	5% β-mercaptoethanol	
	2% SDS	
	0.05% bromophenolblue	
Stripping buffer	1M Tris-HCl (pH6.7)	3.125ml
	20% SDS	5ml
	dH$_2$O	42ml
	β-mercaptoethanol	0.35ml
50x TAE buffer	Tris-base	242g
	Glacial acetic acid	57.1ml
	0.5M NA$_2$EDTA (pH8.0)	100ml
	H$_2$O	up to 1000ml
Tail lysis buffer	50mM EDTA	in water
	50mM Tris-HCl (pH8.0)	

Solution	Ingredients	
	0.5% SDS	
10x TBS	500mM Tris-HCl (pH7.4)	
	1.5M NaCl	in water
TBST	1x TBS	
	000.05% Tween-20	
TE	10mM Tris-Hcl (pH7.5)	in water
	1mM EDTA	

Buffers for CsCl-Plasmid Preparation

Solution	Ingredients	
SolutionI	50mM Glucose	in water
	25mM Tris-HCl (pH8.0)	
	10mM EDTA	
SolutionII	0.2M NaOH	in water
	1% SDS	
SolutionIII	5M Kaliumacetate	
	glacial acetic acid	115ml
		ad to 1l water
Water saturated n-butanol	5M NaCl	Mix, wait until the
	n-butanol	phases separate and
		the lower NaCl
		phase becomes
		salt-saturated

Buffers for in-situ hybridisation

Solution	Ingredients	
BCIP-stock	50mg/ml BCIP	in 100% dimethylformamide
Blocking Solution	2% Blocking Reagent	
	20% heat inactivated FCS	in TBST
Denhard's Solution (100x)	2%BSA	In water-DEPC
	2% Polyvinil Pyrolidine (PVP-40)	
	2% Ficoll	
Hybridisation buffer	100% deionized Formamide	50ml
	20x SSC	25ml
	20mg/ml yeast tRNA	1.25ml
	10mg/ml Heparin	1ml
	0.5M EDTA (pH8.0)	1ml
	10% Tween-20	1ml
	10% Chaps	1ml
	50x Denhard's solution	1ml
	water-DEPC	ad to 100ml
	1M citric acid	to pH5
NBT-stock	75mg/ml NBT	in 70% dimethylformamide
NTMT	1M Tris-HCl (pH9.5)	20ml
	1M MgCl$_2$	10ml
	1M NaCl	20ml

Solution	Ingredients	
	10% Tween-20	10ml
	water	ad to 200ml
	1M HCl	to pH 9.5
	1M Levamisol (add before use)	1ml
Proteinase K-buffer	50mM Tris	
	5mM EDTA	in PBS
RNaseA buffer	NaCl	29.23g
	1M Tris-HCl (pH7.5)	10ml
	0.5M EDTA	2ml
	water	ad to 1l
SSC (20x)	NaCl	17.65g
	triSodiumdihydrate	8.82g
	water-DEPC	to 100ml
	1M citric acid	to pH 5
TAE-buffer	0.1M triethanolamin (pH8.0)	50ml
	add slowly while stirring	135µl
	acetic anhydride	

2.2 Molecular Biology Methods

2.2.1 Bacterial Manipulation

Transformation of competent bacteria

For transformation of plasmid-DNA into *E.coli*, the XL1-Blue Competent Cells (Stratagene) were used as described in the according manual. After transformation the bacteria were plated on LB-agar plates containing a selective antibiotic. After incubation at 37°C overnight, a single colony can be picked and expanded in LB medium containing the selection antibiotic and used for DNA preparation.

Purification of Plasmid-DNA

To amplify plasmid DNA, a colony of *E.coli* that were transformed with the according plasmid before, was grown in 50 ml of LB medium overnight. From the pellet of this culture, the plasmid-DNA was isolated using the QIAGEN Plasmid Kits as described in the according manual.

CsCl Plasmid Preparation

For CsCl plasmid preparation 500ml of plasmid containing bacterial overnight culture were pelleted at 5000rpm at 4°C for 10min and the supernatant was discarded. The bacterial pellet was resuspended in 20ml of solution I and after 10min of incubation at room temperature 40ml of solution II were added. The mixture was incubated on ice for 10min before 30ml of ice-cold solution III were added, followed by 10min incubation on ice. The lysed bacteria were then pelleted again via centrifugation for 10min at 9000rpm at 4°C. The DNA-containing supernatant was filtered and the DNA was precipitated by addition of 0.6 volumes of isopropanol and 10min incubation at room temperature. After 10min centrifugation at 9000rpm at 4°C the supernatant was discarded, the pellet was air-dried and resuspended in 30ml of TE-buffer.

Exactly 33.4g of CsCl were added to 30ml of the DNA-solution, mixed until the CsCl was completely dissolved and 0.5ml of Ethidiumbromide were added. The solution was then transferred to Beckmann Quickseal Tubes and the tubes were closed with the apposite equipment. The exactly balanced tubes were centrifuged overnight at 45000rpm in an ultracentrifuge. The DNA-band, which was visualized by UV-light, was removed using an injection-needle and a syringe. To remove the ethidiumbromide, the DNA-solution was then added an equal volume of water-saturated n-butanol and the organic and the aqueous phase were mixed by vortexing. After the organic and the aqueous phase had separated, the upper organic phased was removed using a Pasteur pipette. This extraction was repeated until the pink colour had disappeared from the organic as well as from the aqueous phase.

To precipitate the DNA from the CsCl-DNA-solution, three volumes of water and 8 volumes of ethanol were added and the precipitation was performed overnight at 4°C. To collect the precipitate, the mixture was centrifuged for 30min at 4200rpm at 4°C. The pellet was washed with 70% ethanol, air-dried and dissolved in 500µl TE-buffer.

2.2.2 Analysis of DNA-molecules

Agarose-Gelelectrophoresis of DNA-molecules

Double stranded DNA fragments with a length between 150 bp and 10 kbp can be separated according to their length on an agarose gel. For this purpose a suspension of agarose (0.8-2%) in 1xTAE-buffer was cooked until the agarose was completely dissolved. After cooling to about 50°C, 0.5µg/ml Ethidiumbromide was added before the solution was poured into the gel apparatus. When the gel was solidified, the DNA mixed with loading dye was applied on the gel and electrophoresis was performed in 1xTAE buffer at 120V for 30min. The DNA bands then could be visualized under UV-light.

Preparation of DNA-Fragments from an agarose gel

The DNA-fragments separated by agarose-gelelectrophoresis visualized by UV-light can be excised with a sterile scalpel from the gel. Afterwards this DNA was isolated from the gel using the QIAGEN Gel Extraction kit according to the included manual.

Preparation of DNA-Fragments from an agarose gel for microinjection

For the preparation of DNA-Fragments from an agarose gel for microinjection was performed using an agarose-digesting enzyme, agarase, from Biozym according the included manual.

Isolation of DNA from tissue

For isolation of DNA from murine tissue, the QIAGEN DNeasy tissue kit was used according to the included manual.

2.2.3 Polymerase Chain Reaction (PCR)

The Polymerase Chain Reaction (PCR) is used for amplification of specific regions of a DNA-target. Usually PCR was performed in an 30µl reaction mix containing 3µl of 10x Taq-Polymerase buffer, 1µl of 2mM dNTP-mix, 0.5µl of 20pM forward and reverse Primer and

0.3µl Taq-Polymerase, filled up with water. The PCR reaction typically consists of 20-40 repeated temperature changes called cycles. After an initialization step for 10min at 95°C follows a cycling of the denaturation step (usually for 30sec at 95°C), the annealing step (the temperature depends on the primers that are used) and the elongation step (30sec-1min at 72°C). Finally before cooling down the reaction mix, there is an additional elongation step at 72°C for 10min. All PCR reactions were performed as described above as long as there are no other conditions mentioned.

2.2.4 Mutation-Analysis

Isolation of DNA from paraffin-sections

For the isolation of DNA from tissue sections, after an H&E staining the sections were not mounted but air-dried. 25µl of ProteinaseK-buffer (containing 20mg/ml ProteinaseK) were propounded into a 1.5ml reaction tube. 10µl of ProteinaseK-buffer were directly pipetted on the region to be isolated from the section and the tissue was scraped from the glass slide using a sterile scalpel, transferred to the prepared reaction tube and incubated overnight at 37°C. After inactivating the ProteinaseK by incubating the samples at 92°C for 30min, the samples were centrifuged at 12000rpm and the DNA was isolated from the supernatant. For this purpose ProteinaseK-buffer was added to a final volume of 450µl and 250µl 6M NaCl were pipetted to the samples and they were incubated for 5min at room temperature. After 10-15min of centrifugation at 12000rpm, the supernatant was transferred to a fresh reaction tube and 600µl of Isopropanol were added. After incubating the samples for 5min at room temperature, they were centrifuged at 12000rpm for 10-15min and the pellet was first washed with 600µl 70% Ethanol and later with 100% Ethanol. Finally, the pellet was dried and dissolved in sterile Millipore water.

PCR for KRas Exon1 and LKB1 Exon6

To have enough material for sequencing KRas Exon1 and LKB1 Exon6 to detect mutations, before PCR was performed as described above to amplify the DNA isolated from paraffin-sections. First a PCR was performed with primers that bind adjacent to the Exon of interest and afterwards an additional PCR was done using primers that lead to the amplification of the complete Exon of interest. All primers used for the mutation-analysis are listed in Table 2-1.

Primer	Sequence	PCR-conditions
KRas_S_OUT KRas_AS_OUT	5'-GGCTGAGGCGGCAGCGCTGTG-3' 5'-GCTGAGGTCTCAATGAACGGAAT CC-3'	50°C annealing temperature 40 cycles
KRas_S KRas_AS	5'-GGCTGAGACGGCAGGGGAA-3' 5'-CTTGCTAACTCCTGAGCCTG-3'	50°C annealing temperature 40 cycles
LKB_6OUTS LKB_6OUTAS	5'- GGGGTCACACTGTAAGTGTC-3' 5'- TGGGGGGAAGCAATCTCAGA-3'	50°C annealing temperature 40 cycles
LKB_6S LKB_6AS	5'- ACCCTGTAGCAGATGGGGGG-3' 5'- CCTCCCATCCTGGCGGACAA-3'	50°C annealing temperature 40 cycles

Table 2-1 PCR-conditions for Mutationanalysis.

Sequencing of KRas Exon1 and LKB1 Exon6

Before sequencing the PCR-products were purified via gelextraction as described above with the Gelextraction-Kit of QIAGEN. The DNA was eluted with 30µl of water and for sequencing, 4µl of the DNA was mixed with 1µl of the primer KRas_S, KRas_AS, LKB_6S and LKB_6AS, respectively, and with 25µl of Millipore water and the samples were sent for sequencing to StarSEQ for sequencing. The resulting sequences were compared with the published sequences of KRas and LKB1 with carefully searching for doublepeaks in the sequences indicating a heterozygous mutation.

2.2.5   Enzymatic Manipulation of DNA

Restriction Digestion of DNA using Restrictionendonucleases

Restrictionendonucleases bind doublestranded DNA specifically and cut in or next to their target sequence containing 4-8 basepairs. Depending on the enzymes used, the digestion of

the DNA results in blunt or sticky ends. For analytical digestion 1-3μg DNA were incubated with 1-3 units of the restrictionendonuclease for 2hrs at the enzyme-specific temperature in a final volume of 20μl containing the according buffer. For a preparative approach 10μg of plasmid were digested using up to 20 units of enzyme in a final volume of 50μl. The composition of the according buffers and the reaction conditions are described in the catalogue of the enzyme supplier.

Dephosphorylation of digested plasmid-DNA

To prevent religation of linearized plasmid-DNA, the DNA was treated with Calf Intestine Alkaline Phosphatase (CIAP) before ligation, which is removing the 5'-phosphate-groups from the DNA-ends. This reaction was performed in the reaction mix of the restrictionendonuclase-digestion reaction. For this purpose 1/10 of the final volume 10x CIAP-buffer and 1μl CIAP was added and the reaction was incubated for 30min at 37°C. Finally the reaction was stopped by heating to 85°C for 15min. The dephosphorylated DNA was then purified from an agarose gel.

Purification of PCR-products

To remove the nucleotides and the Taq-Polymerase-buffer from the PCR-product, the PCR reaction was purified using the QIAGEN PCR Purification kit according to the included manual.

Phosphorylation of PCR-products

To increase the effectivity of the ligation reaction into a CIAP-treated vector, the PCR-fragments were phosphorylated on the 5'-ends using the T4-Polynucleotide-Kinase. For this purpose, 15.5μl of the PCR-product were incubated with 2μl of 10xbuffer, 1μl T4-Polynucleotide-Kinase and 1.5μl Ribose-ATP for 30min at 37°C. To inactivate the enzyme, 1μl of 0.5M EDTA was added and the EDTA was extracted by the same volume of

chloroform. To assure, that there is no chloroform left in the mix, the DNA was finally purified from an agarose gel.

Ligation of DNA-fragments

DNA-Ligases catalyze the formation of a phosphodiesterbinding between neighbouring 5'-phosphate- and 3'-hydroxylgroups of double stranded DNA-molecules. For this reaction, the concentration of the insert was about three times higher related to the vector-concentration. To a final volume of 15µl, 1.5µl 10xligation buffer and 1-2 units of T4-Ligase were added. The reaction was performed for 2hrs at 22°C or overnight at 14°C.

2.2.6   Isolation of RNA

RNA-Isolation from cells and tissue

For isolation of RNA from cells, after removal of the medium 1ml of Trizol-reagent was directly added on the cells. In case of shock-frozen organs, the tissue was mechanically homogenized at 4°C using a homogenizer in 1ml of Trizol-reagent. The procedure of RNA-isolation was performed as described in the protocol provided by the manufacturer.

For isolation of RNA from rare samples, i.e. the neural tube explants, the QIAGEN RNeasy-kit was used. The RNA-isolation was performed as described in the manual included in the kit.

The RNA was dissolved and eluted, respectively, using RNase-free water and was stored at -80°C.

Quantification and determination of Quality of RNA

The concentration of the isolated RNA was determined by measuring the absorbance at 260nm (A_{260}) using a spectrophotometer. An absorbance of 1 unit at 260nm equals 44µg of RNA per ml. The ration between the absorbance values at 260 and 280nm, which should be between 1.7 and 2.1, gives an estimate or RNA purity.

2.2.7 RT-PCR

cDNA -synthesis

Total RNA obtained from eukaryotic cells or tissue, was treated with RNase-free DNaseI to remove DNA contamination from the RNA-sample. For this purpose 1μg RNA was filled up to a volume of 9μl with RNase-free water and 1μl DNaseI-buffer was added to the reaction mix. After pipetting 1μl of DNaseI to the sample, the mix was incubated for 30min at 37°C. The reaction was stopped by the addition of 1μl 25mM EDTA and heating to 65°C for 10min. The first strand synthesis was performed, using the sample directly from the DNaseI-treatment with the Fermentas first strand synthesis kit and random hexamer primers as described in the according manual.

The cDNA was used as a template for RT-PCR and qPCR, respectively.

Real-Time-PCR

Depending on the cDNA-quality, 0.5-2μl of cDNA obtained from cDNA-synthesis described above was used as template for real-time PCR analysis. 10μl of the Finnzymes SYBR Green master-mix, the template cDNA, 0.5μM of the primers specific for the gene of interest or for the housekeeping gene, respectively, and 0.4μl of the dye ROX as an internal control were used in a 20μl reaction. To calculate the relative amount of the transcript of the gene of interest, the amplification efficiency was raised to the power of the threshold cycle (C_t-value). This gives the number of cycles necessary for the product to be detectable. The resulting value was normalised to the level of the housekeeping gene for all samples in the same experiment. Assays were performed in triplicates following the manufacturer's instructions in a Rotor-Gene 2000 detection system.

2.2.8 Microarray

Microarray experiments and analysis were performed by Ellen Leich at the Institute for Pathology at University of Würzburg using Affimetrix Gene Chip products.

2.3 Biochemistry Methods

2.3.1 Measurement of Protein concentration

For the measurement of protein concentration in the BCA-Kit from Thermo Scientific Pierce was used according to the included manual. BSA was used as a standard control.

2.3.2 SDS-PAGE

Proteins can easily be separated by size by electrophoresis in a polyacrylamide gel under denaturing conditions. 5x SDS-loading buffer was used to denature 20-50μg of protein sample and the diluted samples were then heated at 95°C for 5min. The denatured protein samples were then separated in a gel composed of two layers, the separating gel and the stacking gel with a lower concentration of acrylamide to insure that the proteins simultaneously enter the separating gel. The composition of the gel is indicated in Table 2-2.

	Separating Gel	Stacking Gel
3M Tris-HCl, pH 8.8	2.5 ml	
1M Tris-HCl, pH 6.8		1.3 ml
Acrylamide/bisacrylamide 29:1 (30%)	2.7-6.5 ml	1.1 ml
10% SDS	200 μl	100 μl
ddH$_2$O	14.4-10.6 ml	7.6 ml
10% APS	200 μl	100 μl
TEMED	20 μl	10 μl

Table 2-2 Components of a separating and a stacking gel.

After preparation and solidifying of the gel at room temperature, the gel was put into a running chamber and this chamber was filled with running buffer. The denatured samples were then loaded into the wells of the stacking gel as well as a protein ladder for mass determination and 45mA were applied until the running front of loading dye was on the

bottom of the gel. The due to the SDS negatively loaded proteins are running from the anode to the kathode.

2.3.3   Immunoblotting

After SDS-Gelelectrophoresis the proteins were transferred by electroblotting from the gel to a nitrocellulose-membrane. SDS-gels were blotted at 400mA in blotting buffer for 1hr. After the transfer, the membrane was incubated with blocking buffer containing 5% slim milk in PBS for 1hr at room temperature or over night at 4°C. To detect the protein of interest, after blocking, the membrane was incubated with the primary antibody diluted in PBS (1:50-1:10000, depending on the antibody) for 2hrs at room temperature or overnight at 4°C. Before applying the secondary antibody, the membrane was washed at least three times for 10min with PBS-0.3%Tween. The appropriate peroxidase-conjugated secondary antibody was diluted in PBS (1:100-1:10000, depending on the antibody) and incubated with the membrane for 45 min at room temperature. An additional washing step was performed before the membrane was incubated for 1min at room temperature with a 1:1 mixture of the ECL-solutions I and II. The incubation of the peroxidase bound to the secondary antibody with the ECL-solutions leads to the emission of light photons, which can be detected on an X-Ray film.

2.3.4   Immunoblot-stripping

To reprobe the same nitrocellulose membrane with the bound proteins with another antibody, it is possible to remove the primary and secondary antibodies using stripping buffer and incubating the membrane for 30min at 50°C. After stripping and washing, the membrane can be blocked and reprobed as described above.

2.3.5   Luciferase-Reportergene-assay

For the Luciferase-Reportergene-assay, samples were prepared in lysis buffer containing 0.25M Tris, pH7.6, 1% Triton-X100. Tissue samples were homogenized in the lysis-buffer at 4°C, cell culture samples were lysed directly on a 6-well dish. After centrifugation at 11000rpm for 10min at 4°C, the luciferase of the supernatant was measured in a luciferase assay using a Berthold luminometer and the luciferin substrate. Finally the protein concentrations were measured as described above and luciferase activity was normalized to the protein concentration.

2.4   Eukaryotic Cell Culture Techniques

All handling of cell cultures was performed using a clean bench. To the media used for the cell lines as described, 10% fetal calf serum was added and 1% Penicillin/Streptomycin was used to avoid contamination. To passage the adherent cell lines, the cells were washed with PBS, treated with Trypsin-EDTA for 3-5min and the splitted as required. The cultures were kept in an incubator at 37°C in a humidified atmosphere with 5% CO_2.

2.4.1   Freezing cell lines

By addition of an anti-freezing compound like DMSO, eukaryotic cell lines can be stored in liquid nitrogen for several years. For this purpose, the trypsinized cells were spun down in a centrifuge (1000rpm, 5min, room temperature), the pellet was washed with PBS, counted using a Neubauer chamber and diluted in ice-cold medium containing 20% FCS and 10% DMSO to obtain at least $1\text{-}2\text{x}10^6$ cells per ml. 1ml of this cell suspension was then transferred into a cryotube and stored at –80°C for at least 24hrs. For prolonged storage the cryotubes were then transferred to liquid nitrogen.

For reculturing of the frozen cells, the cell suspension was defrosted at 37°C and immediately put into prewarmed medium. To remove the toxic DMSO, the cells were spun down

(1000rpm, 5min, 37°C) and the pellet was resuspended in warm medium and cultured at 37°C as described before.

2.4.2 Transient Transfection of cells using Lipofectamine

For transient transfection of adherent cells with plasmid-DNA, the cells were seeded the day before transfection to reach about 70% confluency at the time of transfection in medium without Penicillin/Streptomycin. The transfection was performed according to the recommendations in the manual. The day after transfection the medium was changed to normal culture medium. Antibiotics for selection of the transfected cells were added 48hrs after transfection. Expression of a transfected vector was tested 48hrs after transfection.

2.4.3 Viral infection of cell lines

For virus production the amphotrophic retrovirus producer cell line Phoenix was transfected with the viral plasmid using Lipofectamine as described above. 24hrs after transfection the medium of the virus producing cell line was changed to a minimal amount to have a high virus concentration in the supernatant. Cells for infection were seeded to be about 50% confluent on the day of infection. 48hrs after transfection, the virus containing supernatant of the virus-producing cells was collected and centrifuged at 500rpm at 4°C to pellet cell debries and was used immediately. Before pipetting the virus-containing supernatant onto the cells to be infected, it was mixed 1:1 with fresh medium and 8μg/ml of Polybrene was added.

2.4.4 Soft-agar-assay

The soft-agar-assay was performed using cells 24hrs after virus-infection or cells transfected with a plasmid containing a selectable marker selected for at least 5days. First, the bottom agar was prepared using an autoclaved stock of 5% Sea Plaque Agarose, which was microwaved and mixed with D-MEM-medium to a final concentration of 0.5% Agarose. For the bottom agar 5ml of 0.5% Agarose was used per 60mm dish. When the bottom agar was

solid, for the topagar the 5% stock was diluted to 0.6% Agarose with medium and stored in a waterbath at 40°C. Dilutions of the cells were prepared in 1ml of medium (10^3 to 10^6 cells per 60mm dish) and then mixed 1:1 with the 0.6% Agarose and poored on top of the bottom agar. After solidifying the soft-agar-assay was incubated in a wet chamber at 37°C for 21-28days. For quantification the colonies were counted and categorized by size. If necessary for the experiment, colonies were picked using a Pasteur pipette and were subsequently grown under adherent cell culture conditions.

2.4.5 Cultures of Neural Tube Explants (Jontes et al.)

Fibronectin-coating of cell-culture dish

For coating of the cell-culture dish with the extracellular adhesion molecule fibronectin, the dish was incubated with 2.5% fibronectin in PBS for one hour at room temperature. Finally the dish was washed with sterile millipore water and stored at 4°C until use.

Preparation and culturing of Neural Tube Explants

For culturing of neural tubes, embryos in the age of E9.5 were isolated from the pregnant female and were transferred into cold PBS. Using a stereolupe, the neural tube was separated from the rest of the embryo and transferred to fibronectin-coated dish containing prewarmed D-MEM-Medium. The head of the embryo was kept at –20°C for genotyping. The neural tube explants were cultured in D-MEM medium containing 5nM Endothelin-3. The medium was changed every other day.

2.4.6 Analysis of cultured cells via Immunocytochemistry

Immunocytochemistry

For immunocytochemical staining of cultured cells, the cells were grown on sterile coverslips, washed three times with PBS and fixed for 15min at room temperature using 4%PFA-PBS.

After fixation the cells were washed three times for 5min with PBS and blocked with blocking solution containing the blocking reagent indicated in Table 2-3 and 0.3% TritonX-100 for 1hr at room temperature. The primary antibody was diluted as indicated in Table 2-3 in blocking solution and incubated at 4°C overnight on the cells. Before incubation with the secondary antibody diluted in blocking solution as indicated in Table 2-3 for 2hrs at room temperature, the cells were washed three times for 5min with PBS. The cells were washed again three times for 5min with PBS and if the secondary antibody was biotinylated, the cells were then incubated with streptavidin-Alexa555 diluted 1:200 in 0.2% TritonX-100 for 1hr. Otherwise or after this step, after washing three times for 5min, the cells were counterstained with DAPI diluted 1:200 in PBS at 37°C for 15min. After washing with Millipore water, the cells were mounted with mowiol and stored at 4°C until fluorescence microscopy.

staining	blocking reagent	dilution primary antibody	secondary antibody	dilution secondary antibody
p75/Sox10	1% BSA	Sox10 1:50 p75 1:250	rabbit-α-mouse-biot. Goat-α-rabbit-Alexa488	1:200 1:200
chicken Myc	4% donkey serum	1:10000	donky-α-rabbit-Cy5	1:200
GATA4	4% donkey serum	1:100	donky-α-goat-Alexa647	1:200
GATA6	4% donkey serum	1:50	donky-α-rabbit-Cy3	1:200
VEGF	4% donkey serum	1:500	donky-α-rabbit-Cy3	1:200

Table 2-3 Antibody conditions for Immunocytochemistry.

Quantification of p75/Sox10 positive cells

For quantification of the percentage of neural crest stem cells in the neural tube explants, after staining the cultured cells for p75 and Sox10, explants of two wildtype and two B-Raf-deficient embryos were quantified. Using a fluorescent microscope all cells were counted according to being positive for the counterstaining DAPI and all double-positive cells were counted.

2.5 Histological Methods

2.5.1 Preparation of tissue-sections

Paraffin-embedded tissue sections

The fresh tissue was washed with PBS and fixed in 4% PFA in PBS at 4°C overnight. After washing with PBS, the tissue was deposited in 70% ethanol and stored at 4°C until the embedding procedure. Paraffinization step involves 40min in 50% ethanol, 40min in 70% ethanol, 40min in 80% ethanol, 40min in 90% ethanol, 40min in 95% ethanol, 3x 40min in 100% ethanol, 2x 30min in chloroform:ethanol (1:1), 30min in chloroform. All procedures were performed at RT. Afterwards the tissue was transferred into melted paraffin and incubated for 1h at 65°C and then in fresh paraffin 2hrs or overnight at 65°C. Finally the tissue was casted into paraffin blocks. These blocks were then sectioned into 6-10μm microsections and used for the further histological analysis after drying for at least one night.

Cryosections

The fresh tissue was washed with PBS and fixed in 4% PFA in PBS at 4°C overnight. After washing with PBS, the tissue was transferred into 30% sucrose in PBS and incubated at 4°C until the tissue was fallen to the bottom of the tube. Before embedding on dry ice with OCT, the tissue was washed with PBS. The blocks were sectioned into 6-10μm microsections and used for further histological analysis. The blocks and the sections were stored at −80°C until use.

2.5.2 H&E-staining

For histological analysis of paraffin sections, the tissue was stained with H&E. As indicated in first the paraffin has to be removed from the sections, then the tissue is stained with H&E, dehydrated and mounted with Entellan.

reagent	incubation time
Xylol	2x 10min
100% Ethanol	3x 5min
70% Ethanol	10min
Millipore water	5min
Hematoxilyn	30sec
tap water	5min
Millipore water	5min
Eosin	20sec
Millipore water	5min
70% Ethanol	10min
100% Ethanol	3x 5min
Xylol	2x 10min

Table 2-4 H&E staining of paraffin sections.

2.5.3   Immunohistochemistry for Cytokeratin7

After deparaffinization instead of H&E-staining, the paraffin sections can be stained immunohistochemically using a specific antibody. For this purpose, an antigen-retrieval step was performed using 10mM Citrate buffer, pH6.0 and cooking the tissue in the microwave for 15min. After cooling down at room temperature, the sections were washed with tap water and then three times for 5min with PBS. Before incubation with the primary antibody, the sections were blocked for 1hr at room temperature with 1%BSA, 0.1% TritonX-100 in PBS. The primary antibody was diluted 1:200 in blocking solution and was applied on the tissue overnight at 4°C. Afterwards the sections were washed three times for 5min with PBS. The secondary antibody (Goat-anti-mouse-biotinylated) was diluted 1:200 in blocking solution and the sections were incubated for 90min at room temperature. Before applying the A+B reagent that was prepared 30min before 1:1 for 30min at room temperature, the tissue was washed three times for 5min with PBS. Afterwards the sections were washed again three times for 5min with PBS and incubated with DAB (1ml DAB + 0.8ml 30%H_2O_2) until the brown colour appeared. The reaction was stopped with tap water for 5min and afterwards the tissue was counterstained shortly with hematoxylin, washed with tap water, dehydrated and mounted with Entellan.

2.5.4 In-situ Hybridization

Cloning of Sox10, Mitf, DCT and Tyrosinase cDNA into pcDNA3

cDNAs of different neural crest and melanocyte development markers were cloned in order to synthesize riboprobes for in-situ hybridization. The cDNA obtained from RNA from the murine B16 melanoma cell line using the Fermentas first strand synthesis kit and the random hexamer primers was used as a template for RT-PCR using primers specific for the different markers. The resulting fragments were digested with restrictionendonucleases, to create sticky ends and were cloned into the pcDNA3-vector (Invitrogen) for in-vitro transcription for probe generation (Table 2-5). In the case of Tyrosinase, the primers were designed with overhangs to introduce a NotI and a XbaI restriction site into the DNA-sequence.

Gene	Primer	PCR-Fragment-Size	Enzymes used for cloning	Fragment Size
DCT	DCT-RT-for DCT-RT-rev	765 bp	KpnI XbaI	506 bp
Tyrosinase	Tyrosinase-NotI-for Tyrosinase-XbaI-rev	858 bp	NotI XbaI	290 bp
Mitf	Mitf-RT-for Mitf-RT-rev	822 bp	KpnI BamHI	626 bp
Sox10	Sox10-RT-for Sox10-RT-rev	693 bp	EcoRV	693 bp

Table 2-5 Cloning of plasmids for in-vitro transcription.

In-situ hybridisation-riboprobe synthesis

Probe	Enzyme	RNA-Polymerase
DCT-Sense	HindIII	Sp6-Polymerase
DCT-Antisense	XbaI	T7-Polymerase
Tyrosinase-Sense	XbaI	T7-Polymerase
Tyrosinase-Antisense	BamHI	Sp6-Polymerase
Mitf-Sense	HindIII	Sp6-Polymerase
Mitf-Antisense	NotI	T7-Polymerase
Sox10-Sense	NotI	T7-Polymerase
Sox10-Antisense	BamHI	Sp6-Polymerase

Table 2-6 Linearization of Plasmid-DNA for DIG-labelling via in-vitro transcription.

The cDNA-containing plasmids were linearized as described in Table 2-6. The linearized plasmid were then gel-isolated and used as templates for antisense and sense Digoxigenin

(Addya et al.) -labeled riboprobe synthesis. The in-vitro transcription was performed as described for the DIG RNA labeling kit (Roche) using 1μg of linearized plasmid DNA.

The riboprobes were then purified through a precipitation step by addition of 2.5μl 4M LiCl and 75μl 100% Ethanol and incubation for at least 2 hours at −20°C. The riboprobes were pelleted via centrifugation at 4°C, the pellet was washed with 70% Ethanol and resuspended in 75μl DEPC-treated water. To control the length and integrety of the probes, gelelectrophoresis was performed before using the riboprobes for in-situ hybridisation.

In-situ Hybridisation

After thawing the sections for at least 30 min at room temperature and drying them for 2 hours at 40°C, the tissue was fixed for 5 min using 4% PFA in PBS (pH7.5). To permabilize the cells, the sections were treated with 0.3% Triton X-100 in PBS for 15 min and with 0.2μg/ml Proteinase K in Proteinase K buffer for 5 min at room temperature and fixed again for 5 min at room temperature. For acetylation, the tissue was incubated for 10 min at room temperature in TEA-buffer. Between all treatments, the sections were washed with PBS.

The tissue was then prehybridized in hybridisation buffer for 1 hour at room temperature. Before adding the riboprobes to the hybridisation buffer, they were denatured by incubation at 80°C for 5 min. For hybridisation 500ng/ml riboprobe was added to the prewarmed hybridisation buffer. The sections were incubated with the riboprobe containing hybridisation buffer overnight at 63°C. Prehybridisation and hybridisation were performed in a box saturated with 5x SSC and 50% foramide and the slides were covered by a rectangular piece of parafilm to avoid evapuration. After hybridisation, the sections were washed with prewarmed 2x SSC, 50% formamide for 1 hour at 63°C and then equilibrated in prewarmed RNaseA-buffer for 20 min at 37°C. To reduce the background, the single-strand RNA was removed by RNaseI-treatment (20 μg/ml RnaseI-buffer) for 30 min at 37°C.

Before blocking the tissue for 1 hour at room temperature with blocking solution, the sections were washed for 30 min in TBST. To detect the DIG-labeled riboprobes, the tissue was then incubated with alkaline-phosphatase-coupled anti-digoxigenin antibody diluted 1:2000 in blocking solution overnight at 4°C. To avoid evaporation, this was performed in a box saturated with water and the slides were covered with rectangular pieces of parafilm.

Excess antibody was removed by washing the tissue several times in TBST and the sections were then equilibrated in NTMT. Color development was performed overnight at 4°C using 4.5μl NBT and 3.5μl BCIP per ml NTMT buffer in a box saturated with NTMT buffer and covered with rectangular pieces of parafilm. When the color had the desired intensity, the staining was sections were washed with PBS and then fixed with 4% PFA in PBS (pH7.5) for 15 min at room temperature. After washing with PBS the sections were mounted with mowiol.

2.6   *In-vivo experiments*

All animal experiments were performed according the German law for animal protection. Animals were sacrificed via cervical dislocation unless described differently.

2.6.1   Generation of transgenic mice

For microinjection the pBi5-B-Raf^{V600E}-EGFP plasmid-DNA was prepared by CsCl plasmid preparation as described before. To remove the vector-backbone 50μg of DNA were digested using the restrictionendonucleases XbaI and PvuI and the resulting 5.4kb fragment was isolated from a low-melting agarose gel using the agarose digesting enzyme agarase as described by the manufacturer. The DNA was dissolved in injection buffer for microinjection. Finally, purified DNA-fragment was injected into the pronucleus of fertilized mouse eggs by Hildegard Troll and the resulting mice were genotyped by PCR as described in the next paragraph.

2.6.2   Genotyping of transgenic mice

For gaining DNA for genotyping the mouse tails were cut in the age of 3-4 weeks and the mice were marked by earmarks. The tails were lysed by the addition of 190µl of tail lysis buffer and 12µl of 0.4mg/ml ProteinaseK and incubation overnight at 54°C. The resulting lysate was then centrifuged at 10000rpm for 5min and the supernatant was diluted 1:10 with water and was used as a template for a PCR-reaction as described above with primers for genotyping listed in the material part.

2.6.3   Transplantation-experiments

For subcutaneous injection of A549 and A549 J5-1 cells, the cells were washed two times with sterile PBS after trypsinisation and were counted. 10^6 cells were subcutaneously injected in 100µl of sterile PBS into Rag1$^{-/-}$-mice. The tumour size was measured weekly and the animals were sacrificed when the first tumours in the different groups were close to 2cm of diameter. Under anaesthetic the animals were perfused using 4% PFA-PBS and the primary tumours, the lungs, the livers and the lymph nodes were collected for histology.

2.6.4   Neural Tube Explants

Fibronectin-coating of cell culture dish

For culturing the neural tube explants, the cell culture dish was before coated with the cell adhesion molecule fibronectin. For this purpose, 8µg fibronectin were diluted in 300ml of sterile PBS per well of a 24-well-plate. The solution was pipetted onto the dish and incubated for 1hr at room temperature. After this the fibronectin-solution was removed and the dish was washed three times with sterile Millipore water and was then used immediately or stored at 4°C.

Preparation of the neural tube

Time-matched pregnant mice were sacrificed via cervical dislocation, the skin was opened and with a different, sterile surgery set, the uterus was prepared and opened and the embryos were transferred to sterile PBS. Using a stereolupe, the neural tube of the embryos was prepared and transferred to the fibronectin-coated dish already containing D-MEM-medium including Endothelin-3. The head of the embryos were stored at -20°C for genotyping.

Culturing Neural Tube Explants

The neural tubes were cultured on fibronectin-coated dish in D-MEM-medium containing 5nM Endothelin-3 at 37°C for 2-5 days. The medium was changed every other day.

2.7   Statistical Analysis

Statistical analyses of data sets were performed using the Graphpad Prism version 4.0 software. For all tests, statistical significance was considered to be at $P<0.005$.

3 Results

3.1 *Generation of a transgenic mouse model for melanocyte-specific and inducible expression of B-RafV600E*

The goal of this part of the thesis was to establish a mouse model that expresses the human oncogenic B-Raf^{V600E} in melanocytes. For this purpose the tetracycline-inducible system was chosen. The promoter used in this system contains a tetracycline-responsible element (*TetO*), which can be bound by the reverse tetracycline-controlled transcription activator protein (rtTA) in the presence of doxycycline to induce the transcription of the gene of interest (Zhu et al., 2002). This mouse can then be combined with a strain that expresses the rtTA under the control of a tissue-specific promoter, in this case in the melanocytes for example driven by the DCT- or the Tyrosinase-promoter. The resulting bitransgenic mice would express the oncogenic B-Raf^{V600E} tissue-specific in the presence of doxycycline. The tissue-specific and inducible expression of B-Raf^{V600E} is crucial to obtain viable offspring, since it is known that the constitutive expression of C-Raf as well as the tissue-specific, but constitutive expression of B-Raf^{V600E} under control of the Tyrosinase promoter is embryonal lethal (unpublished data Rapp et al., Marais et al.).

3.1.1 Construction of pBi5-B-Raf^{V600E}-EGFP

To generate transgenic mice conditionally expressing the constitutive active B-Raf^{V600E}, a plasmid was used that encodes the B-Raf^{V600E}-sequence and the reporter gene Luciferase, controlled by a bidirectional CMV promoter unit, that contains a tetracycline-responsible element (*TetO*) (Figure 3-1). To be able to distinguish the exogenous B-Raf^{V600E} from the endogenous wild type B-Raf, an EGFP-tag was introduced into the pBi5-B-Raf^{V600E} that was previously generated by PD Dr. R.Götz. For this purpose, a plasmid that was generated by Dr. C.Xiang was used that contained the wild type B-Raf tagged with EGFP. Both plasmids were

cut using the restriction endonucleases Mph1103I and SalI and the EGFP-tagged C-terminal part of B-Raf was combined with the N-terminal V600E-mutation containing part in the pBi5 vector. The DNA was linearized and purified for pronucleus injection, which was performed by Hildegard Troll.
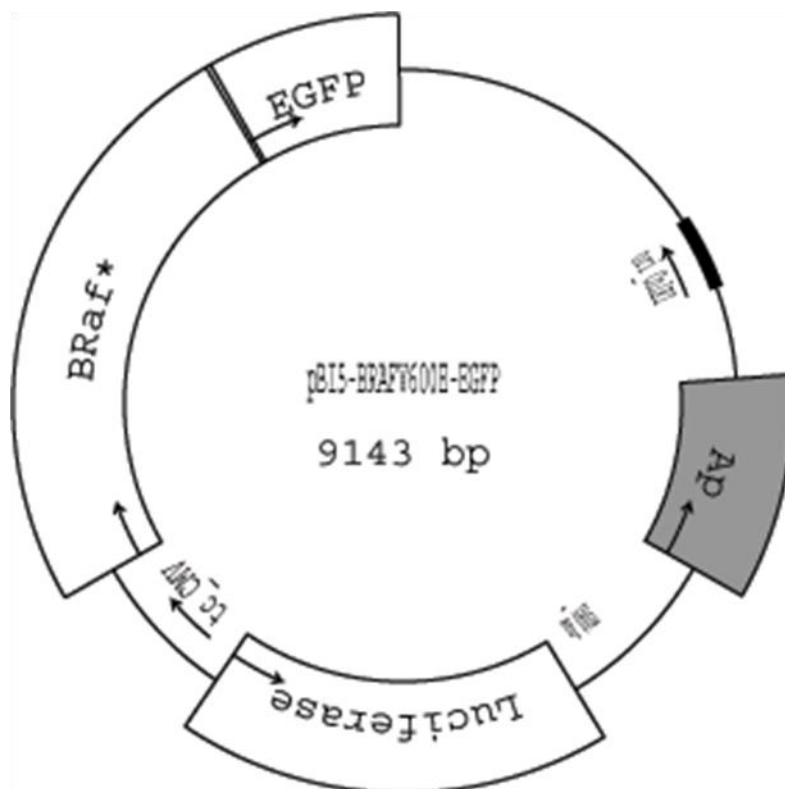
Figure 3-1 Design of a vector for tetracycline-regulated transgene expression. The plasmid contains a bidirectional tetracycline-regulatory CMV promoter element controlling in one direction the oncogenic version of human B-Raf tagged with EGFP and in the other direction the reporter gene Luciferase.

3.1.2   In vitro analysis of B-Raf^{V600E}-EGFP expression and functionality

To test the resulting pBi5-B-Raf^{V600E}-EGFP construct, the fibroblast cell line NIH3T3, stably expressing the tetracycline-controlled transcriptional activator (tTA), was transfected with the plasmid using Lipofectamine reagent. Western blot analysis showed, that the protein level of B-Raf was elevated in the cells 48hrs post transfection ("On"-status) and that the expression could be turned off by the addition of Doxycycline ("Off"-status) to the cell culture medium (Figure 3-2 A). More quantitative analysis was possible due to the additional reporter gene

Luciferase for the promoter activity. The Luciferase was expressed in the absence of

A

B
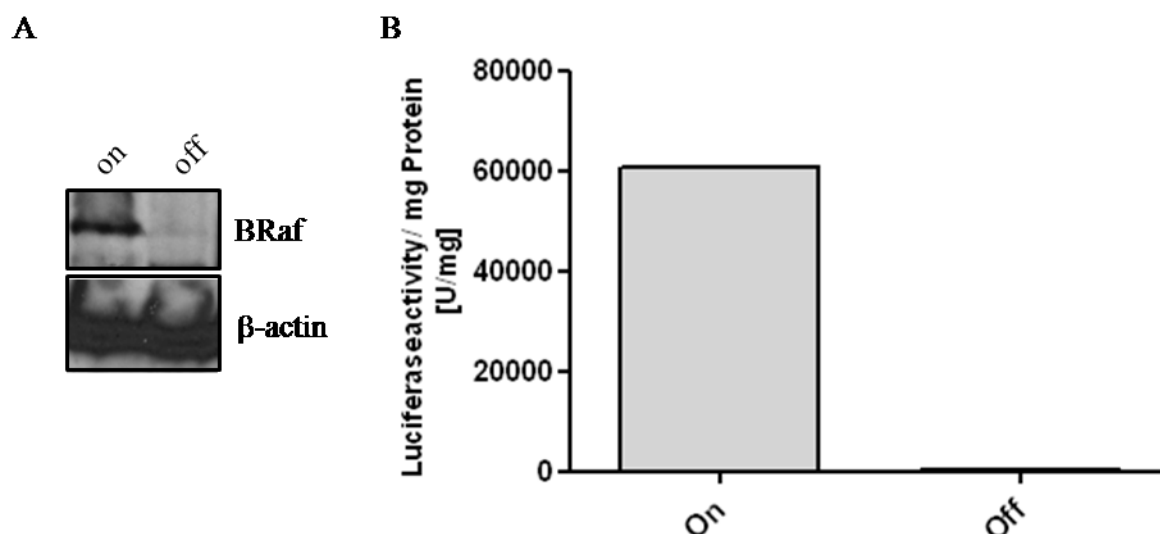
Figure 3-2 Conditional Expression of B-Raf^{V600E} in NIH3T3-tTA cells. **A** Western Blot analysis shows the expression of the B-Raf-protein in dependency on the tetracycline-controlled transactivator protein tTA and Doxycycline (1000μg/ml) 48 hrs post transfection. B-Raf was detected using a C-terminal B-Raf antibody. **B** Analysis of the cells with a luciferase assay shows elevated luciferase levels only in the "On"-status of the tetracycline-inducible CMV-promoter.

Doxycycline, while after treating the cells with Doxycycline the Luciferase activity per mg of

protein was about 160 times lower than detected in the "On"-status (Figure 3-2 B).

A

B
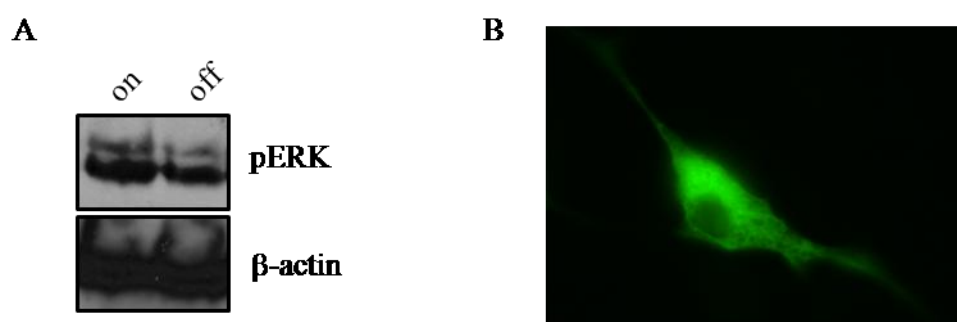
Figure 3-3 Expression of EGFP-tagged B-Raf^{V600E} in NIH3T3-tTA cells. **A** Western Blot analysis shows elevated pERK levels using a phospho-specific ERK antibody in the "On"-status. **B** The transgenic B-Raf^{V600E} can be detected via fluorescence microscopy.

To examine whether the EGFP-tagged B-Raf^{V600E} protein was functional, a Western Blot for

pERK was performed. As shown in Figure 3-3 A in the absence of Doxycycline the pERK-

levels in NIH3T3-tTA cells that were starved for 24 hrs (reducing the FCS amount from 10%

to 0.5%) were higher compared to Doxycycline-treated cells, indicating that the kinase

activity of the exogenous B-Raf^{V600E}-EGFP is functional. To show, that the EGFP-tag can be detected by fluorescent microscopy, the cells were fixed and analyzed using a fluorescent microscope. As shown in Figure 3-3 B, the green fluorescent cells could only be detected in the absence of Doxycycline. These data show, that the regulation of the B-Raf^{V600E}-EGFP and the luciferase-expression using Dox is working and that the resulting protein is functional in respect to the kinase activity and the EGFP-tag.

3.1.3   Generation and Characterization of transgenic B-Raf^{V600E}-EGFP founder lines

To generate transgenic mice, pBi5-B-Raf^{V600E}-EGFP was cut with the restrictionendonucleases XbaI and PvuI to remove the vector backbone. The resulting 5445 bp fragment containing the bidirectional inducible promoter and the B-Raf^{V600E}-EGFP as well
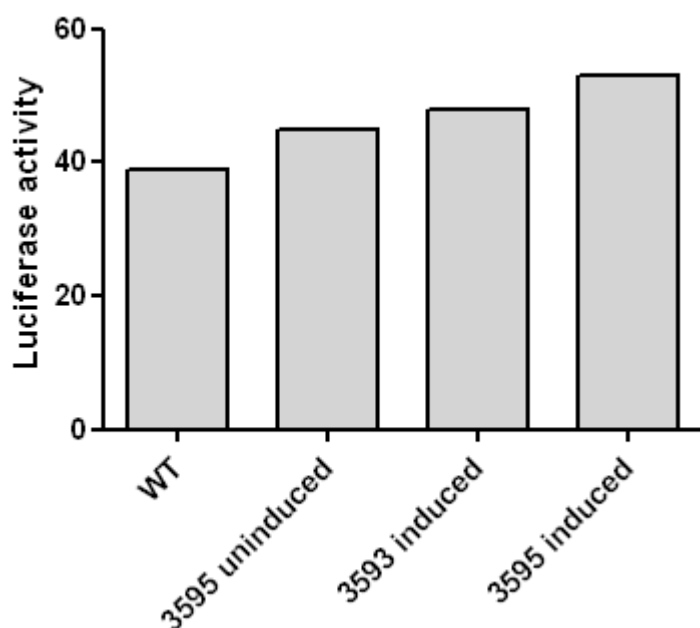
Figure 3-4 Luciferase-assay from lung lysates of induced tet-o-B-Raf^{V600E}-EGFP/SpC-rtTA bitransgenic animals. No difference was observed in the luciferase activity in samples from induced animals from both founder lines when compared to samples from not-induced or wildtype animals.

as the luciferase was isolated by gelextraction from an agarose gel and was injected in the pronucleus of fertilized mouse oozytes and the resulting mice were genotyped by PCR. From the six positively (2832, 2772, 2831, 2833, 3593, 3595) genotyped animals, only two (3593,

3595) were transmitting the transgene to their offspring. These founder animals were crossed with the well established *SP-C-rtTA* inducer mice that express the rtTA in lung alveolar type II epithelial cells (Perl et al., 2002a) to generate bitransgenic (*SP-C-rtTA*/*TetO-B-Raf*^{V600E}-*EGFP*) animals. Analysis of luciferase activity in lung tissue extracts of Dox-induced bitransgenic mice, that were induced for one week with Dox-food and additional daily injections, showed no increased luciferase levels in both founder lines (Figure 3-4), suggesting no expression of the transgene.

3.2   *The Role of B-Raf in Melanocyte Development*

This part of the thesis addresses the role of B-Raf in murine melanocytes to gain insights into its physiological role in healthy melanocytes versus melanoma cells. Since B-Raf-deficient embryos die during embryonal development, the role of B-Raf in the early embryonal melanocyte development was determined. As mentioned already in the introduction an important step during tumour development from a benign tumour to malignant metastatic cancer might be tumour cell reprogramming by which the tumour cells gain features that are comparable with properties of precursor cells during developmental processes.

3.2.1   Expression of Melanocyte Development markers in the Neural Tube at day E11.5

To address whether the precursors of the melanocytes, the neural crest stem cells and the melanoblasts, are present in the absence of B-Raf, RT-PCR was performed using RNA isolated from neural tubes prepared from E11.5 wildtype and B-Raf$^{-/-}$ embryos. As described in the introduction, during the early melanocyte development, the precursors are located in the neural crest and are positive for the neural crest marker Sox10. When the cells exit the neural tube and start to migrate, the expression of the transcription factor Mitf, which is said to be the master regulator in melanocyte development, is unregulated. Melanoblasts migrate dorsolaterally and express first the melanogenic enzyme dopachrome-tautomerase (DCT) and later also Tyrosinase (Le Douarin, 2003). As shown in Figure 3-5 the neural crest marker

Sox10 is expressed in the neural tube of wildtype as well as of B-Raf-deficient embryos. The same is true for one of its target genes *Mitf*. Furthermore even the melanogenic enzyme
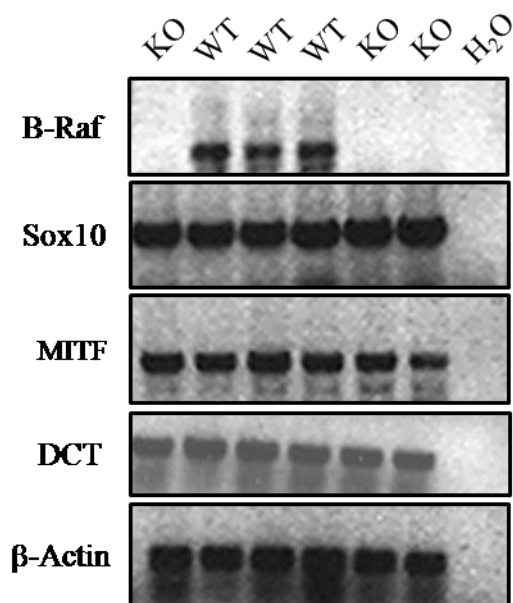
Figure 3-5 RT-PCR from RNA of the neural tubes of E11.5 embryos shows the expression of the neural crest stem cell marker *Sox10* as well as the melanocyte development markers *Mitf* and *DCT* in the presence and absence of B-Raf respectively.

DCT, which is a melanoblast marker and involved in the melanin synthesis is expressed in the presence as well as in the absence of B-Raf in the neural tube of E11.5 embryos Figure 3-5. These data suggest that B-Raf is not necessary for the expression of these genes involved in melanocyte development.

3.2.2 Neural Crest Stem Cells in Neural Tube Explants

To gain more quantitative insights into the neural crest stem cell population in wildtype versus B-Raf$^{-/-}$ embryos, the neural tubes from E9.5 wildtype and B-Raf$^{-/-}$ embryos were isolated and cultured for five days in D-MEM-medium containing Endothelin-3 on fibronectin-coated cover slips. At early stages a high percentage of all neural crest stem cells in these neural tube explant cultures are early neural crest stem cells and express the neural crest stem cell markers p75 and Sox10 (Kleber et al., 2005). As shown in Figure 3-6 A, most of the cells in the migratory front of the neural tube explants are positive for both markers in

the presence as well as in the absence of B-Raf. When the double positive cells were counted in the complete explants, there was no significant difference between the number of cells expressing both markers in the B-Raf-deficient neural tube explants compared to the wildtype cultures (Figure 3-6 B). These data suggest that B-Raf is not necessary for the early neural crest development.

A

B
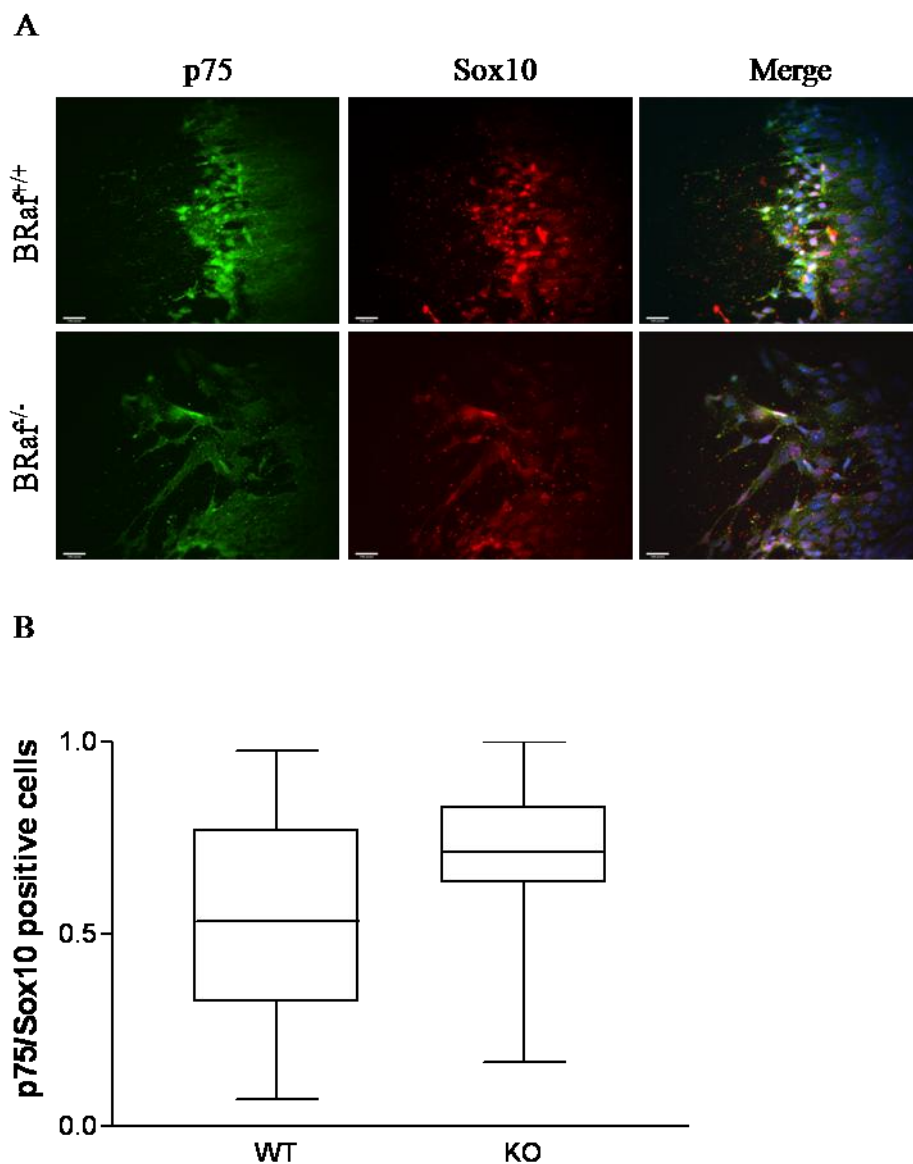
Figure 3-6 Neural crest stem cell markers in neural tube explants cultured for 5 days in the presence of Endothelin-3 in the presence and absence of B-Raf respectively. **A** Immunocytochemistry for the neural crest stem cell markers p75 and Sox10 shows that there are double positive cells in the migratory front of the neural tube explant cultures in the presence as well as in the absence of B-Raf. **B** The Quantification of the p75/Sox10 double positive cells in two cultures of WT and KO embryos, respectively, shows, that there is no reduction of the neural crest stem cells in the absence of B-Raf.

3.2.3 Neural Crest Development *in vivo* in B-Raf-deficient embryos

Since it was published earlier that B-Raf plays an important role in migration of cortical

neurons in the developing brain (Camarero et al., 2006), an in-situ hybridization was
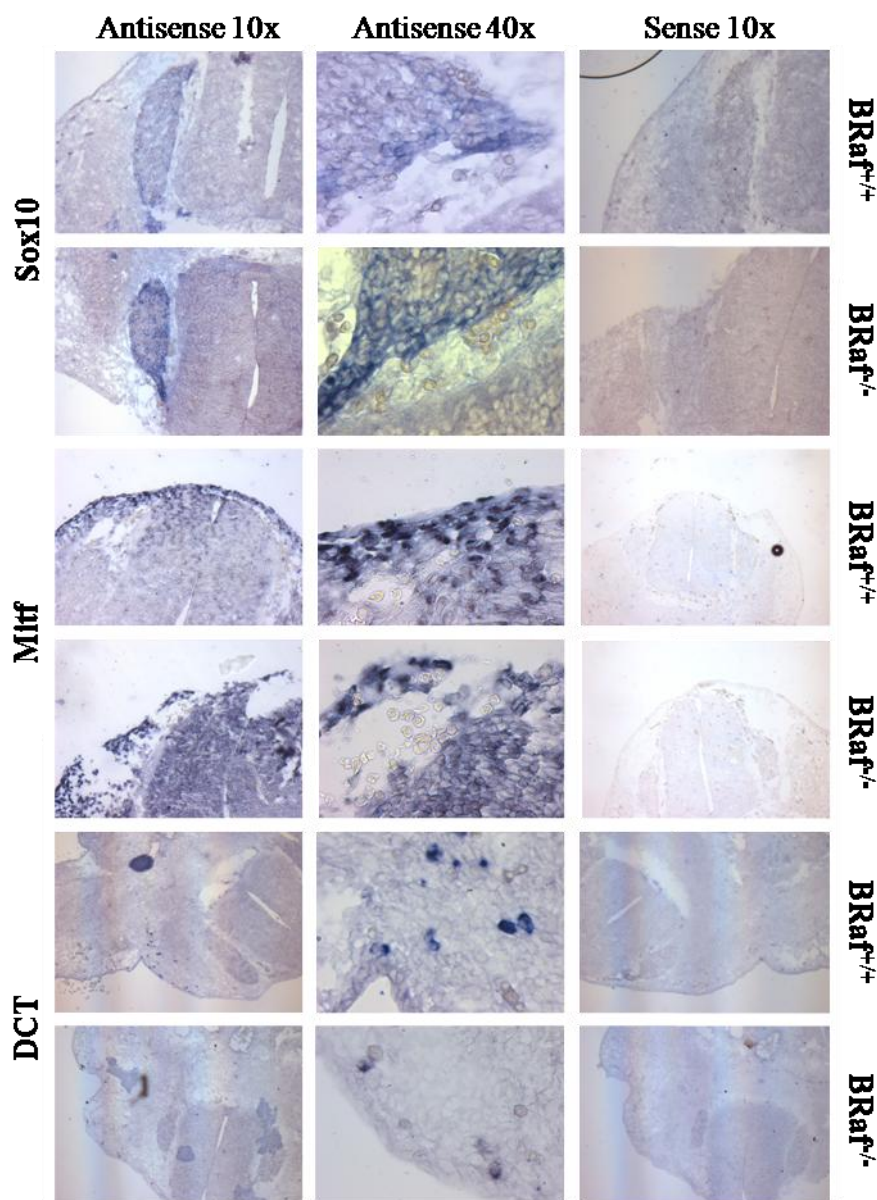
Figure 3-7 in-situ hybridization on horizontal sections of E11.5 embryos shows no difference in localization of cells expressing the neural crest stem cell marker Sox10 as well as of cells expression the melanoblast markers Mitf and DCT in B-Raf-deficient embryos compared to wildtype animals.

performed to see the localization of the melanoblast precursors in the wildtype and B-Raf$^{-/-}$

embryos. As shown in Figure 3-7, there are *Sox10*-positive cells present in the migratory

stream from the neural crest stem cell population to the dorsal root ganglia in the wildtype as

well as in the B-Raf-deficient embryos. Furthermore the in-situ hybridization showed the *Mitf*-expressing cells in the migration staging area and in the dorsolateral migratory pathway of the neural crest derived cell population in the presence and absence of B-Raf. The melanoblast localization was detected using probes for the melanogenic enzyme *DCT*. As indicated in Figure 3-7 the melanoblast are located independently of B-Raf-expression in the dorsolateral part of the embryos next to the epidermis.

3.3   *Myc-induced metastasis in NSCLC*

In this part of the thesis, a transgenic mouse model for metastasis in NSCLC was used to determine the differences in the gene expression profiles of non-metastatic lung tumours compared to liver metastases of primary lung tumours. As described in the introduction, transgenic mice expressing oncogenic C-Raf under the control of the SpC-promoter in the alveolar type II pneumocytes develop premalignant adenoma with high penetrance, but lacking spontaneous progression. In contrast the expression of c-Myc targeted to lung alveolar type II cells leads to late tumour development with a relatively low penetrance. When these two transgenes are combined in compound animals, a phenotypic switch of the tumour cells from a cuboidal to a columnar shape was observed. Furthermore, in 24% of the bitransgenic animals metastases were found in liver or lymphnodes (Rapp et al., 2009).

3.3.1   **Mutation analysis of primary tumours and metastasis of SpC-c-Myc and SpC-C-Raf-BxB/SpC-c-Myc animals**

Since the tumour development in the SpC-c-Myc animals was delayed and the number of tumour foci was lower when compared to the compound mice, a screen for secondary mutations in Exon1 of the oncogene *KRas* and in Exon6 of the tumour suppressor *LKB1*, which is mutated in 34% of human NSCLC (Shah et al., 2008), was performed (partly by Valentina Serafin). As shown in Table 3-1 in all tumours of single transgenic SpC-c-Myc animals, a secondary mutation was found and mutations in *KRas* Exon1 and *LKB1* Exon6

were mutually exclusive with one exception. In the bitransgenic compound animals on the other hand, only in a small fraction of animals a mutation in *KRas* Exon1 was identified, while they were all negative for mutations in *LKB1* Exon6. These results suggest an inhibition of the tumour suppressor gene *LKB1* by the mitogenic cascade in lung alveolar type II cells.

Genotype	ID-number	*KRas* Exon1	*LKB1* Exon6
SpC-c-Myc	2	[G12->D]	
	6389	[G12->D]	[G279->S]
	8445	-	[P275->S]
	8530	[G12->D]	-
	8898	-	[P275->S]
	9119	[G12->D]	-
	10466	-	[P275->S]
	11163	[G12->C]	-
	12084	[G12->D]	-
	12926	[G12->D]	-
SpC-C-Raf-BxB/SpC-c-Myc	468	[G12->D]	-
	10219	-	-
	10416	-	-
	10617	-	-
	10621	-	-
	11136	-	-
	11501	-	-
	11528	-	-
	11556	-	-
	11560	[G12->D]	-

Table 3-1 Mutation analysis of primary tumours. The long latency tumours of the SpC-c-Myc mice carry frequently mutations in the oncogene *KRas* or in the tumour suppressor gene *LKB1*.

The discovery of the high frequency of mutations in *KRas* Exon1 in the primary tumours of the SpC-c-Myc single transgenic animals suggested that it might be possible to use these mutations as markers for lineage tracing in the metastases. In Table 3-2 it is shown that the metastases of the single transgenic SpC-c-Myc animals were negative for the *KRas* mutation detected in the primary lung tumour with only one exception. In the mouse number 16740, which had multiple organ metastases, the *KRas* mutation in the primary lung tumour was similar to the mutation found in the liver metastasis. These results suggest that metastasis is an early event.

Genotype	ID-number	lung KRas Exon1	liver KRas Exon1
SpC-c-Myc	1	-	n.m.
	44	-	n.m.
	46	-	n.m.
	1895	[G12->D]	-
	8445	-	-
	8530	-	n.m.
	11163	[G12->C]	n.m.
	14226	-	-
	16740	[G12->C]	[G12->C]
	22620	[G12->D]	-
	30424	-	-
	30413	-	-
SpC-C-Raf-BxB/SpC-c-Myc	322	-	n.m.
	10219	-	-
	10617	-	n.m.
	10621	-	-
	11176	-	n.m.
	11501	-	n.m.
	11518	-	-
	14203	[G12->C]	n.m.
	16479	-	-
	17623	-	n.m.

Table 3-2 Mutation analysis of primary tumours and the corresponding metastases. The metastases of the primary tumours in the SpC-c-Myc transgenic animals do not carry the same *KRas* Exon1 mutations as the primary tumours (n.m.: no metastases).

3.3.2 Gene expression analysis of primary tumours of SpC-c-Myc and of compound animals

To investigate the differences in the gene expression profile of the SpC-C-Raf-BxB/SpC-c-Myc lungs compared to the SpC-C-Raf-BxB and wild type lungs, qPCR was performed for a panel of candidate genes (Table 3-3), that are known to be involved in processes like: organ development, Wnt-signalling, regulation of transcription, cell-adhesion or cell-cell-signaling, vasculogenesis, neuronal tissue or Type-II-pneumocytes, stem cell maintenance, the cell cycle and in tumourigenesis, that are necessary for cell-cycle progression and that are involved in cytokine-signaling. Furthermore, this list contains candidate proteins and genes expressed in hematopoietic cells picked from microarray data and the transgenes c-Myc and C-Raf-BxB. Surprisingly, the only gene that was found to be highly significantly upregulated in the SpC-

C-Raf-BxB/SpC-c-Myc compound compared to the single transgenic SpC-C-Raf-BxB and wildtype animals, respectively, was the *Synuclein* α (*SNCA*), which is expressed normally in the brain and is involved in Alzheimer and Parkinson's disease and dementia (Bisaglia et al., 2009).

Gene	wt	CRaf-BxB	Cpd	CRaf-BxB/wt	p-value	Cpd/CRaf-BxB	p-value
57578[1]	0,000556	0,000492	0,00062	0,884363	0,85554	1,261603	0,672598
AFP[2]	0,0012966	0,000649	0,00083882	0,50028169	0,1133043	1,2931772	0,3621580
AQP5[10]	0,0916433	0,170599	0,18930793	1,86155041	0,3030432	1,1096693	0,8877917
ASCI[6]	0,1849785	0,079031	0,12063433	0,42724555	0,3248567	1,5264133	0,3984433
AXUD1[2,3]	0,00896	0,007458	0,006047	0,832355	0,713729	0,810866	0,415423
CCL19[6]	2,279920	1,678303	3,85955363	0,7361237	0,245285	2,2996761	0,3236408
CCR7[6]	0,0099881	0,003929	0,00606607	0,39338607	0,3415127	1,5438542	0,194230
CD44[5]	0,3832155	0,381220	0,44394464	0,99479378	0,4947715	1,1645353	0,3665909
CDCA7L[4]	0,011819	0,012814	0,011878	1,084237	0,894375	0,926946	0,892581
CLECSF8[5,6]	0,001205	0,001336	0,001142	1,108763	0,834706	0,854758	0,709895
C-RAF[16]	0,1474777	13,63718	16,5425	92,4694917	**0,0001**	1,2130438	**0,0131**
DBPHT2[2]	6,87E-05	2,65E-06	3,02E-06	0,038629	0,3816	1,13783	0,789521
ENOL[9]	0,000991	0,000588	0,001262	0,59257	0,141969	2,148539	0,078509
ERAF[7]	0,002035	0,001201	0,00057	0,590368	0,405218	0,474445	0,196053
ERFI[8]	10,30684	8,84907	12,5388	0,858562	0,819747	1,416962	0,179143
FOXD3[2]	8,2213734	1,849395	1,13315397	0,22494959	0,0804918	0,6127162	0,2914543
FZD10[2,3]	0,0035117	0,003329	0,00380563	0,94787817	0,1640242	1,1432983	0,4274523
HBBBH1[7]	0,588658	0,082675	0,142033	0,140447	0,15272	1,717962	0,365726
IFI202B[7]	0,023095	0,008267	0,0135190	0,3579665	0,0328788	1,6352768	0,154656
JAGGED[2]	0,1010275	0,076452	0,06243959	0,7567462	0,3286535	0,8167145	0,3576276
KLF4[11]	0,1410194	0,116246	0,0698515	0,82432319	0,14085	0,6008961	0,0380691
LATS[12]	0,386345	0,604052	0,265197	1,563504	0,196018	0,439031	0,085538
MALAT1[13]	2,5765939	2,291542	2,45155872	0,8893685	0,3272480	1,0698295	0,3956217
MYC[16]	0,0105068	0,012967	0,03177759	1,23413090	0,5143	2,4506908	**0,0251**
NEURODI[9]	0,4172601	0,557438	1,45343679	1,33594875	0,4288621	2,6073509	0,3112298
NOTCH1[2]	0,0537009	0,058160	0,04705475	1,08303617	0,358757	0,8090564	0,2870955
NOTCH2[2]	0,0393950	0,046429	0,04709058	1,17855955	0,2673994	1,0142428	0,4847522
NOTCH3[2]	0,0229184	0,028635	0,02340299	1,24942743	0,2361030	0,8172892	0,2608844
NOTCH4[2]	9,4745859	0,247757	0,36855509	0,02614966	0,1866442	1,4875655	0,2487878
ODC[2]	0,209083	0,277562	0,190878	1,32752	0,598424	0,687696	0,511083
PBK[14]	0,002272	0,002323	0,003345	1,022465	0,944062	1,43993	0,261408
RSAD2[15]	0,738283	0,435451	0,728339	0,589816	0,191024	1,672607	0,077373
SHTM1[1]	0,01396	0,020894	0,013205	1,496665	0,307386	0,632002	0,256547
SNCA[9]	0,002285	0,00669	0,14804	2,927831	0,361006	22,12732	**0,009796**
SNCG[9]	0,9851209	0,215649	0,41625916	0,21890617	0,0472698	1,9302621	0,4667407
SYB[9]	1,2336177	0,010366	0,01573141	0,00840291	0,1869330	1,5175998	0,1659027
SYK[2]	0,651939	0,086118	0,06986264	0,13209524	0,3847539	0,8112431	0,5781639
TIAM2[2,13]	0,0104784	0,006825	0,00579676	0,65129778	0,2526831	0,8493979	0,3797876
TMP4[12,13]	0,426306	0,391205	0,354294	0,917664	0,626968	0,905647	0,721871

Table 3-3 Candidate Genes. wt: wildtype, Cpd: compound SpC-C-Raf-BxB/SpC-c-Myc. [1]hypothetical protein, [2]organ development, [3]regulated by Wnt-signalling, [4]regulation of transcription, [5]cell-adhesion, [6]cell-cell-signalling, [7]hematopoetic cells, [8]vasculogenesis, [9]expressed in neuronal tissue, [10]Type-II-pneumocytes, [11]stem cell maintenance, [12]regulation of the cell cycle, [13]involved in tumourigenesis, [14]cell-cycle progression, [15]cytokine-signalling, [16]transgenes.
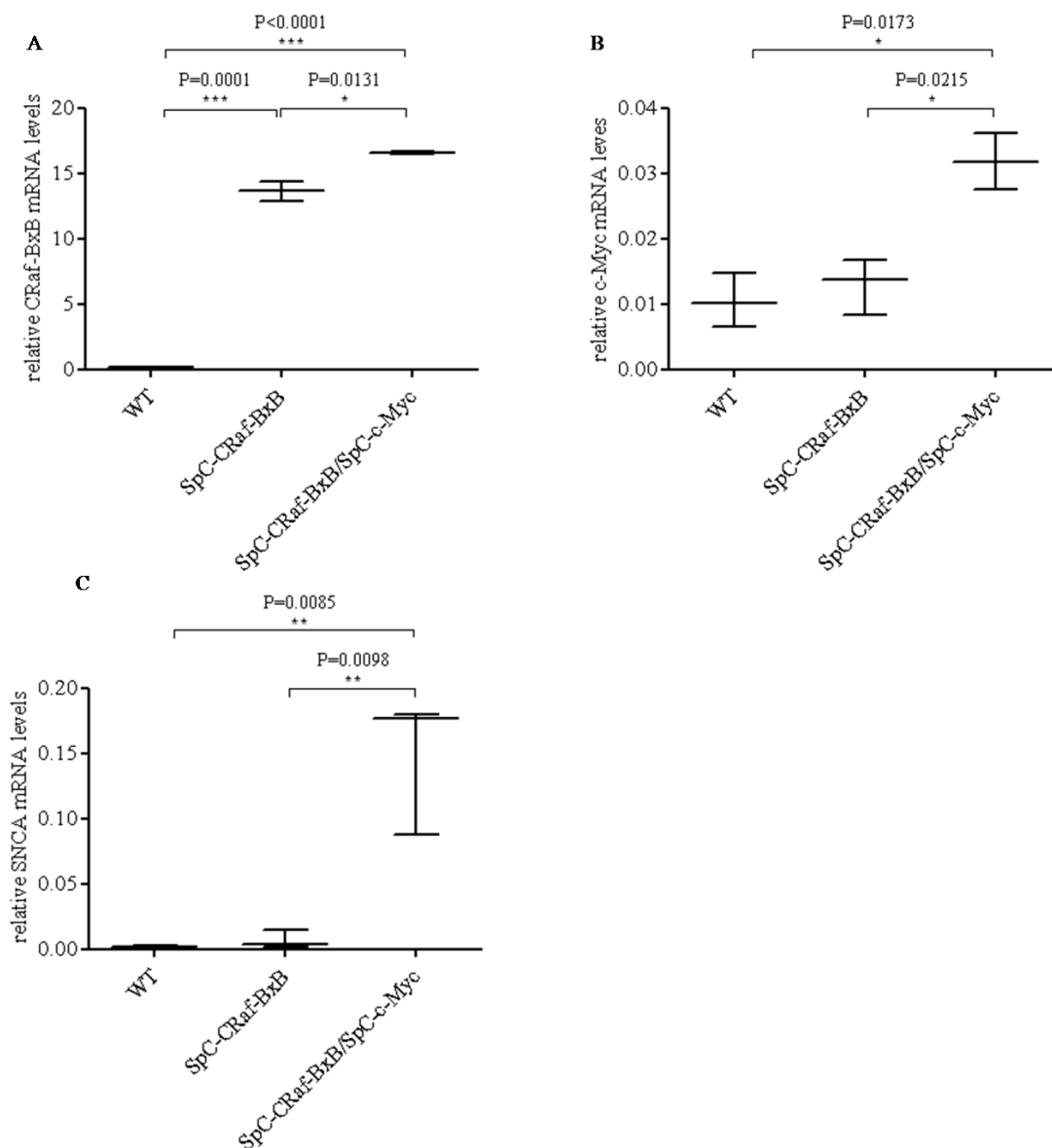
Figure 3-8 qPCR analysis of total lung RNA of wildtype, SpC-C-Raf-BxB and SpC-C-Raf-BxB/SpC-c-Myc bitransgenic animals (>10 months). **A** The relative mRNA-levels of *C-Raf-BXB* are increased highly significant in the SpC-C-Raf-BxB and in the compound animals when compared to the wildtype mice (n=3 for all genotypes). **B** The relative mRNA-levels of *c-Myc* are significantly higher in the bitransgenic animals compared to the wildtype and the SpC-C-Raf-BxB mice, respectively (n=3 for wildtype and SpC-C-Raf-BxB, n=2 for compound). **C** qPCR analysis for the neuroendocrine gene *Synuclein* α shows a highly significant increase of mRNA levels in the compound mice versus the wildtype and the single transgenic SpC-C-Raf-BxB animals, respectively (n=3 for SpC-C-Raf-BxB, n=2 for wildtype and compound).

(Figure 3-8 C). The expression of the transgene *C-Raf-BxB* was as expected highly significantly different in the SpC-C-Raf-BxB and SpC-C-Raf-BxB/SpC-c-Myc compound mice when compared to the wildtype animals (Figure 3-8 A). Furthermore the expression of the *c-Myc* transgene in the compound mice lead to a significant increase in the *C-Raf* mRNA

levels when compared to the single transgenic SpC-C-Raf-BxB animals. The relative mRNA levels of *c-Myc* were also highly significantly higher in the SpC-C-Raf-BxB/SpC-c-Myc compound animals when compared to the wildtype and SpC-C-Raf-BxB single transgenic mice (Figure 3-8 B), respectively, confirming the possibility to detect changes in the gene expression in the tumour cells using total lung RNA in qPCR analysis. These data suggest a neuroendocrine character of the columnar tumours.

3.4 *Generation and Analysis of a human NSCLC cell line expressing chicken c-Myc*

The goal of this part of the thesis was to generate a c-Myc-expressing NSCLC cell line to test whether the expression of c-Myc is sufficient to induce tumour progression to metastasis and to obtain a human cell culture system that is comparable to our NSCLC mouse model.

3.4.1 Introduction of chicken c-Myc into the human NSCLC cell line A549

To obtain a c-Myc-expressing cell line, chicken c-Myc was introduced into the non-metastatic human NSCLC cell line A549 using the J5-virus (Kurie et al., 1990). Since this virus has no marker for eukaryotic selection, the infected cells were seeded in soft agar and the resulting clones were picked after two weeks of incubation at 37°C. These clones were afterwards tested by immunocytochemistry using an antibody specific for chicken c-Myc. As shown in Figure 3-9 the clone with the strongest expression of chicken c-Myc was the clone A549 J5-1. Furthermore, immunocytochemistry was performed for the GATA family transcription factors 4 and 6 (GATA4 and 6, respectively), which were observed to be markers for the lineage switch from cuboidal (GATA6) to columnar shape (GATA4) tumour cells in our transgenic NSCLC mouse model (Rapp et al., 2009). GATA6 is expressed

normally   in   the   alveolar   type

	Chicken-Myc	Merge		Chicken-Myc	Merge
A549			**A549 J5-34**		
A549 J5-1			**A549 J5-36**		
A549 J5-12			**A549 J5-37**		
A549 J5-15			**A549J5-38**		
A549 J5-17			**A549 J5-39**		
A549 J5-23			**A549 J5-40**		
A549 J5-31			**A549 J5-41**		
A549 J5-33					
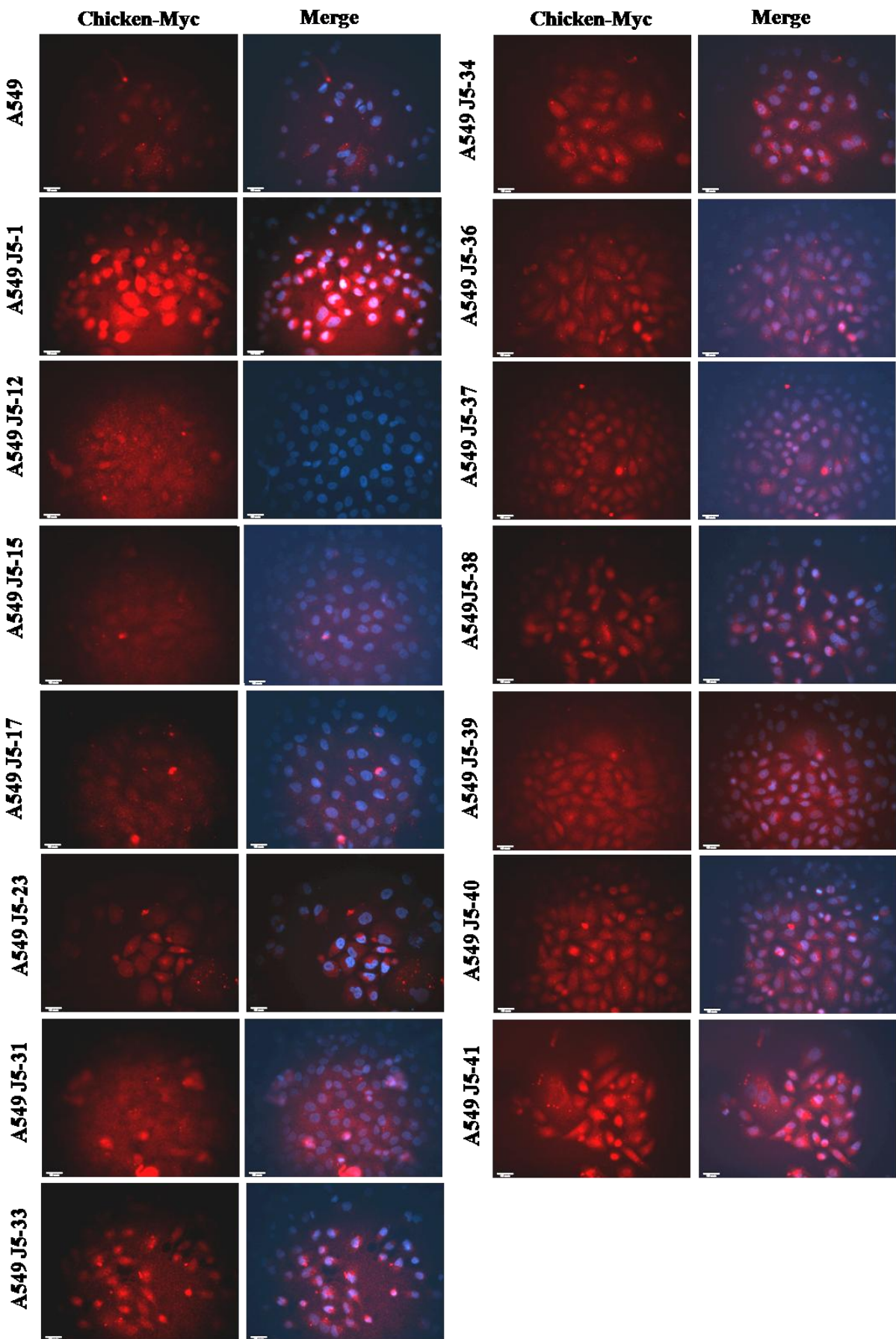
Figure 3-9 Immunocytochemistry for chicken c-Myc in the J5-transformed A549 clones shows that the clones express the exogenous chicken c-Myc on different levels. The clone with the highest chicken c-Myc expression level was the clone 1 (referred to as A549 J5-1).

II pneumocytes, where it drives the expression of the transcription factor TTF-1, which is necessary for SpC-promoter activity (Liu et al., 2002), and was recently shown to be involved in epithelial stem cell development and airway regeneration (Zhang et al., 2008). GATA4 on the other hand is necessary for the maintenance of the intestine in adult mice. As shown in Figure 3-10 in A549 J5-1 ectopic de novo expression of GATA4 has been observed in addition to GATA6 when compared to the parental cell line A549. This clone was used to perform the further experiments. As shown in Figure 3-11 A the clone A549 J5-1 has a different morphology compared to the parental cell line A549, when grown in adherent culture. The ability to grow anchorage-independently A549 J5-1 cells was compared in a soft agar assay. Although the A549 J5-1 cells are growing slower in adherent culture than the parental cell line (data not shown), when grown in soft agar, the size and number of colonies was highly significantly higher when compared to the A549 cells (Figure 3-11 B-D). These results show that the expression of c-Myc in the human NSCLC cell line A549 highly significantly increases the ability for anchorage-independent growth.

	GATA4	Merge	GATA6	Merge
A549				
A549 J5-1				
A549 J5-12				
A549 J5-23				
A549 J5-31				
A549 J5-34				
A549 J5-39				
A549 J5-41				
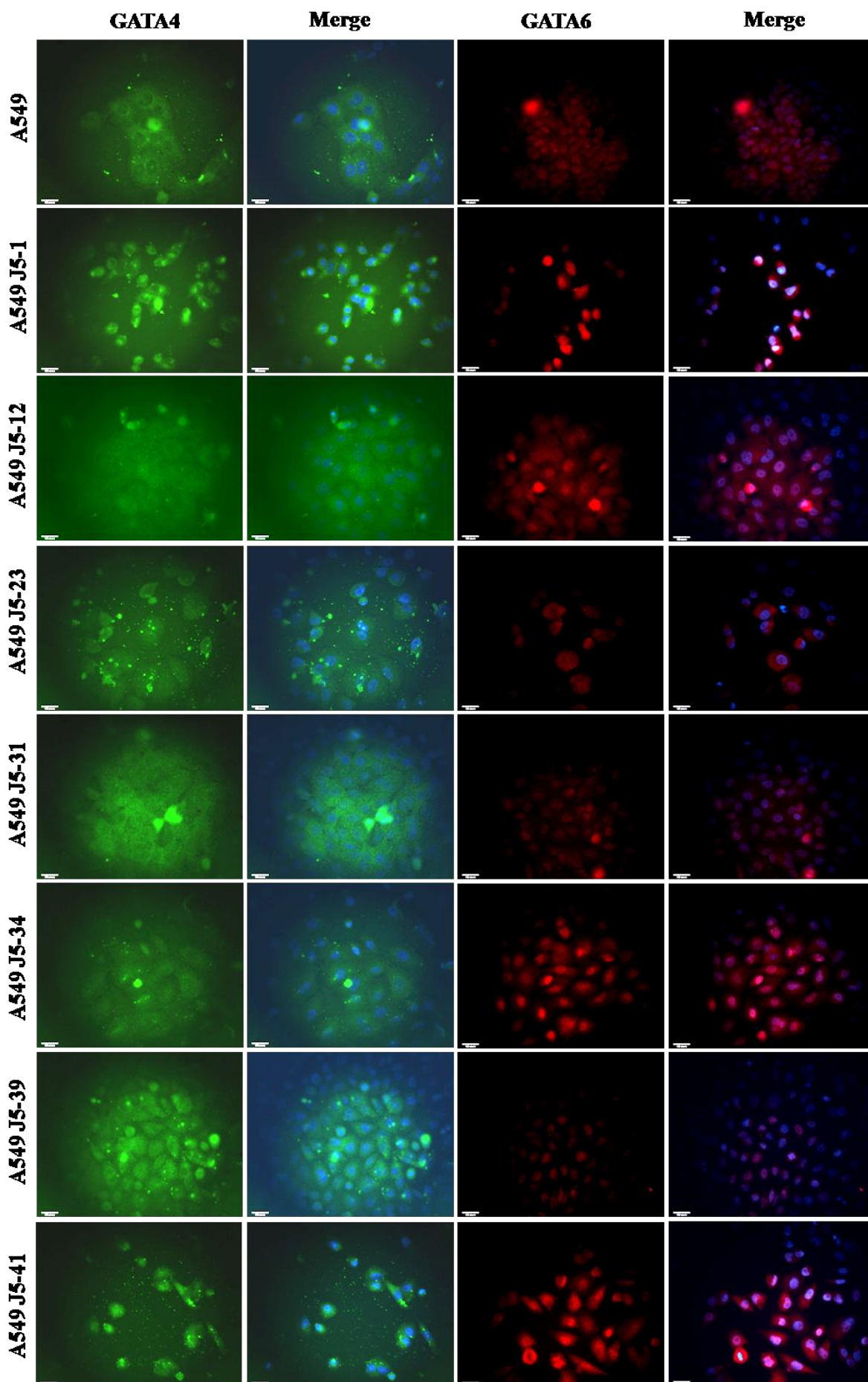
Figure 3-10 Immunocytochemistry for the in the mouse model identified markers for tumor progression GATA4 and GATA6 on several different A549 J5 clones showed that GATA6 was relatively high in the parental cell line as well as in the low chicken c-Myc expressing clones, while GATA4 levels were clearly elevated in the clones J5-1 and J5-41.
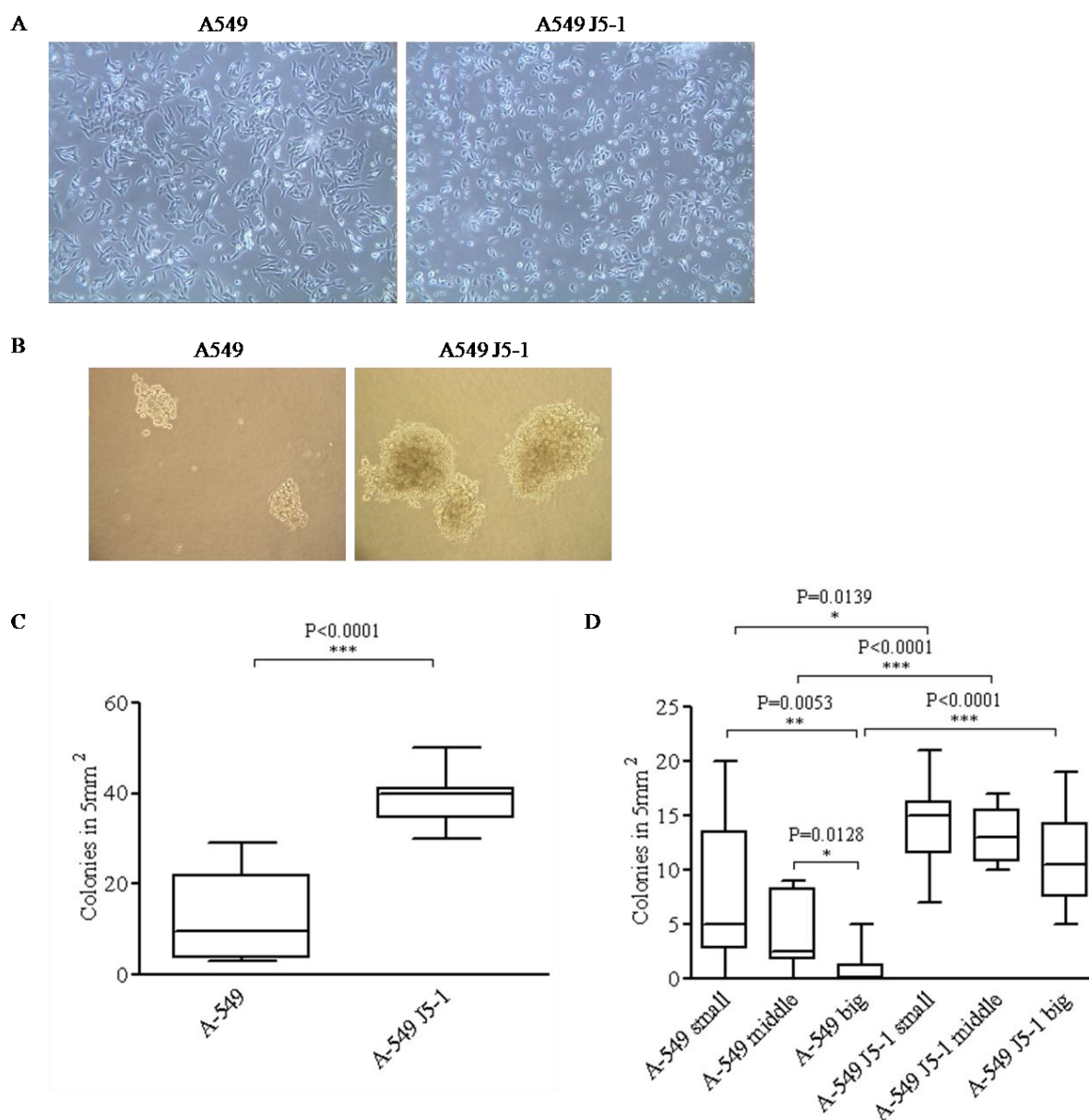
Figure 3-11 Characterization of the clone A549 J5-1. **A** After introduction of chicken c-Myc, the cells change their morphology and tend to detach. **B** Growing in soft-agar resulted in bigger colonies in the case of the clone A549 J5-1 (10000 cells where seeded and grown for 21 days). **C** The number of colonies in $5mm^2$ was highly significantly higher for the A549 J5-1 when compared to the parental A549 (12 squares were counted). **D** Counting the colonies of different size showed a highly significant increase of the number for the colonies that were of big and intermediate size, respectively, while the difference looking at the colonies that were of small size revealed in a slight, but significant increase in the number.

3.4.2 Expression levels of GATA4 and GATA6 in A549 J5-1

To have a more quantitative indicator for GATA4 and GATA6 expression in A549 J5-1 compared to A549, qPCR-analysis was performed using primers specific for human *GATA4* and *GATA6* as well as for the GATA4-target gene *mucin2* (van der Sluis et al., 2004) and for *chicken c-Myc*. As shown in Figure 3-12 A a 4-fold increase of *GATA4* mRNA levels could be shown with high significance. As observed by immunocytochemistry, the mRNA levels of *GATA6* were also highly significantly increased about 2-fold (Figure 3-12 B). Furthermore, when qPCR was performed with primers specific for the GATA4-target gene *mucin2*, an about 10-fold, highly significant increase was observed in the mRNA level (Figure 3-12 C) showing, that the detected GATA4 protein is nuclear. The exogenous chicken c-Myc in A549 J5-1 served as a positive control for this experiment. As shown in Figure 3-12 D, significantly higher levels of *chicken c-Myc* mRNA levels could be detected in the clone A549 J5-1 when compared to the parental cell line A549. These results confirm the expected elevated expression levels of *chicken c-Myc*, *GATA4*, *GATA6* and *mucin2*.

3.4.3 Expression of neuroendocrine markers in the A549 J5-1 cells

Since in the analysis of total lung RNA of wildtype, SpC-C-Raf-BxB single transgenic and SpC-C-Raf-BxB/SpC-c-Myc compound animals the only highly significantly upregulated gene was the *SNCA* and the expression of the immature neuroendocrine marker PGP9.5 was observed in the vasculature of columnar tumours of the SpC-c-Myc single transgenic and of the SpC-C-Raf-BxB/SpC-c-Myc compound mice (Rapp et al., 2009), qPCR-analysis was performed to check the expression levels of more neuroendocrine markers. Tumours with neuroendocrine character arise from neural crest-derived neuroendocrine pulmonary cells, but usually not from the alveolar type II pneumocytes (Borczuk and Powell, 2007). As already described for the total lung RNA of compound animals (Figure 3-8 C) highly significantly

increased mRNA levels were observed for *SNCA* and *PGP9.5* specific primers in the
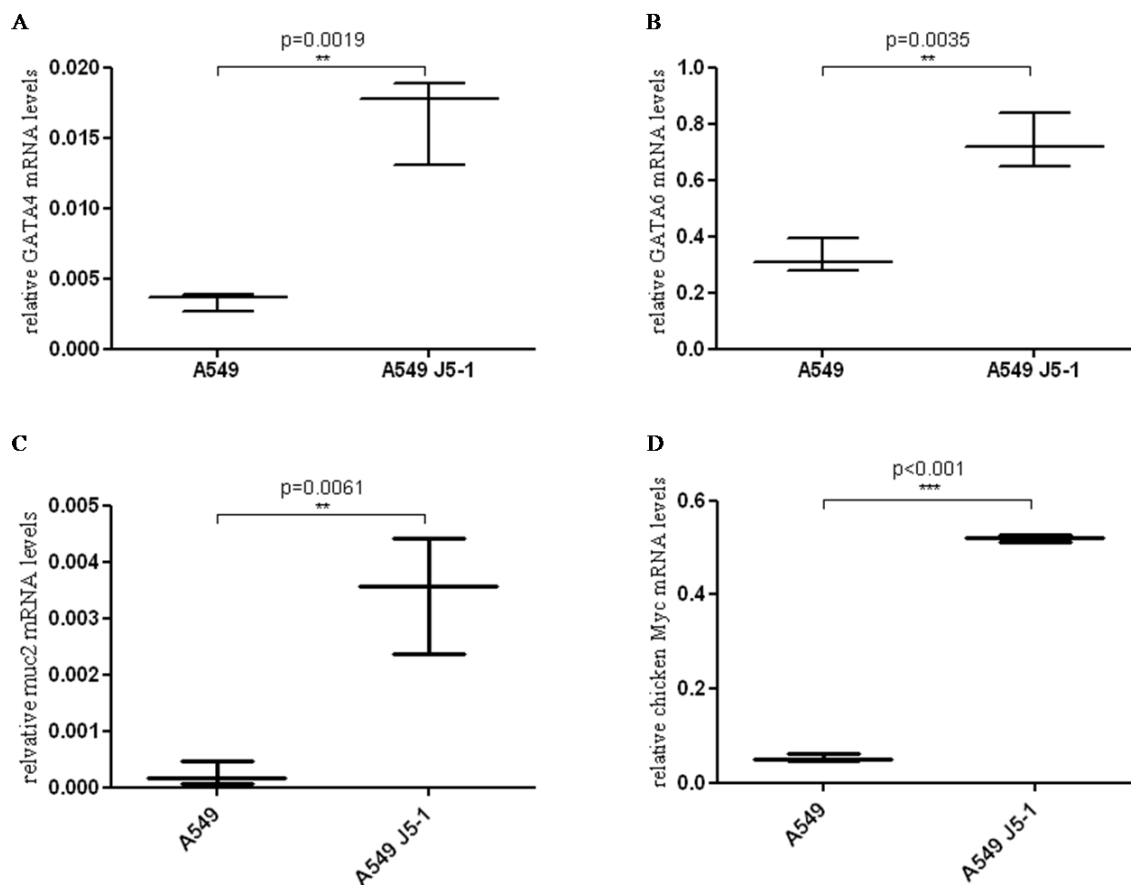

Figure 3-12 qPCR analysis of the clone A549 J5-1 compared to the parental A549 cell line. **A+B** qPCR with primers specific for *GATA4* and *GATA6* shows that there is a highly significant about 4-fold and 2-fold, respectively, increase in the relative GATA4 and GATA6 mRNA levels in the J5-1 clone. **C** Using primers specific for the GATA4 target gene *mucin2* shows an about 10-fold increase of the relative mRNA levels mucin2. **D** Performing qPCR using primers specific for chicken c-Myc shows a highly significant difference in the expression of the oncogene.

chicken c-Myc expressing cells A549 J5-1 when compared to the parental cell line A549

(Figure 3-13 A+B). Furthermore, significantly increased mRNA levels were observed for the

neuroendocrine marker and Wnt-signalling target (Kuwabara et al., 2009) *NeuroD1* and the

neuroendocrine marker *Synaptobrevin* in the A549 J5-1 cells when compared to the parental

A549 cell line (Figure 3-13 C+D). In contrast to the other three assayed neuroendocrine

markers, qPCR-analysis with primers specific for the neuroendocrine-specific Enolase,

Enolaseγ, showed a highly significant downregulation of this neuroendocrine enzyme upon

expression of chicken c-Myc when compared to the parental A549 cell line (Figure 3-13 E).

These data confirm the induction of *SNCA* and *PGP9.5* by the expression of c-*Myc*, but show

that c-Myc does not induce a full neuroendocrine character of the tumours.
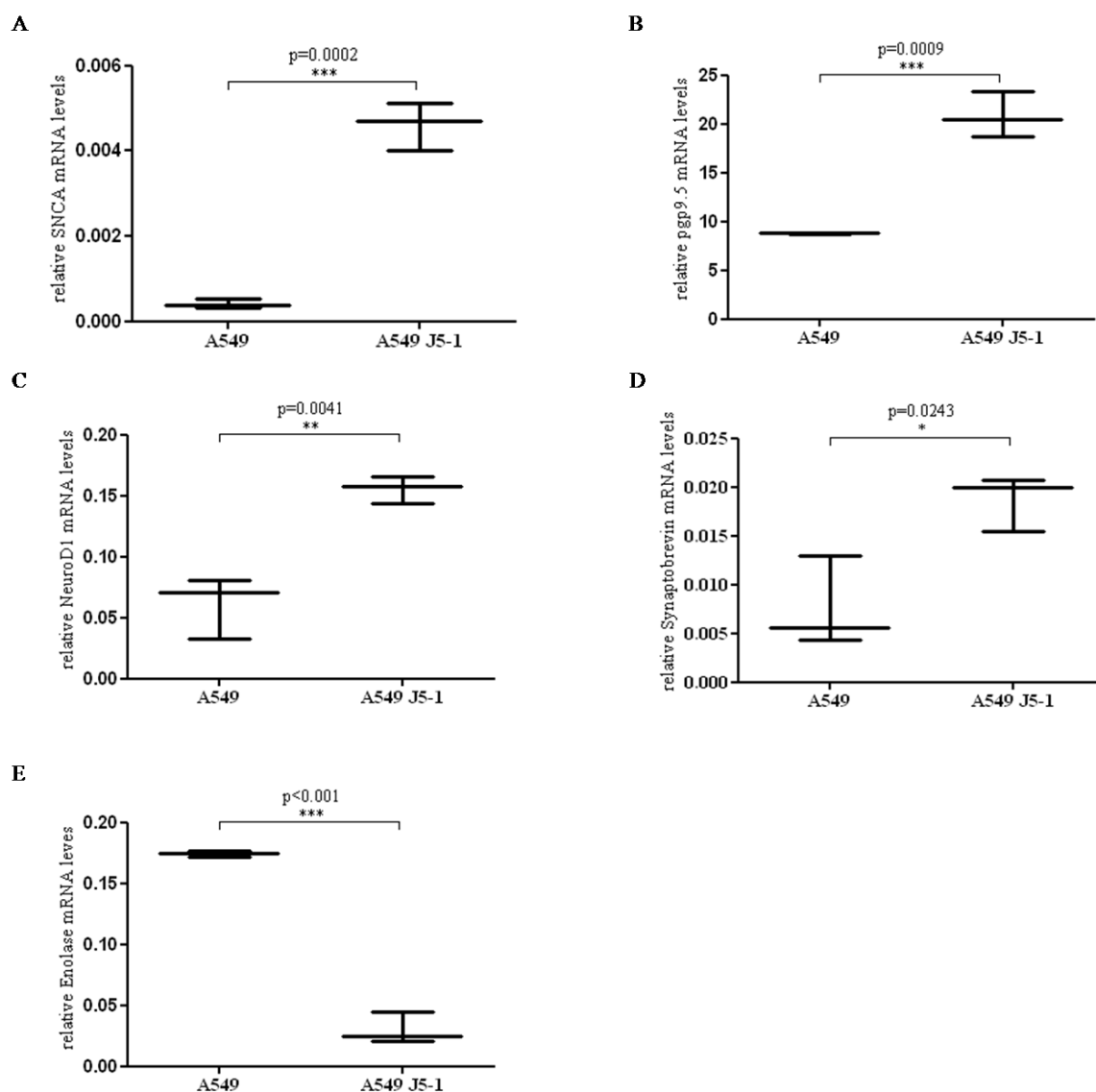
Figure 3-13 qPCR analysis of the expression of neuroendocrine markers in the A549 J5-1 cells compared to the parental A549 cell line. **A** qPCR with primers specific for the neuroendocrine marker *SNCA* shows a highly significant 5-fold increase in mRNA levels of this gene in the presence of chicken c-Myc. **B** qPCR with primers specific for the immature neuroendocrine marker *PGP9.5* shows a highly significant 2-fold increase in mRNA levels of this gene in the presence of chicken c-Myc. **C** qPCR with primers specific for the neuroendocrine marker *NeuroD1* shows a highly significant 3-fold increase in mRNA levels of this gene in the presence of chicken c-Myc. **D** The relative mRNA levels of the neuroendocrine marker *Synaptobrevin* were significantly higher in the A549 J5-1 cells when compared to the parental A549 cells. **E** qPCR with primers specific for the immature neuroendocrine marker *Enolaseγ* shows a highly significant 4-fold decrease in mRNA levels of this gene in the presence of chicken c-Myc.

3.4.4   Transplantation of A549 J5-1 in Rag1$^{-/-}$-mice

If the expression of c-Myc is sufficient to induce metastasis, the transplantation of a chicken c-Myc expressing clone of the human non-metastatic NSCLC cell line A549 in immunodeficient animals should give rise to metastasis. To test this possibility, Hildegard Troll and Fatih Ceteci injected 10^6 A549 and A549 J5-1 cells, respectively, subcutaneously in Rag1$^{-/-}$ animals. As shown in Figure 3-14 A, the tumour incidence in the animals injected with the chicken c-Myc expressing A549 J5-1 cells was higher than in the mice transplanted with
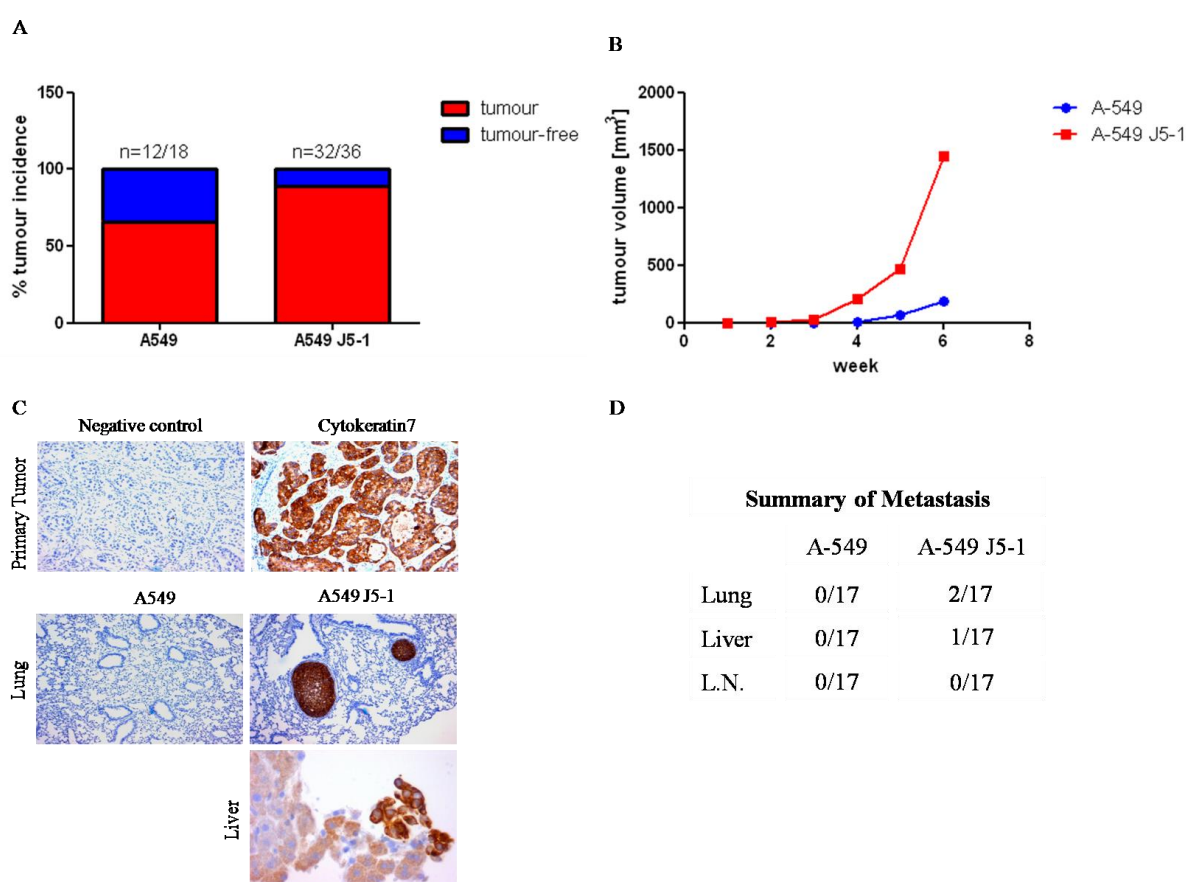
Figure 3-14 Transplantation of A549 and A549 J5-1 cells, respectively, in Rag$^{-/-}$-mice. **A** The tumour incidence in A549 J5-1 injected animals was higher than in the mice injected with the parental A549 cell line. **B** The tumour growth in the animals injected with the chicken c-Myc expressing cells was accelerated when compared with the mice injected with the parental cell line. **C** Staining for the human Cytokeratin7 showed positive cells in the primary tumour and in lung and liver of animals injected with the A549 J5-1 cells. **D** Metastasis after screening of the organs for Cytokeratin7-positive cells were detected in 2 lungs and 1 liver of mice injected with A549 J5-1, but in no organ of animals injected with the parental cell line A549.

the parental cell line A549. Furthermore, accelerated tumour growth was observed in the

A549 J5-1 transplanted animals when compared to the animals injected with the control cells

(Figure 3-14 B). The tumours consisting of the A549 J5-1 cells were growing so fast, that the animals had to be sacrificed as soon as six weeks after transplantation to not exceed the allowed 2cm of tumour size. After sacrification the lungs, livers and lymphnodes of the transplanted animals were screened for expression of the human specific cytokeratin7 to be able detect the human A549 cells in any organ. The transplanted primary tumours were all positive for cytokeratin7 and in two lungs and one liver of the animals injected with A549 J5-1 cells human cells could be observed (Figure 3-14 C). All in all in two lungs and one liver of the mice transplanted with A549 J5-1 cells, human cells could be detected by the cytokeratin7 staining, while in the organs isolated from mice transplanted with the control parental cell line A549 no cytokeratin7-positive cells could be detected (Figure 3-14 C). These results show that c-Myc is sufficient to induce metastases in the human NSCLC cell line A549.

3.4.5 shRNA-mediated GATA4 knockdown inhibits the ability of anchorage-independent growth in A549 J5-1

To test the role of the consistently upregulated marker GATA4 upon c-Myc-expression in the SpC-c-Myc single transgenic and in the SpC-C-Raf-BxB/SpC-c-Myc compound tumours and in the human NSCLC cell line A549 in the induction of metastasis, we performed an shRNA-mediated knockdown of GATA4 in the A549 J5-1 cells. For this the cells were infected with 5 different shRNA-producing viruses (sh24-sh28) and qPCR-analysis for the expression of the GATA4-target gene *mucin2* was performed. As shown in Figure 3-15 A, the mRNA levels of *mucin2* was significantly higher in A549 J5-1 cells when compared to the parental cell line A549. Only the A549 J5-1 cells infected with the shRNA25 producing virus did not have elevated levels of the GATA4-target gene *mucin2* indicating an efficient knock down of the

transcription factor GATA4. When a soft agar assay was performed to test the ability of
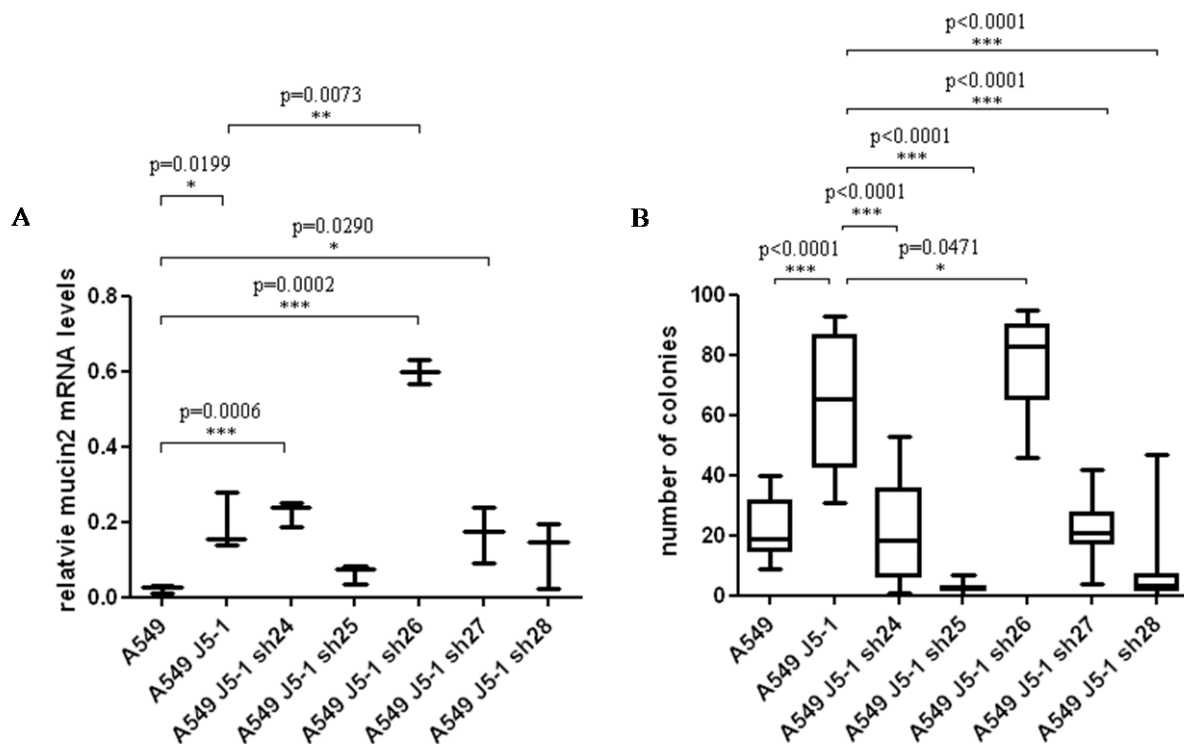
Figure 3-15 shRNA-mediated knockdown of GATA4 in A549 J5-1. **A** qPCR-analysis for the GATA4-target gene *mucin2* showed a significant upregulation of its expression in A549 J5-1. The only shRNA that efficiently knocked down the expression of the GATA4 target gene *mucin2* was the sh25. **B** The soft agar assay with the A549 J5-1 cells showed a highly significantly reduction in the number of colonies in the A549 J5-1 cells infected with the shRNA25-expressing virus.

anchorage-independent growth of the cells, the A549 J5-1 cells infected with the virus

producing the shRNA25 did hardly form any colonies (Figure 3-15 B). These data suggest

that the expression of GATA4 is necessary for the induction of anchorage-independent

growth by c-Myc.

3.4.6   Induction of DNA-demethylation upon c-Myc-expression

The regulatory significance of epigenetic regulation of upstream and downstream genes of a

single transcription factor has been shown to occur in the GATA gene family of transcription

proteins in lung cancer cell lines, where the promoter-hypermethylation correlated with gene-

silencing (Guo et al., 2004). To test the possibility of the induction of genes that are involved

in DNA-demethylation by c-Myc, qPCR-analysis was performed using primers specific for

GADD45α, β and *γ. GADD45* genes are stress inducible and function in many
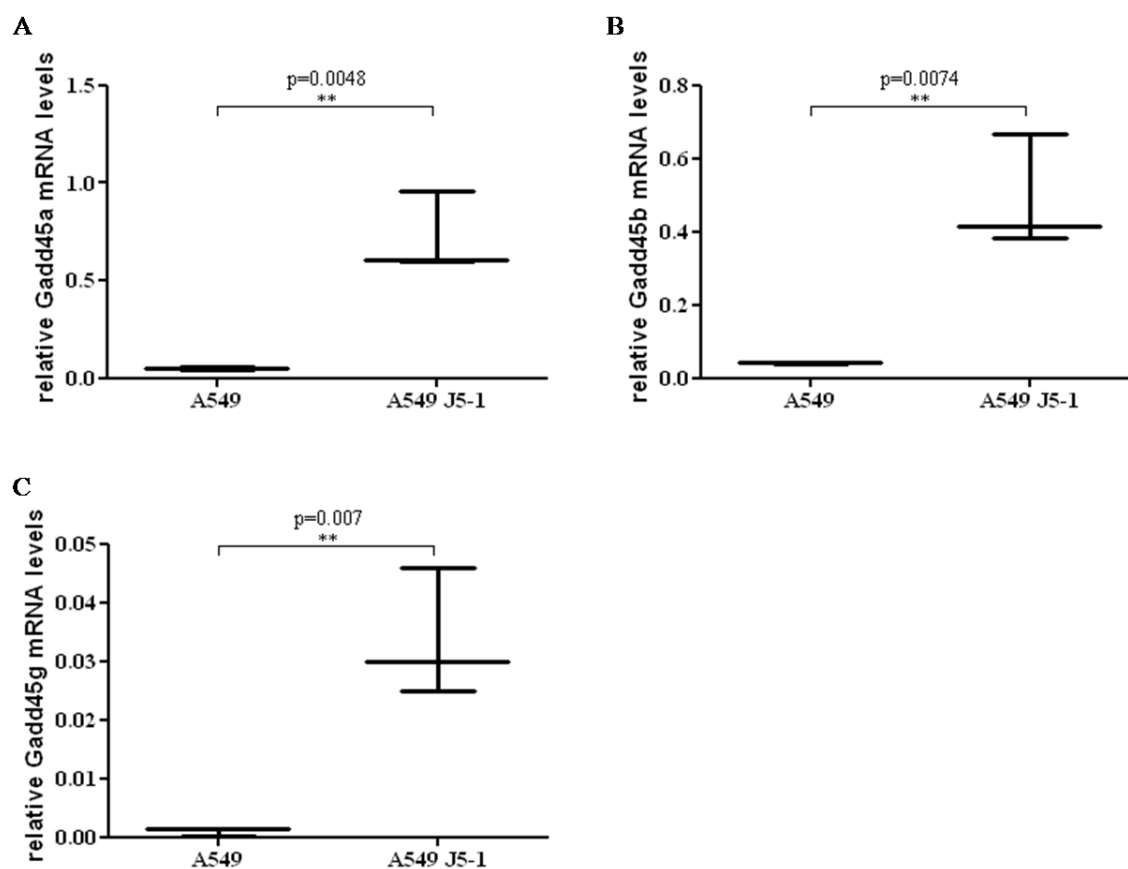
Figure 3-16 qPCR-analysis for expression levels of *GADD45* genes. **A** The mRNA levels of *GADD45α* were highly significantly increased in the A549 J5-1 cells when compared to the parental A549 cell line. **B** *GADD45β* expression levels were highly significant higher in the chicken c-Myc expressing cells when compared to the parental cell line. **C** *GADD45γ* expression was highly significantly elevated upon the expression of chicken c-Myc.

biological processes like the cell cycle, senescence, apoptosis and nucleotide excision repair.

GADD45α was shown to have a key role in active DNA demethylation and to promote global

DNA demethylation (Barreto et al., 2007). As shown in Figure 3-16 the expression levels of

all *GADD45* genes were increased in the chicken c-Myc expressing A549 J5-1 cells when

compared to the mRNA levels in the parental A549 cell line, suggesting an induction of

overall promoter-DNA-demethylation in the c-Myc-expressing cells.

Furthermore, qPCR-analysis was performed testing the expression levels of the *p53* gene

family, the products of which act upstream of the *GADD45* genes in the nucleotide excision

repair (Smith and Seo, 2002). The *p53* gene family has three members, the p53, p63 and p73,
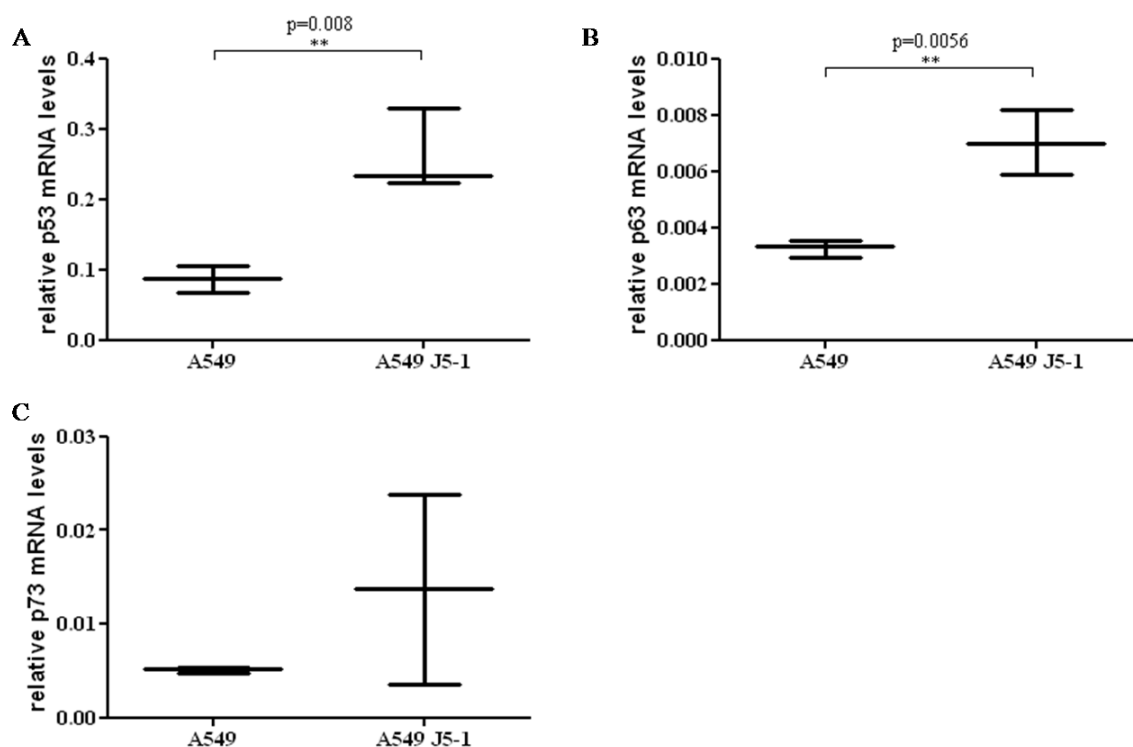
Figure 3-17 q-PCR-analysis for the expression levels of the *p53* family genes. **A** The mRNA levels of *p53* were highly significantly elevated in the A549 J5-1 cells when compared to the parental A549 cells. **B** *p63* expression was highly significantly induced by the expression of chicken c-Myc when compared to the parental A549 cell line. **C** No significant change in the relative mRNA levels of *p73* was observed in the A549 J5-1 cells when compared to the parental A549 cell line.

which are all transcription factors involved in development, differentiation and cell response

to stress (Bourdon, 2007). As shown in Figure 3-17, the relative mRNA levels of *p53* and *p63*

were highly significantly increased in the A549 J5-1 when compared to the parental cell line

A549, while there was no significant difference observed in the expression levels of *p73*.

These data suggest that in the NSCLC cell line A549 the expression of chicken c-Myc leads

to an upregulation of the expression of *p53* and *p63* and by this to an upregulation of the

GADD45 family genes.

3.4.7 Upregulation of angiogenesis markers in the chicken c-Myc expressing A549

Since c-Myc has been reported to induce angiogenesis (Knies-Bamforth et al., 2004) and in

tumours of the SpC-c-Myc single transgenic and SpC-C-Raf-BxB/SpC-c-Myc compound

animals a significant increase in blood and lymph vessels was observed (Rapp et al., 2009), immunocytochemistry for VEGF was performed. As shown in Figure 3-18 an induction of VEGF-expression was observed in the chicken c-Myc expressing A549 J5-1 cells when compared to the parental A549 cell line. These data together with the observation of VEGF-expression in the vessels of the tumours of the SpC-c-Myc single transgenic and the SpC-C-Raf-BxB/SpC-c-Myc compound animals suggest that c-Myc induces angiogenesis via upregulation of VEGF.
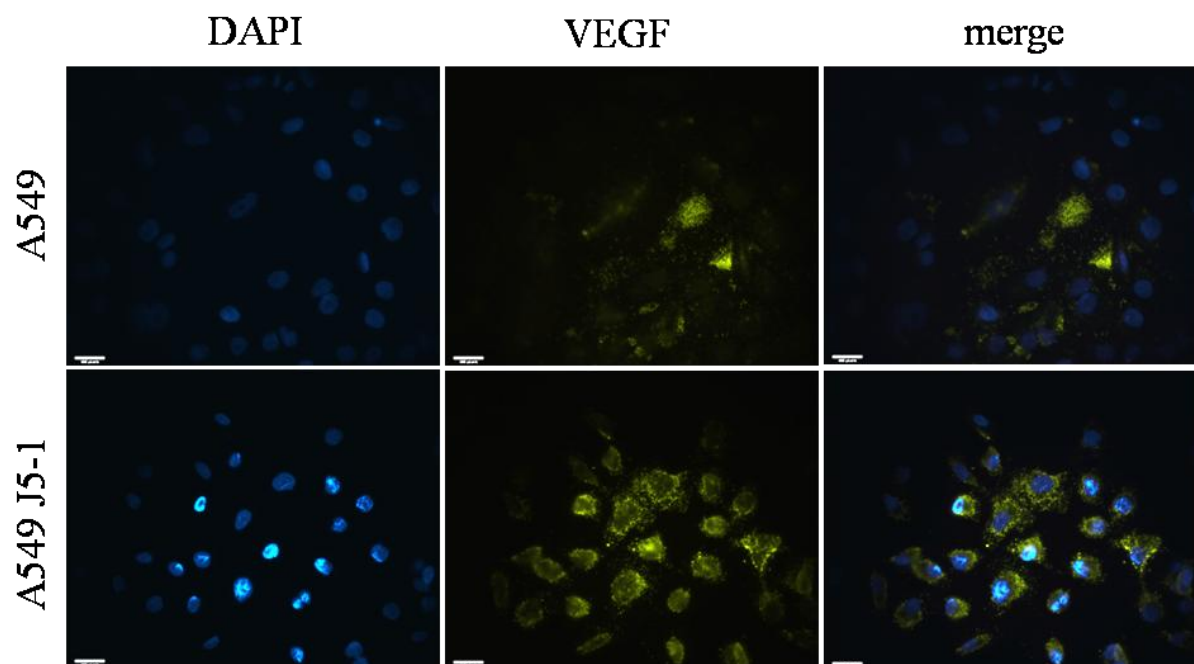
Figure 3-18 Immunocytochemistry for the angiogenesis marker VEGF shows that there is an upregulation of this protein in the chicken c-Myc expressing cells compared to the parental cell line.

3.4.8 Expression of the pluripotency genes *Klf4* and *Sox2* and the lung development gene *Sox9* in A549 J5-1 cells

To test the expression of markers involved in pluripotency, reprogramming and early lung development, qPCR-analysis was performed using primers for specific genes involved in these processes. Sox2 is a transcription factor that regulates embryonic stem cell pluripotency and is involved in lung development. Furthermore, it has been published, that Sox2 is expressed in NSCLC and neuroendocrine lung tumours (Sholl et al., 2009). Upon expression

of chicken c-Myc in the A549 cells, significantly elevated *Sox2* mRNA levels have been observed when compared to the parental A549 cells (Figure 3-19 A). The Krüppel-like factor 4 (Klf4) is a zinc-finger type transcription factor, that is important in
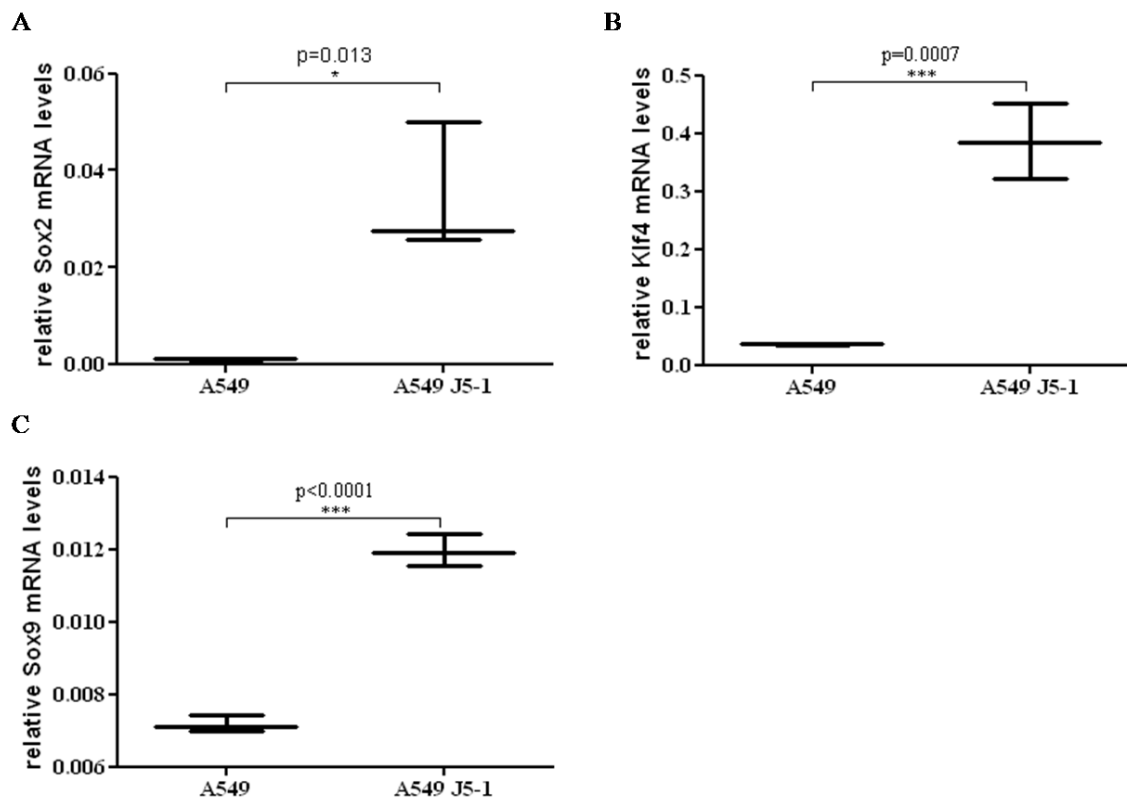
Figure 3-19 qPCR-analysis of the pluripotency genes *Klf4* and *Sox2* and the early lung development gene *Sox2*. **A** The relative mRNA levels of *Sox2* were significantly higher in the A549 J5-1 when compared to the parental A549 cells. **B** qPCR-analysis of the expression levels of *Klf4* showed a highly significant increase upon expression of chicken c-Myc. **C** The expression levels of *Sox9* were highly significantly higher in the A549 J5-1 cells when compared to the parental A549 cell line.

reprogramming differentiated fibroblasts into inducible pluripotent stem cells and is involved as an oncogene in many tumours (Evans and Liu, 2008). As shown in Figure 3-19 B the relative mRNA levels of *Klf4* were highly significantly higher in the chicken c-Myc expressing cells when compared to the parental A549 cell line. Sox9 is a transcription factor that is expressed at high levels during lung development (Perl et al., 2005). The relative mRNA levels of *Sox9* were highly significantly increased in the A549 J5-1 cells when compared to the parental A549 cells (Figure 3-19 C). These data suggest that the expression of c-Myc in the human NSCLC cell line induces the acquisition of progenitor cell features,

which was also observed in the SpC-c-Myc single transgenic and SpC-C-Raf-BxB/SpC-c-Myc compound animals (Rapp et al., 2009).

3.4.9 Upregulation of *tert* in A549 J5-1

Telomerase activation is observed in about 90% of human cancers, while most healthy tissues contain inactivated telomerase (Kim et al., 1994). Telomerase activation occurs after genomic instability in the early stages of carcinogenesis lead to telomere shortening and by this reduced cell survival. Telomerase activation induces genomic stability and assures cell
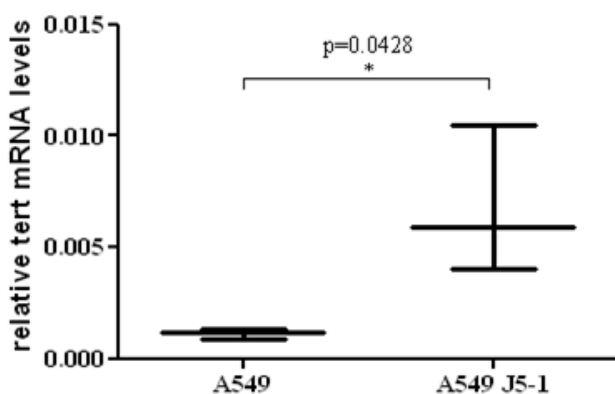
Figure 3-20 qPCR-analysis using primers specific for *telomerase*. The relative mRNA levels of *tert* are significantly higher in the A549 J5-1 when compared to the parental A549 cell line.

survival (Kim et al., 1994). Furthermore, it was published, that telomerase can be activated by c-Myc (Wang et al., 1998) and for this reason in the following qPCR-analysis was performed to test the expression levels of *telomerase* in the A549 J5-1 cells in comparison to the parental A549 cell line. As shown in Figure 3-20 the mRNA levels of *telomerase* were significantly higher in the chicken c-Myc expressing A549 J5-1 cells when compared to the parental A549 cell line.

3.4.10 Microarray analysis of chicken c-Myc expressing A549

To get an overall overview about the Myc-induced changes in the gene expression profile in the A549 cells, microarray analyses were performed including the RNA isolated from A549 and from A549 J5-1 cells. The microarray and the analysis of the data were done by Ellen

Leich, Institute for Pathology, University of Würzburg. In Figure 3-21 are shown the data oritinate from the analysis of differentially expressed tissue-specific genes. The lung-specific genes are only a small fraction of organ-specific genes being down- and upregulated after the expression of chicken c-Myc in the A549 cells, respectively (Figure 3-21 A). Figure 3-21 B it is shown that the number of genes accounting for organ identity that is downregulated by the expression of chicken c-Myc in the A549 cells is about fivefold higher than the number of genes accounting for organ identity that is upregulated by the expression of chicken c-Myc in the A549 cells. This observation indicates that the expression of c-Myc in NSCLC cells at least partially leads to the loss of organ identity.
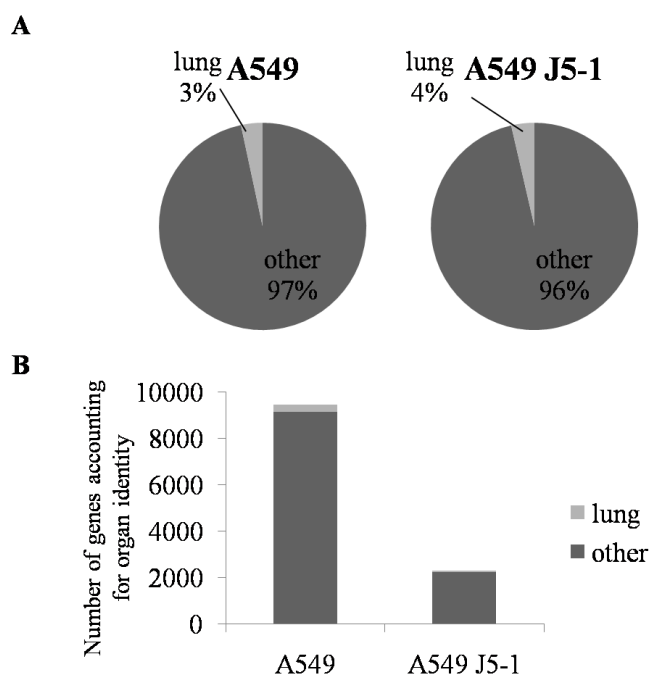
Figure 3-21 Expression of tissue-specificity genes in A549 and A549 J5-1. **A** The fraction of lung-specific genes of all genes down- and upregulated upon the expression of c-Myc in the A549 cells. B The number of down- and upregulated genes upon c-Myc-expression accounting for organ identity.

Furthermore, the differentially expressed genes in A549 versus A549 J5-1 were assigned to biological processes. In Figure 3-22 are shown the biological processes that are significantly different in A549 and A549 J5-1. Not surprisingly, the observed differences included biological processes that are known to be influenced by Myc, like signal transduction, cell differentiation, cell proliferation and cell growth, but also processes involved in metastasis,

like cell motility, cell morphology, localization of the cell, inflammatory response, chemotaxis and taxis. Interestingly, cellular processes that are involved in imprinting were also changed significantly upon c-Myc-expression in the A549 cells.
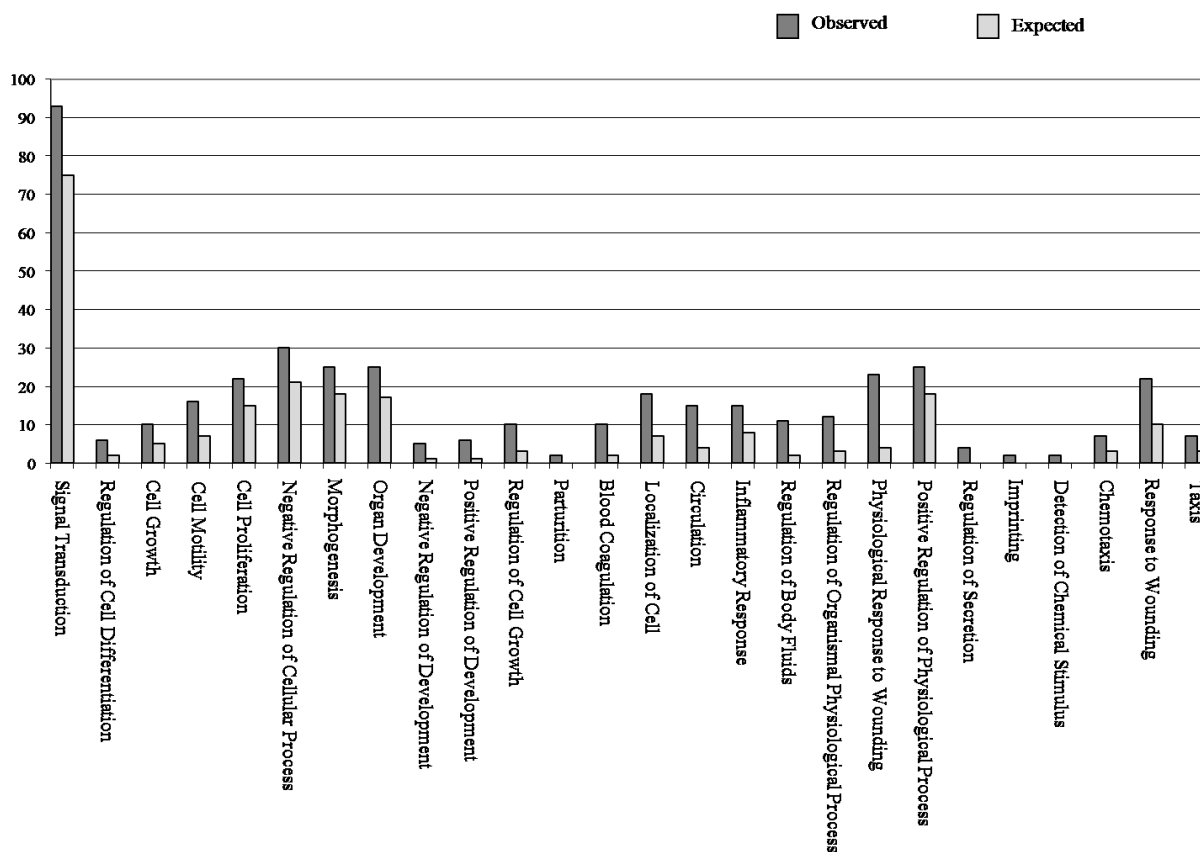
Figure 3-22 Gene ontology analysis for biological processes (Ashburner et al., 2000) for the genes differentially expressed in A549 and A549 J5-1. Shown are only the significantly different biological processes, p<0.05 by hypergeometric test.

In regard to signal transduction the differentially expressed genes were assigned to specific pathways. In Table 3-4 are shown the ten most significantly enriched curated gene sets from pathway analysis of the genes upregulated in A549 J5-1. In Table 3-5 the ten most significantly enriched curated gene sets highlighted by pathway analysis of the genes downregulated in A549 J5-1 are listed. Not surprisingly, the most significant hit in the analysis of the genesets upregulated in the A549 J5-1 cells was the Myc oncogenic signature and on the third position of this analysis one can find the Myc-targets that were identified by ChIP analysis in diverse cell lines (Fernandez et al., 2003), supporting the authenticity of the

analysis tool used and the quality of the array data. The knockdown of KRas in A549 was

shown to upregulated a specific set of genes (Sweet-Cordero et al., 2006), which was among

the most significantly downregulated gene sets in the A549 J5-1, indicating a stimulation of

A

Curated Pathways_GSEA	Genes that account for enrichment	P-Value
MYC_ONCOGENIC_SIGNATURE	RABEPK; SLC19A1; HK2; DUSP2; MYBBP1A; SLC6A15 C16ORF14	4.39E-04
BRCA1_OVEREXP_DN	RABEPK; SLC19A1; GAL; BOP1; SLC7A5; CCDC85B	7.86E-04
FERNANDEZ_MYC_TARGETS	GAL; ID2; WT1; TERT; MAGEA3; SLC19A1	1.06E-03
ADDYA_K562_HEMIN_TREATMENT	ID2; APOC1; TXNIP; HBA1	1.27E-03
BAF57_BT549_DN	HK2; GAL; PPIF; TLE4; SLCO4A1; LOC129293; C12ORF24; ADAMTS1	1.35E-03
IRINOTECAN_PATHWAY_PHARMGKB	BCHE; CYP3A4	2.25E-03
ZHAN_MULTIPLE_MYELOMA_VS_NORMAL_DN	APOC1; WNT10B; GLDC	2.51E-03
SARCOMAS_GISTROMAL_UP	BCHE; GUCY1A3	2.68E-03
WELCSH_BRCA_DN	SLC19A1; BOP1	3.15E-03
PENG_RAPAMYCIN_DN	SLC7A5; ID2; PPIF; WNT10B; CYCS; P2RX5	3.35E-03

B

Curated Pathways_GSEA	Pathway description
MYC_ONCOGENIC_SIGNATURE	Genes selected in supervised analyses to discriminate cells expressing c-Myc oncogene from control cells expressing GFP.
BRCA1_OVEREXP_DN	Downregulated by induction of exogenous BRCA1 in EcR-293 cells
FERNANDEZ_MYC_TARGETS	MYC target genes by ChIP in U-937,HL60 (leukemia),P493 (B-cell),T98G (glioblastoma),WS1 (fibroblast)
ADDYA_K562_HEMIN_TREATMENT	Selected differentially expressed genes in K562 cells after hemin treatment
BAF57_BT549_DN	Down-regulated following stable re-expression of BAF57 in Bt549 breast cancer cells that lack functional BAF57
IRINOTECAN_PATHWAY_PHARMGKB	
ZHAN_MULTIPLE_MYELOMA_VS_NORMAL_DN	The 50 most significantly down-regulated genes in MM in comparison with normal bone marrow PCs
SARCOMAS_GISTROMAL_UP	Top 20 positive significant genes associated with GI stromal tumors, versus other soft-tissue tumors.
WELCSH_BRCA_DN	Genes downregulated by BRCA1
PENG_RAPAMYCIN_DN	Genes downregulated in response to rapamycin starvation

Table 3-4 A GSEA annotation for curated gene sets upregulated in A549 J5-1 (Xie et al., 2005), (Subramanian et al., 2005). Annotations were performed using genes that were at least 1.5 times differentially expressed between the two phenotypes A549 and A549 J5-1. B description of the in A listed pathways.

the mitogenic cascade upon Myc-expression. Furthermore, the pathway analysis of the A549

J5-1 suggests a downregulation of the breast cancer associated tumour supressor gene *BRCA1*

since two of the ten most significantly upregulated gene sets upregulated in A549 J5-1 include genes that are downregulated by this tumour supressor. Interestingly, among the gene sets that were downregulated upon c-Myc-expression in the A549 cells, were genes that are specifically upregulated during the ageing process of the kidney and liver, indicating a more differentiated status of the A549 cells when compared to the A549 J5-1 cells.

In Table 3-6 are shown the ten most significant hits for transcription factor binding motif gene sets that were upregulated in the A549 J5-1 cells, in Table 3-6 the ten most significant hits for transcription factor binding motif gene sets that were downregulated in the A549 upon c-Myc-expression. An interesting gene set that was upregulated in the A549 J5-1 contains a binding site for the Myc-associated zinc-finger protein MAZ, which binds in the promoter region of Myc regulating transcription initiation as well as termination (Bossone et al., 1992). These data are consistent with negative autoregulation of endogenous Myc that regulates its own transcription (Cleveland et al., 1988; Goodliffe et al., 2005). On the other hand, among the gene sets identified to be downregulated in the A549 J5-1 cells were the genes containing a binding site for Myc itself, suggesting a negative feedback regulation of Myc-target genes upon their induction by Myc. Furthermore, gene sets have been identified in the analysis of transcription factor binding motifs to be upregulated in A549 J5-1 cells that are regulated by the mitogenic cascade, indicated by the gene set containing a binding site for the transcription factor Ets2, which is regulated transcriptionally and posttranscriptionally by the mitogenic cascade and inhibits apoptosis via induction of the transcription of the anti-apoptotic Bcl-XL (Yordy and Muise-Helmericks, 2000). The downregulation of gene sets that contain a binding motif for the E4F1 transcription factor, which induces cell cycle arrest via interaction with the tumour suppressors p14[ARF] and p53 (Le Cam et al., 2006), upon c-Myc-expression in the A549 cells on the other hand supports the induction of cell cycle progression genes by Myc-expression. Additionally, genes containing a binding site for Sp1 and for NFATc, which

A

Curated Pathways_GSEA	Genes that account for enrichment	P-Value
BAF57_BT549_UP	FN1; COL15A1; C1S; COL5A1; COL1A1; RARRES1; PGM2L1; COL6A3; MAP3K8; GNG2; SRPX; MATN2; CFI; C8ORF4; KIAA1462; NRIP1; GALNT12; SDC2; MMP2; IRS1; STEAP1; TGFB2; LBH; MARCKS; CA12 ITGB8; IGFBP4; POSTN; ABCA1; INHBB; BTBD11; KLRC2; CGNL1; LMCD1; ZBTB1; BOC; FLJ14213; HMCN1	8.32E-23
AGEING_KIDNEY_SPECIFIC_UP	FN1; COL15A1; C1S; COL5A1; COL1A1; RARRES1 PGM2L1; COL6A3; SERPINE2; FBN1; TPM1; FGG; C1R; STS; NRP1; HGF; PROM1; PXDN; NFKBIZ; RBMS3; MMP7; SYTL2; NOV; C11ORF9; RAB34; MGLL; ABCC3; PKIB; BICC1; DCDC2	2.92E-18
AGEING_KIDNEY_UP	FN1; COL15A1; C1S; COL5A1; COL1A1; RARRES1 PGM2L1; MAP3K8; GNG2; SERPINE2; FBN1; TPM1; FGG; C1R; STS; NRP1; HGF; PROM1; PXDN; NFKBIZ RBMS3; MMP7; SYTL2; NOV; C11ORF9; RAB34; CUGBP2 CXCL1; CD14; PTPRE; SPON2; SAMD9; CD38; ST8SIA4; SHANK2; C4ORF18; APBB1IP; ARL4C; QPCT; DOCK11	3.01E-16
BOQUEST_CD31PLUS_VS_CD31MINUS_UP	FN1 ; COL15A1 ; MAP3K8 SRPX ; MATN2 ; CFI ; C8ORF4 ; KIAA1462 ; NRIP1 SERPINE2 ; CUGBP2 ; CXCL1 ; CD14 ; PTPRE ; RNASE4 ; CES1 ; CFH ; WNT5A ; SOX4 ; AGTR1 ; SEPP1 ; THBS1 ; IL15 ; SLC2A3 ; RGS2 ; NEDD9 ; PTGER2; IL8; CXCR7; MAST4; CTSS; PFKFB3; TLR3; LMO7 ; SLC1A1 PDLIM5; TNFSF10; PGCP ; PTPRM; TSPAN7; ANGPTL4 MTUS1; DKK1; CTSH; MICAL2; FRMD4B; GPR64 ; CYP26B1 ; SCG5 ; GREM1 ; DOK5	3.05E-16
BOQUEST_CD31PLUS_VS_CD31MINUS_DN	FN1 ; C1S ; COL5A1 ; COL1A1; COL6A3; SRPX GALNT12 ; SDC2 ; MMP2; IRS1; STEAP1; SERPINE2 FBN1; CUGBP2; SPON2; RNASE4 ; CES1 ; CFH WNT5A ; IGFBP3 ; ALDH1A1; HNMT; SPOCK1; TMEM45A COL5A2; PCDH9; PLA2G4A; ITGBL1; SETBP1; CRISPLD2	2.23E-13
CORDERO_KRAS_KD_VS_CONTROL_UP	C1S; COL5A1; COL1A1; MAP3K8; MATN2; TGFB2; LBH; SERPINE2; TPM1; SOX4; IGFBP3; HGD; IGFBP7; MYL9; SLC16A4; NCF2; DKK3	1.13E-12
HSIAO_LIVER_SPECIFIC_GENES	FN1; C1S; CFI; FGG; C1R; RNASE4; CES1; AGTR1; SEPP1; ALDH1A1; HNMT; HGD; DAB2; IGFBP1; CP APOH; F5; FGB; FGA; FGL1; ITIH2; CFHR1	1.14E-08
TAKEDA_NUP8_HOXA9_10D_UP	FN1; CFI; GALNT12; SERPINE2; STS; SAMD9 CD38; SOX4; THBS1; IL15; ALDH1A1; SPOCK1; TMEM45A; PTGS2; RBPMS; HPGD; GBP1; OAS1	7.54E-08
RUTELLA_HEMATOGFSNDCS_DIFF	C1S; RARRES1; SDC2; MMP2; MARCKS; STS; NRP1 MGLL; ABCC3; CUGBP2; CXCL1; CD14; RNASE4; CES1; SLC2A3 ; RGS2; NEDD9 ; PTGER2 ; SPOCK1; IGFBP7; DAB2 ; CCNG2; OPTN; CTSD; SLC7A7; LXN; F2RL1; CXCL5; NAT1; FKBP1B; NRG1; KMO; FLJ10357; CSF2RA; MYO15B; RAB20	9.05E-08
HYPOXIA_REVIEW	COL5A1; CA12; HGF; SLC2A3; IL8; IGFBP3; IGFBP1; CP; PTGS2; CCNG2; IGF2; EDN1	9.25E-08

B

Curated Pathways_GSEA	Pathway description
BAF57_BT549_UP	Up-regulated following stable re-expression of BAF57 in Bt549 breast cancer cells that lack functional BAF57
AGEING_KIDNEY_SPECIFIC_UP	Up-regulation is associated with increasing age in normal human kidney tissue from 74 patients, and expression is higher in kidney than in whole blood
AGEING_KIDNEY_UP	Up-regulation is associated with increasing age in normal human kidney tissue from 74 patients
BOQUEST_CD31PLUS_VS_CD31MINUS_UP	Genes overexpressed 3-fold or more in freshly isolated CD31+ versus freshly isolated CD31- cells
BOQUEST_CD31PLUS_VS_CD31MINUS_DN	Genes overexpressed 3-fold or more in freshly isolated CD31- versus freshly isolated CD31+ cells
CORDERO_KRAS_KD_VS_CONTROL_UP	Genes upregulated in kras knockdown vs control in A549 cells
HSIAO_LIVER_SPECIFIC_GENES	Liver selective genes
TAKEDA_NUP8_HOXA9_10D_UP	Effect of NUP98-HOXA9 on gene transcription at 10 d after transduction UP
RUTELLA_HEMATOGFSNDCS_DIFF	The 672 significantly changing genes
HYPOXIA_REVIEW	Genes known to be induced by hypoxia

Table 3-5 A GSEA annotation for curated gene sets upregulated in A549 (Xie et al., 2005), (Subramanian et al., 2005). Annotations were performed using genes that were at least 1.5 times differentially expressed between the two phenotypes A549 and A549 J5-1. B description of the in A listed pathways.

induce and are induced by VEGF, respectively, and by this have both been reported to promote tumour angiogenesis (Kulkarni et al., 2009; Song et al., 2009), were among the most significantly upregulated gene sets in the A549 J5-1, reflecting the induction of angiogenesis by Myc. Surprisingly, the Sp1-target genes were also upon the most significant gene sets

A

Motif Geneset_GSEA	Genes that account for enrichment	P-Value
GGGCGGR_V$SP1_Q6	WT1; TLE4; MAZ; POLR3G; ID4; COL4A6; PRDM13; TRIM14; CBX5; SLC6A15; OIP5; GNG4; PTGES2; GLDC	7.85E-04
CAGGTG_V$E12_Q6	WT1; TLE4; MAZ; POLR3; CXORF;15 HES6; NRCAM; ANKRD2; WNT10B; P2RX5; GUCY1A3	1.16E-03
TGGAAA_V$NFAT_Q4_01	ID4; COL4A6; DLX1; FLI1; PDE3B; ID2; CCL5	1.39E-03
CTTTGT_V$LEF1_Q2	PRDM13; CXORF15; HES6; NRCAM; DLX1; PTPRG; OSBPL6; BCHE	2.18E-03
GGGAGGRR_V$MAZ_Q6	WT1; ID4; COL4A6; PRDM13; ANKRD; DLX1; FLI1; PTPRG; DAPP1; HRK; ADAMTS1	4.37E-03
RYTTCCTG_V$ETS2_B	PTPRG; DAPP1; PPIF	5.51E-03
V$CEBPGAMMA_Q6	ID4; PRDM13; DLX1; FLI1; PTPRG; G0S2; CYCS	7.03E-03
TGACCTY_V$ERR1_Q2	DLX1; G0S2; PRRX2	7.61E-03
TTGTTT_V$FOXO4_01	ID4; COL4A6; PRDM13; TRIM14; CXORF15; DLX1; FLI1; PDE3B; ID2; TXNIP; UGT8	1.08E-02
CAGCTG_V$AP4_Q5	TLE4; PRDM13; HES6; WNT10B; P2RX5; DLX1; HIST1H2BF	1.41E-02

B

Motif Geneset_GSEA	Genes with promoter regions [-2kb,2kb] around transcription start site containing the motif
GGGCGGR_V$SP1_Q6	CTTTGT which matches annotation for LEF1: lymphoid enhancer-binding factor 1
CAGGTG_V$E12_Q6	CAGGTG which matches annotation for TCF3: transcription factor 3
TGGAAA_V$NFAT_Q4_01	NNNGNCAGTTN which matches annotation for MYB: v-myb
CTTTGT_V$LEF1_Q2	GGGCGGR which matches annotation for SP1: Sp1 transcription factor
GGGAGGRR_V$MAZ_Q6	TWTTTAATTGGTT which matches annotation for NKX6-1: NK6
RYTTCCTG_V$ETS2_B	ANCAATCAW which matches annotation for PBX1: pre-B-cell leukemia transcription factor 1
V$CEBPGAMMA_Q6	CTBATTTCARAAW which matches annotation for CEBPG: CCAAT/enhancer binding protein (C/EBP), gamma
TGACCTY_V$ERR1_Q2	CACGTGS which matches annotation for MYC: v-myc myelocytomatosis viral oncogene homolog (avian)
TTGTTT_V$FOXO4_01	CAGCTG which matches annotation for REPIN1: replication initiator 1
CAGCTG_V$AP4_Q5	NTGCGTGGGCGK which matches annotation for EGR3: early growth response 3

Table 3-6 A GSEA annotation for motif gene sets higher expressed in A549 J5-1 (Subramanian et al., 2005). Annotations were performed using genes that were at least 1.5 times differentially expressed between the two phenotypes A549 and A549 J5-1. B description of the in A listed motifs.

identified to be downregulated in the A549 J5-1 cells, suggesting that the presence and absence of Myc can both activate the same transcription factors, but resulting in different sets of target genes. As many as four transcription factors identified in the transcription factor

A

Motif Geneset_GSEA	Genes that account for enrichment	P-Value
SCGGAAGY_V$ELK1_02	TRIM46; PDE5A; CLMN; SHANK2; INSIG2	3.64E-11
GGGCGGR_V$SP1_Q6	TRIM46; PDE5A; NDN; RAB3IP; WNT5A; ALS2CR8; BMP4; ABCA1; PFKFB3; KCNJ2; COL1A1; SOX4; ARHGAP26 DLG3; MARCKS; CYP26B1; CCNG2; AXIN2; CYP24A1;CPNE4; TCEA3; ITGB8; RASSF2; TGFB1I1; NRP2; SERPINI1; IGF2; THBS3; MYH10; GPR37; MLLT3; PPARA; HPGD; PLCB1; HAS2; BAMBI; ITGBL1; POLD4; MAML2; SLC16A2; ENO2; NEDD9; CNTN1; RAB34; IGFBP7; MUC1; DSC2; MAOB; OPTN; ABCC3; MLPH	1.45E-06
RCGCANGCGY_V$NRF1_Q6	NDN; RAB3IP; WNT5A; ALS2CR8; NBEA; VAV3; SGCB	1.86E-06
CACGTG_V$MYC_Q2	TRIM46; BMP4; ABCA1; PFKFB3; TGFB2; FXYD2; PLA2G4A; MTUS1; MICAL2; ARMCX2	6.74E-06
MGGAAGTG_V$GABP_B	CLMN; NDN; BMP4; PCDH7; PKIB; CTSS; AGPAT4	9.14E-05
GTGACGY_V$E4F1_Q6	TGFB2; PCDH7; PKIB; LTBP1; CRH; WSB1; CHGB	6.51E-04
GATTGGY_V$NFY_Q6_01	BMP4; KCNJ2; COL1A1; SOX4; ARHGAP26; DLG3; MARCKS; CYP26B1; CCNG2 L;TBP1; ANK3; FGD4; GCA; CDH6; PCDH9; IRS1; MMD; SORT1	8.24E-04
V$HNF1_Q6	RAB3IP; AXIN2; FXYD2; FGA; FGB; SEMA3A; NRP1; UGT1A6; RNASE4; C11ORF9; SLC4A4; IGFBP1; ANXA13; CLDN10; F2RL1; SPINK1	1.67E-03
V$CEBPB_02	RAB3IP; WNT5A; KCNJ2; CYP24A1; CPNE4; PLA2G4A; PCDH7; FGA; FGB; MAP2K6; COL4A3; COL4A4; RBPMS; CP; KCNE3	5.39E-03
V$HNF1_01	RAB3IP; TCEA3; FXYD2; PLA2G4A; FGA; SEMA3A; NRP1; UGT1A6; RNASE4; C11ORF9; SLC4A4; IGFBP1; ANXA13; DAB2	6.26E-03

B

Motif Geneset_GSEA	Genes with promoter regions [-2kb,2kb] around transcription start site containing the motif
SCGGAAGY_V$ELK1_02	SCGGAAGY which matches annotation for ELK1: ELK1, member of ETS oncogene family
GGGCGGR_V$SP1_Q6	which matches annotation for SP1: Sp1 transcription factor
RCGCANGCGY_V$NRF1_Q6	RCGCANGCGY which matches annotation for NRF1: nuclear respiratory factor1
CACGTG_V$MYC_Q2	CACGTG which matches annotation for MYC: v-myc myelocytomatosis viral oncogene homolog (avian)
MGGAAGTG_V$GABP_B	MGGAAGTG which matches annotation for GABPA: GA binding protein transcription factor, alpha subunit 60kDa GABPB2: GA binding protein transcription factor, beta subunit 2
GTGACGY_V$E4F1_Q6	GTGACGY which matches annotation for E4F1: E4F transcription factor 1
GATTGGY_V$NFY_Q6_01	GATTGGY. Motif does not match any known transcription factor
V$HNF1_Q6	WRGTTAATNATTAACNNN which matches annotation for TCF1: transcription factor 1, hepatic; LF-B1, hepatic nuclear factor (HNF1), albumin proximal factor
V$CEBPB_02	NKNTTGCNYAAYNN which matches annotation for CEBPB: CCAAT/enhancer binding protein (C/EBP), beta
V$HNF1_01	GGTTAATNWTTAMCN which matches annotation for TCF1: transcription factor 1, hepatic; LF-B1, hepatic nuclear factor (HNF1), albumin proximal factor

Table 3-7 GSEA annotation for motif gene sets higher in A549 (Subramanian et al., 2005). Annotations were performed using genes that were at least 1.5 times differentially expressed between the two cell lines A549 and A549 J5-1. B description of the in A listed motifs.

binding motif analysis of gene sets upregulated in the A549 J5-1 cells are involved in dedifferentiation or early embryonal developmental processes, clearly showing that these are affected by the expression of c-Myc. I.e. Sp1 plays a crucial role in mediating early events of physiological mucous epithelial cell differentiation of bronchial epithelial cells (Hong et al., 2008), Tcf3 is expressed during embryonal lung development in the primordial and alveolar epithelium (Tebar et al., 2001), Lef1 is involved in the development of multiple organs (Eastman and Grosschedl, 1999) and MAZ protein levels show an increase upon differentiation of ES cells (Tarasov et al., 2008). Additionally, among the most significantly downregulated gene sets upon c-Myc-expression in the A549 cells were two transcription factors identified that are involved in differentiation and the expression of organ-specific genes, GABPB2, which is involved in B-cell lineage differentiation and HNF1, which is a liver-specific transcription factor (Servitja et al., 2009). Interestingly, the above mentioned transcription factor Lef1 has also been recently identified to be one of the mediators of chemotactic invasion and colony outgrowth in lymph node derived lung adenocarcinoma cells (Nguyen et al., 2009), consistent with the metastatic potential of the A549 J5-1 cells. Additionally, a gene set containing a binding site for the transcription factor FoxO4 was among the most significantly upregulated gene sets identified for A549 J5-1 cells. FoxO4 is known to activate amongst others the transcription of the DNA-damage responsive Gadd45a (Kobayashi et al., 2005), which was shown to be upregulated in the A549 J5-1 cells in the qPCR experiments shown before.

Not only genetic and epigenetic alterations of protein encoding genes are responsible for tumour development. Over the past few years also many microRNAs have been implicated in various human cancers (Croce, 2009). MicroRNAs are small, 19-22 nucleotide long, non-coding RNAs that inhibit gene expression at the posttranscriptional level. Given the frequency with which microRNA target sequences are conserved within 3'UTRs, it is estimated that 20 to 30% of all human genes are targets for microRNAs (Peter, 2009). Therefore a GSEA

annotation was also performed for microRNA targets upregulated and downregulated in c-Myc-expressing A549 cells in comparison to the parental cell line A549. An upregulation of microRNA target genes can be interpreted as a downregulation of the corresponding microRNA. In Table 3-8 the ten most significantly upregulated microRNA target gene sets in the A549 J5-1 cells are shown, in Table 3-9 the ten most significantly downregulated microRNA target gene sets in the A549 J5-1 cells. First of all, the upregulation of the micro-

microRNA targets_GSEA	Genes that account for enrichment	P-Value
TGTTTAC,MIR-30A-5P,MIR-30C,MIR-30D,MIR-30B,MIR-30E-5P	BNC1; GLDC	3,87E-03
TGGTGCT,MIR-29A,MIR-29B,MIR-29C	DUSP2; TUBB2B	8,49E-03
TTTGCAC,MIR-19A,MIR-19B	ID4; PTPRG	8,82E-03
TGCTGCT,MIR-15A,MIR-16,MIR-15B,MIR-195,MIR-424,MIR-497	TLE4; SLC7A2; G0S2	9,74E-03
ACCAAAG,MIR-9	ID4; FLI1	1,09E-02
ACTGTGA,MIR-27A,MIR-27B	ID2; ECE2	1,48E-02
CAGTATT,MIR-200B,MIR-200C,MIR-429	FLI1; ID2	1,59E-02
GCACTTT,MIR-17-5P,MIR-20A,MIR-106A,MIR-106B,MIR-20B,MIR-519D	BNC1; DUSP2; TXNIP; SOLH	2,63E-02
AATGTGA,MIR-23A,MIR-23B	PPIF; DLX1	2,78E-02
GTGCCTT,MIR-506	TLE4; PPIF ;NRCAM; PRDM13; TRIB3; NUDCD2	3,17E-02

Table 3-8 GSEA annotation for microRNA target gene sets upregulated in A549 J5-1 (Subramanian et al., 2005). Annotations were performed using genes that were at least 1.5 times differentially expressed between the two cell lines A549 and A549 J5-1.

microRNA targets_GSEA	Genes that account for enrichment	P-Value
TGAATGT,MIR-181A,MIR-181B,MIR-181C,MIR-181D	ST8SIA4; MYH10; WSB1; PDLIM5; ITGB8; NPTXR; GREM1; SLC2A3; ARNT2	1,79E-04
GTGCCTT,MIR-506	ST8SIA4; MYH10; WSB1; NRP2; NAV1; PCDH9; NRP1; SESTD1; FOXQ1; RAB34; FAM62B; PLCB1; SHANK2; ABCA1; FLRT3; DAPK1; FLJ10357; PDE5A; COL5A1	5,11E-04
CTGAGCC,MIR-24	RASSF2; NEDD9	6,02E-04
TGCTGCT,MIR-15A,MIR-16,MIR-15B,MIR-195,MIR-424,MIR-497	NRP2; NAV1; PCDH9; PDLIM5; SLC4A4; LPHN2; MMD; KCNJ2; COBLL1; HAS2; RSPO3; AXIN2; ARMCX2; RNF43; CLDN2	9,18E-04
GTGCAAT,MIR-25,MIR-32,MIR-92,MIR-363,MIR-367	SOX4; CXCL5; FBN1; SDC2; DSC2	1,35E-03
CTACCTC,LET-7A,LET-7B,LET-7C,LET-7D,LET-7E,LET-7F,MIR-98,LET-7G,LET-7I	SLC4A4; COL1A1; PGM2L1; COL5A2; SYT11; MGLL; CGNL1; DKK3	1,70E-03
ATTCTTT,MIR-186	LPHN2; CACNB3; WNT5A; HNMT	1,72E-03
CTCAGGG,MIR-125B,MIR-125A	ST8SIA4; SLC4A4; SORT1; MTUS1; LBH; ABHD6	1,95E-03
TGTTTAC,MIR-30A-5P,MIR-30C,MIR-30D,MIR-30B,MIR-30E-5P	ST8SIA4; MYH10; NRP2; NRP1; MMD; SOX4; CUGBP2; YPEL2; NRIP1; RGS2; IRS1; FHOD3; INSIG2; SEMA3A; CYP24A1; SGCB	3,07E-03
TGCCTTA,MIR-124A	MYH10; NRP2; NAV1; SESTD1; FOXQ1; RAB34; FAM62B; KCNJ2; CACNB3; PPARA; PTPRE; BTBD11; MLLT3; RBMS3; CNTN1	3,13E-03

Table 3-9 GSEA annotation for microRNA target gene sets upregulated in A549 (Subramanian et al., 2005). Annotations were performed using genes that were at least 1.5 times differentially expressed between the two cell lines A549 and A549 J5-1.

RNAs miR-24 and Let-7, which both target Myc-RNA (Lal et al., 2009; Sampson et al., 2007), in the c-Myc-expressing A549 cells is consistent with a negative feedback regulation

of Myc upon its expression (Cleveland et al., 1988). Furthermore, the ability of Myc to promote cell growth and proliferation was reflected in this analysis by the upregulation of gene sets that are targets of microRNAs responsible for suppression of cell growth, i.e. miR-30 (Wu et al., 2009); blocking G(1)/S-transition, like miR-195 (Xu et al., 2009); and that inhibit proliferation, like miR-9 does via targeting of NFκB (Guo et al., 2009); and the downregulation of gene sets that are targets of microRNAs that increase proliferation, like themiR-92, which targets p63 (Manni et al., 2009), in A549 J5-1 cells. Additionally, target genes of the microRNA miR-200 were found to be among the most significantly upregulated gene sets in this analysis upon c-Myc-expression. The miR-200 inhibits the ability to metastasize in tumour cell lines derived from mice that develop metastatic lung adenocarcinoma owing to expression of mutant KRas and p53 via targeting genes involved in EMT (Gibbons et al., 2009). Although in the SpC-C-Raf-BxB/SpC-c-Myc metastasis model for NSCLC no EMT was observed (Rapp et al., 2009), these data indicate that genes involved in this process are regulated by Myc. The oncogenic potential of Myc is clearly shown by the upregulation of microRNA target gene sets for microRNAs identified to be involved in tumour development, i.e. the tumour suppressor microRNAs miR-15 and -16, in the A549 J5-1 cells. Furthermore, in this analysis a gene set was observed to be downregulated upon c-Myc-expression in the A549 cells, which comprises targets of the microRNA miR-181 that has been shown inhibit hepatic cell differentiation through targeting GATA6 among other genes (Ji et al., 2009). This result indicates a downregulation of GATA6 upon c-Myc expression, which is in line with our observation of a GATA6/GATA4 switch in the c-Myc-expressing tumours in the NSCLC mouse model (Rapp et al., 2009).

4 Discussion

4.1 *Melanoma*

Two strategies were followed to examine the role of B-Raf in melanoma development. The first approach was to generate transgenic animals that express the oncogenic B-Raf^{V600E} melanocyte-specific and inducible. Furthermore B-Raf-deficient embryos were used to determine the role of B-Raf in early embryonal development to gain information about its non-pathological function. Surprisingly, it was observed that the early embryonal melanocyte development is not dependent on B-Raf.

4.1.1 Generation of a transgenic mouse model for melanocyte-specific and inducible expression of B-Raf^{V600E}

The goal of this work was to establish a mouse model to study the role of B-Raf^{V600E} in melanoma development and have a mouse model to test new therapeutic approaches for B-Raf^{V600E}-positive melanoma. To have a flexible system, that can also be used to study the effect of the expression of B-Raf^{V600E} in other organs than the skin, i.e. the lung, and to avoid the risk of embryonal lethality as far as possible, a construct was generated that enables the tetracycline-inducible expression of B-Raf^{V600E} in combination with the tissue-specific expression of rtTA. In principle, it is necessary to express a strong oncogene like B-Raf^{V600E} inducible, because the constitutive expression of an oncogene in many tissues already during early embryonal development is likely to result in embryonal lethality, since the constitutive active mitogenic cascade would interfere with many developmental signaling pathways. Furthermore, to be able to distinguish the transgenic B-Raf^{V600E} from the endogenous wildtype B-Raf, the B-Raf^{V600E} was additionally tagged with EGFP. For being able to test the expression of the construct easily and to later have the possibility of *in vivo* low light imaging, the construct also contains the luciferase, which is expressed under the control of the

bidirectional tetracycline-inducible promoter in the other direction than B-Raf^{V600E}-EGFP. The construct that was generated for this purpose in this work is shown in Figure 3-1. Furthermore, as shown in the results-part, the B-Raf^{V600E} resulting from the expression of this construct in NIH3T3 cells is functional in respect to Erk-phosphorylation, detectable in respect of the EGFP-tag and the Luciferase-activity and inducible by doxycycline. To target the expression of B-Raf^{V600E} to a specific cell type, in our case the melanocytes, the resulting mouse line would have to be combined with a transgenic mouse line expressing the rtTA-protein tissue-specific manner. For the melanocyte-specific transgene expression for this purpose one would chose promoters that drive the expression of members of the Tyrosinase gene family, like the *Tyrosinase-related protein 1* (*TRP1*), *DCT* or the *Tyrosinase.* In mice, in situ-hybridization and *lacZ* reporter assays have shown that *DCT* is expressed in cells of the pigment cell lineage, the melanoblast, melanocytes and cells of the retinal pigment epithelium (Pollock et al.). In migrating melanoblasts the expression of *DCT* starts at the embryonic day E11 and with this starts somewhat earlier than the expression of the two related genes *TRP1* and *Tyrosinase* (Guyonneau et al., 2004). Nevertheless, even if the expression profile of a certain promoter is known, it is difficult to predict the phenotype of the resulting animal. For this reason it is important to make the effort of developing an inducible system, because different promoter/oncogene combinations can more easily be tested.

Surprisingly, as described in 3.1.3, after microinjection of the linearized construct, only two of the founder-lines that were positively tested for the transgene via PCR from tail-DNA were transmitting the transgene to their offspring. Although it has been shown that a very tight regulation of gene expression is possible in the context of the Tet system by the successful expression of the lethal diphtheria toxin gene in transgenic mice (Deuschle et al., 1995), it is sometimes difficult to establish cell lines or transgenic animals where genes encoding potentially toxic products are under Tet control (Lai et al., 2004). These problems mainly result from episomal and multiple copy status of the transferred DNA, a situation when

chromatin suppression is lacking and cumulated expression from multiple copies of the target gene might compromise the survival of candidate cells. Additionally, the conditional expression of a B-Raf^{V600E}-knock-in allel in a Cre/LoxP-approach resulted in combination with the expression of the Cre-recombinase under the control of a CMV-promoter in embryonal lethality at embryonic day E7 (Mercer et al., 2005). This suggests, that a leakiness of the tetracycline-inducible promoter resulting from an integration site in a chromosomal region where chromatin suppression is lacking would lead to a limited survival of the target cells and by this to embryonal lethality or to a mosaic animal not containing transgene bearing cells in any organ that might be affected due to its expression. The probability of an undesirable integration site would be increased if more DNA would be injected into the blastocysts. Furthermore, if the injected DNA integrates in a transcriptionally inactive part of the genome, this will result in viable transgene-positive animals that transmit the transgene in a mendelian ratio to their offspring, which is probably the case for the two transgene-transmitting founder-lines.

To circumvent the problems that we encountered, it might be helpful to combine the generated plasmid with a tetracycline-controlled transcriptional silencer (tTS), which is the fusion of the bacterial Tet repressor and the silencer domain derived from a transcriptional silencer (Forster et al., 1999), i.e. in place of the reporter gene luciferase, to mitigate the leaky expression associated with tetracycline-regulated promoter. By this the gene activity is shut down completely by tTS binding to the promoter in the absence of the inducer doxycycline and thus actively shields the promoter from the endogenous transcriptional machinery. This might provide the possibility to develop a tightly controllable doxycycline inducible gene expression system (Lai et al., 2004).

4.1.2 B-Raf is not involved in early embryonal melanocyte development

In interesting recent publications it was shown that the tumourigenic phenotype of cancer cell lines can be suppressed by the mouse embryonal microenvironment and the developmental plasticity of the tumour cells was manifested as the tumour cells contributed to the formation of normal tissue. When GFP-labeled human metastatic melanoma cells were transplanted into the embryonic chick neural tube, they invaded the chick periphery in a programmed manner along stereotypical neural crest cell migratory pathways and populated peripheral destinations and a subpopulation of these cells even expressed melanogenic markers that could not be detected at the time point of transplantation. Importantly, the transplanted melanoma cells did not form tumours (Kulesa et al., 2006). The other way around, the influence of a tumourigenic microenvironment on melanocytes has been shown to induce the acquisition of tumour cell-like characteristics (Seftor et al., 2005). Furthermore, in expression profiling studies comparing melanoma cell lines with normal melanocytes, pathways were identified that might be involved in the transformation of melanocytes to melanoma, including those involved in embryonal development (Hoek et al., 2004). These data and other reports suggest that the development of metastatic characteristics might be a faulty reversal of ontogeny (Rapp, 2007). As described in the introduction, B-Raf plays an important role in melanoma. For these reasons, in this work, the role of B-Raf in the early embryonal melanocyte development was examined, to gain more information about pathways and events that might also be involved in reprogramming of melanocytes to malignant melanoma cells.

The expression of the neural crest marker Sox10 in neural tubes of E11.5 embryos of B-Raf-deficient animals and the detection of the same amount of p75/Sox10 double-positive cells in neural tube explant cultures of wildtype and B-Raf-deficient embryos suggested a normal early neural crest development in the absence of B-Raf. This was confirmed by in-situ hybridization using Sox10-specific probes showing the localization of the Sox10-positive

cells localized in the migratory stream form the neural crest stem cell population to the dorsal root ganglia.

Furthermore, the results of this work showed that neither the expression of Mitf is impaired in neural tubes of E11.5 embryos, nor the localization of Mitf-positive cells in respect to the neural crest development in E9.5 embryos in the absence of B-Raf. As shown in Figure 3-7, the Mitf-expressing cells in the wildtype as well as in the B-Raf-deficient embryos are located dorsal of the neural tube and along the dorso-lateral migratory pathway. These results were surprising, because B-Raf^{V600E} plays a central role in the regulation of Mitf expression and protein stability in melanoma cell lines. On the one hand, oncogenic B-Raf induces the expression of Mitf via the activation of the mitogenic cascade, which is controlled by the transcription factor BRN2 that targets Mitf is targeted for degradation via phosphorylation by ERK. Long-term inhibition of the constitutively active mitogenic cascade in B-Raf^{V600E}-positive melanoma cells using a MEK-inhibitor leads to an almost complete loss of Mitf expression. Furthermore, it was shown that B-Raf as well as Mitf are essential for melanocyte proliferation, but wildtype B-Raf seems not to regulate Mitf expression in normal melanocytes and also the transcription factor BRN2 is not expressed in mature melanocytes (Wellbrock et al., 2008). BRN2 is a neuronal-specific transcription factor that is expressed in the melanoblasts but becomes downregulated as these cells differentiate into melanocytes (Cook et al., 2003) and that was previously shown to link oncogenic B-Raf to melanoma proliferation (Goodall et al., 2004). Wellbrock et al. showed that BRN2 expression is induced by oncogenic but not by wildtype B-Raf, suggesting that the ability of B-Raf to induce the transcription of BRN2 and by this regulate the expression of Mitf is a newly acquired function of the oncogenic protein (Wellbrock et al., 2008). In line with this, in this work no difference between wildtype and B-Raf-deficient embryos could be shown in respect to Mitf expression and to the localization of Mitf-expressing cells in the melanogenic developmental pathway.

Mitf is considered to be the master regulator of melanocyte biology, mainly because it regulates the expression of the melanogenic enzymes like DCT or Tyrosinase (Levy et al., 2006). As the B-Raf-deficient neural crest stem cells were positive for this master regulator of melanocyte biology it was not surprising to detect DCT expression in the neural tubes of E11.5 wildtype as well as B-Raf-deficient embryos. Furthermore, the dorso-lateral localization of the DCT-positive cells in the in-situ hybridization on sections of E11.5 embryos indicates that unlike in the development of cortical neurons (Camarero et al., 2006), B-Raf is not necessary for migration along the developmental pathways in the melanocyte development.

4.2   NSCLC

Two different models were used to understand the role of c-Myc in the induction of metastasis and tumour cell reprogramming. First of all in the NSCLC metastasis mouse model gene expression profiling was performed to identify pathways that become activated prior to metastasis. Surprisingly, the most significant gene found was a neuroendocrine marker, which usually is a feature of SCLC (Travis et al., 2004). Next Myc was introduced into a non-metastatic human NSCLC cell line. It could be shown that these cells express the same markers that were identified by (Rapp et al., 2009) in the NSCLC mouse model for Myc-induced metastasis and that Myc is sufficient to convert a non-metastatic NSCLC cell line into metastasizing cells. Furthermore, a panel of genes was identified that might be involved in the metastatic conversion upon Myc-expression.

4.2.1   Secondary mutations in long latency SpC-c-Myc single transgenic animals

As described in 3.3.1 the tumour development in single transgenic SpC-c-Myc animals was delayed when compared to the SpC-C-Raf-BxB/SpC-c-Myc compound mice. This demonstrates that Myc alone is incapable to promote tumour formation in this NSCLC model and requires additional mutations to rescue transformation activity due to its deleterious

(apoptotic) single oncogene effects as described in 1.6.1. In this work, a mutation screen was performed and frequent mutations in Exon1 of *KRas* and in Exon6 of *LKB1* were detected in the primary lung tumours of the single transgenic SpC-c-Myc animals. These mutations were exclusive with one exception of the analyzed SpC-c-Myc single transgenic mice, which had a different mutation in Exon6 of *LKB1* (6389). Furthermore, a mutation in Exon1 of *KRas* could only be detected in two, a mutation in Exon6 of *LKB1* in none of the analyzed primary lung tumours of the SpC-C-Raf-BxB/SpC-c-Myc compound animals. This observation is consistent with the mutually exclusive pattern of *Ras* and *Raf* mutations in human tumours (Storm and Rapp, 1993). Furthermore, these data suggest that in the type II-pneumocytes an oncogenic signaling of the mitogenic cascade, i.e. induced by C-Raf-BxB or constitutive active KRas, leads to the inactivation of the tumoursupressor LKB1. In the single transgenic SpC-c-Myc the expansion of the cells in the observed pleomorphic clusters is blocked by the deleterious effects of Myc on cell survival. The activation of the mitogenic cascade via C-Raf-BxB (Rapp et al., 2009) or an activating KRas mutation antagonizes these effects as well as the inactivation of the proapoptotic tumour suppressor LKB1 (Zhong et al., 2008).

4.2.2   Is metastasis an early event

The occurrence of *KRas*-mutations in a high frequency of primary lung tumours in the SpC-c-Myc single transgenic mice suggested the possibility to use these mutation data for lineage tracing from the primary lung tumour cells to the liver and lymph node metastases. Therefore in this work, liver and lymphnode metastases were screened for mutations in Exon1 of *KRas*. Surprisingly, as shown in Table 3-2, all analyzed metastases of the single transgenic SpC-c-Myc mice did not carry a mutation in *KRas* Exon1 with one exception (16740), although they had mutations in this gene in their primary lung tumours. The animal 16740, which had an identical mutation in *KRas* Exon1 in the primary lung tumour and the corresponding liver metastasis had multiple organ metastases, including besides liver pancreas, kidney and brain.

These data strongly indicate that metastasis is an early event and support the suspicion of early seeding of metastasis initiating cells.

4.2.3   Induction of neuroendocrine markers by c-Myc

Although the cell population of the pulmonary neuroendocrine bodies, that is also described as "Clara-like cells" (De Proost et al., 2008) is different from TypeII-pneumocytes expressing the transgenes C-Raf-BxB and c-Myc, in this work a highly significant upregulation of the neuroendocrine marker SNCA has been observed in the lung tumours of the SpC-C-Raf-BxB/SpC-c-Myc compound animals. Hyperplasia of pulmonary neuroendocrine cells is frequently observed in response to acute or chronic lung damage suggesting that they play a role in the regeneration of the pulmonary epithelium after injury (Peake et al., 2000). One could argue that the increased expression of SNCA is rather a consequence of the changes in the normal microenvironment leading to an increase of the SNCA-expressing cell population in the lung than a true effect of the expression of c-Myc in the alveolar type II cells, since this data derived from analysis of total lung RNA. But when we performed qPCR experiments on the c-Myc-expressing A549 J5-1 cells data also showed a highly significant upregulation of SNCA. Furthermore, in this cell culture model for human NSCLC the significant upregulation of more markers of the neuroendocrine system, like pgp9.5, Synaptobrevin and NeuroD1, was observed. SNCA is normally expressed in neuronal tissue and is located in close vicinity to - and is loosely associated with - presynaptic vesicles and thus is considered to play a role in synaptic release of neurotransmitters. Furthermore, it appears to be involved in the etiology of neurodegenerative diseases and has also been reported to play a role in ovarian tumours, but its function in the malignant cells and other nonneuronal tissue remains unclear (Bruening et al., 2000). Synaptobrevin is an integral membrane protein present in synaptic vesicles and is often used as a synaptic marker (Jontes et al., 2004). NeuroD1 has been reported to possibly play a role in the development of neuroendocrine subpopulations in the lung (Ito et al., 2000).

Poulsen et al. showed that the expression of pgp9.5 is not restricted to the neuroendocrine cell population and stated that the constitutive expression of b-Myb in typeII-pneumocytes leads to elevated expression levels of pgp9.5 in the lung (Poulsen et al., 2008). Interestingly, in the data of the microarray comparing genes differentially expressed in A549 versus A549 J5-1 cells the Myb-binding-protein1a (MYBBP1a) was one of the genes accounting for the enrichment of genes of the Myc-oncogenic signature in the A549 J5-1 cells. The only neuroendocrine marker that was significantly downregulated in the qPCR analysis comparing the expression profile of the A549 with A549 J5-1 was Enolase, suggesting the direct regulation of the other analyzed neuroendocrine markers rather than the induction of a master regulator of a complete neuroendocrine phenotype. Summarizing these data, I have shown that the expression of the neuroendocrine genes SNCA, NeuroD1 and Synaptobrevin were significantly upregulated in the typeII-pneumocytes and the A549 cells, respectively, upon c-Myc-expression, although the mechanism and the consequences of the expression of these genes remain to be elucidated. All in all despite the unknown mechanism and role of these neuroendocrine markers, the expression of genes that are characteristic for other tissues is consistent with epigenetic instability or reprogramming events. Furthermore, pgp9.5 was significantly upregulated in qPCR analysis of the A549 J5-1 cells in comparison to the parental A549 cell line and in histological analysis of the lungs of the SpC-C-Raf-BxB/SpC-c-Myc compound and late SpC-c-Myc animals (Rapp et al., 2009). The literature suggests an involvement of b-Myb in the induction of pgp9.5 in typeII-pneumocytes, which is strongly supported by the microarray data of this work. These data suggest an upregulation of b-Myb upon c-Myc-expression, which should be determined via qPCR-analysis in future work.

4.2.4 Myc is sufficient to induce metastasis

If Myc is sufficient to induce metastasis in NSCLC the introduction of c-Myc into a non-metastatic NSCLC cell line should lead to metastatic conversion of these cells. To test this

possibility as described in 3.4 in this work chicken c-Myc was introduced into the human non-metastatic cell line A549 and resulting clones were tested for chicken c-Myc expression. Comparing the ability for anchorage-independent growth in a soft-agar assay of the parental cell line A549 and the high-chicken c-Myc expressing clone A549 J5-1 showed highly significant differences in the size and number of resulting colonies (Figure 3-11). These data suggest an enhanced ability of anchorage-independent growth of the cells upon Myc expression. The high-chicken c-Myc expressing clone A549 J5-1 was also subcutaneously injected into Rag$^{-/-}$-mice and accelerated tumour growths was observed as well as metastasis to lung and liver in a small fraction of the A549 J5-1 injected animals. Since the tumours of the animals injected with A549 J5-1 were growing rapidly, the mice had to be sacrificed as soon as six weeks after transplantation to not exceed the allowed 2cm of tumour diameter. Keeping in mind this short time span of the experiment, it was not surprising that metastasis occurred only with low frequency and this fact suggests that a longer time frame, i.e. possibly by surgical removal of the primary tumour, could increase the metastasis rate in A549 J5-1 injected animals. Additionally, among the identified microRNA targets significantly upregulated in the A549 J5-1 cells, were targets of the microRNA miR-200, which was published to inhibit metastasis (Gibbons et al., 2009). Unfortunately this microRNA was not assessed in the performed microarray. An upregulation of the target genes suggest a downregulation of the corresponding microRNA. Furthermore, among the identified transcription factor targets significantly upregulated in the A549 J5-1 cells, were targets of the transcription factor Lef1, which has recently been identified to be one of the mediators of chemotactic invasion and colony outgrowth in lymph node derived lung adenocarcinoma cells (Nguyen et al., 2009). These data clearly show that Myc is able to convert non-metastatic tumour cells into metastasizing cells. All in all the ability to convert the non-metastatic A549 cells to metastasizing cells via the expression of chicken c-Myc now provides a system to study the events required for this switch in phenotype.

4.2.5 GATA4 in NSCLC

In the lung tumours and liver metastases of the SpC-C-Raf-BxB/SpC-c-Myc compound and the SpC-c-Myc single transgenic animals the expression of the intestine maintenance transcription factor GATA4 was observed. In contrast, GATA4 was absent in the lung tumours of SpC-C-Raf-BxB animals, which expressed instead GATA6, a transcription factor that is involved in airway regeneration, (Rapp et al., 2009). In this work the GATA4- and GATA6-expression of A549 and A549 J5-1 cells was analyzed. In contrast to the switch from GATA6- to GATA4-expression observed in the SpC-C-Raf/SpC-c-Myc compound and SpC-c-Myc single transgenic animals, in the A549 J5-1 an upregulation of both GATA4 as well as GATA6 was seen, as shown in Figure 3-10 and Figure 3-12. Furthermore, to establish functionality of GATA4-protein, qPCR was performed also for the expression of its target gene mucin2, which was in fact significantly upregulated in the A549 J5-1 cells. Although for the human NSCLC cell line A549 the mutually exclusive pattern of GATA4- and GATA6-expression that was observed in the SpC-C-Raf-BxB/SpC-c-Myc compound and SpC-c-Myc single transgenic lung tumours and liver metastases could not been shown, the results clearly demonstrate the induction of GATA4 upon Myc-expression and its functionality by the upregulation of its target mucin2. Interestingly, among the microRNA targets that came up in the microarray comparing the gene expression profile of A549 and A549 J5-1 cells, the microRNA-181 target genes were downregulated in the c-Myc-expressing A549 cells, indicating an upregulation of the corresponding microRNA. The microRNA-181 was published to inhibit hepatic cell differentiation and targets amongst other GATA6 for degradation (Ji et al., 2009). These data suggest that there is a process activated in the A549 J5-1 cells that might lead to the downregulation of GATA6 and consequently TTF1, but other factors might superimpose positive regulation. Furthermore GATA1-activity was shown to be regulated posttranscriptionally via heterodimerization with a cofactor, indicating that this

could be also true for GATA6 and even in the presence of GATA4 as well as GATA6, GATA4 might be dominant (Haenlin et al., 1997).

If loss of organ identity of transformed typeII-pneumocytes is a prerequisite for metastasis as postulated by us (Rapp, 2007) and GATA4 is the mediator by counteracting GATA6 together with its target TTF1, the knockdown of GATA4 in the A549 J5-1 would block the emergence of the metastatic phenotype. To address this issue, A549 J5-1 cells were transfected with GATA4 shRNAs. To confirm the efficient knockdown of GATA4, qPCR on the resulting cell lines was performed and as shown in Figure 3-15, mucin2-expression was significantly reduced. The ability of anchorage independent-growth was tested by growing the cells in soft-agar, which resulted in a significant reduction of the counted colonies upon GATA4 knockdown. These data suggest, that GATA4 knockdown might be capable to at least partially block the metastatic conversion by Myc. To further investigate whether this suspicion is close to reality, a transplantation experiment of the GATA4 knockdown cells into immunodeficient mice might be informative.

Recently it was shown that the overexpression of Hdac1 downregulates the expression of GATA4 in cardiomyocyte formation and that Wnt/Lef1 signalling downregulates the expression of Hdac1 (Liu et al., 2009). Interestingly, the data of the microarray performed with the A549 and A549 J5-1 cells showed an enrichment of genes targeted by the transcription factor Lef1 upregulated in the A549 J5-1 cells, indicating an upregulation of the transcription factor itself. Furthermore, many genes accounting for the enrichment of specific pathways, transcription factor or microRNA targets in the microarray analysis presented in this work are components of WNT-signaling or are involved in the regulation of the latter. All in all this data indicates that WNT/Lef1-signalling might be involved in the regulation of GATA4-expression. Additionally, the involvement of the histone deacetylase Hdac1 suggests an epigenetic mechanism of the regulation of GATA4.

GATA4 is known to be silenced via promoter hypermethylation in primary ovarian, lung and gastrointestinal cancer (Akiyama et al., 2003; Guo et al., 2004; Guo et al., 2006; Wakana et al., 2006). In this work, it was shown that the *GADD45* genes, which play a key role in active DNA demethylation and promote global DNA demethylation via a DNA repair mechanism (Barreto et al., 2007), are significantly upregulated upon c-Myc-expression in the A549 cells. Furthermore, the p53 family members *p53* and *p63* that act upstream of the *GADD45* genes in the nucleotide excision repair (Smith and Seo, 2002) were also shown to be upregulated in the A549 J5-1 cells. Additionally, analysis of the data of differentially expressed genes in A549 and A549 J5-1 cells identified by the microarray performed in this work in respect to cellular processes support an induction of genes involved in the cellular processes of genetic imprinting upon c-Myc expression. The observation that genes that are downregulated upon the expression of the SWI/SNF-chromatin-remodeling-complex subunit BAF57 and targets of the transcription factor FoxO4, which is involved in the regulation of *GADD45* genes (Kobayashi et al., 2005) were found to be significantly upregulated in the A549 J5-1 cells also is in line with these data. Furthermore, among the transcription factors, which came up in the analysis of upregulated transcription factor target genes in A549 J5-1, the transcription factor Ets2 was identified that induces DNA-repair via ERCC5 (Crawford et al., 2007).

All in all these data suggest not only an induction of GATA4 expression in NSCLC upon c-Myc-expression, but furthermore indicate an epigenetic mechanism for the regulation of GATA4-expression via histone deacetylation and promoter demethylation. As GATA4 is not necessary for integrity of the adult lung it may be the ideal target for novel therapeutic approaches.

4.2.6   Further characterization of c-Myc-expressing A549 cells

Myc has been reported to induce angiogenesis in vivo by a VEGF-dependent mechanism (Knies-Bamforth et al., 2004). The finding of this work that Myc is able to induce the

expression of VEGF in the human NSCLC cell line A549 is in line with the previously observed significantly increased VEGF expression and an invasion of blood and lymph vessels in the lung tumours of SpC-C-Raf-BxB/SpC-c-Myc compound and SpC-c-Myc single transgenic animals (Rapp et al., 2009), supporting that Myc induces angiogenesis in NSCLC by upregulation of VEGF expression. Additionally, in the microarray data comparing the gene expression profile of the A549 and A549 J5-1 cells showed an upregulation of target genes for the transcription factor Sp1, which is known to induce VEGF-regulated angiogenesis (Song et al., 2009), and for the transcription factor NFATc, which is induced by VEGF (Kulkarni et al., 2009), upon c-Myc-expression, strongly supporting the before discussed data. Furthermore, in this work the induction of *Sox2*, *Sox9* and *Klf4*-expression was observed upon c-Myc expression in the A549 cells. Sox2 and Klf4 are together with Myc involved in the induction of pluripotent stem cells (Takahashi and Yamanaka, 2006) and *Sox9* is highly expressed during lung development, but absent in the adult lung (Perl et al., 2005), indicating a dedifferentiation of the NSCLC cells upon the expression of Myc. Additionally, the observation of a fivefold reduced expression of tissue-specific genes in the A549 J5-1 cells compared to the A549 parental cell line in the microarray analysis strongly support a loss of organ identity upon Myc-expression. This was also supported by the data on downregulation of genes involved in the ageing process of the kidney and liver-specific genes together with the target genes of the liver-specific transcription factor HNF1 in the A549 J5-1 cells. The combined data indicate a more differentiated status of the A549 cells when compared to the A549 J5-1 cells. Moreover the upregulation of target genes of the transcription factors Sp1, Tcf3, Lef1 and MAZ in the c-Myc expressing cells, which are involved in dedifferentiation or early embryonal development processes is in line with this conclusion.

Finally another tumour-associated gene, *tert*, was upregulated upon c-Myc-expression in the A549 cells going in line with the literature that *tert* is activated by Myc (Wang et al., 1998).

Furthermore *tert* activation assures cell survival after occurrence of genomic instability (Kim et al., 1994).

4.2.7 Microarray-Analysis of the A549 J5-1 cells

Surprisingly, an upregulation of GATA4 expression was not detected in the A549 J5-1 cells in the microarray experiment. On the other hand, the upregulation of a lot of processes, pathways, transcription factor targets and microRNA targets in the A549 J5-1 that we would expect to be induced by Myc-expression, were observed. I.e. among the most significant gene sets identified in the pathway analysis of genes upregulated in the A549 J5-1 cells were the Myc oncogenic signature and the Myc-target genes. Thus the microarray data show the expected changes in the expression profile of the A549 J5-1 cells compared to the A549 cells. The fact that not all Myc targets light up may have several reasons. First of all, as shown in Figure 3-10, the population of A549 J5-1 cells is heterogeneous in respect to GATA4-expression. Furthermore, changes in mRNAs that are expressed at low levels are hardly detectable in the microarray, even if they were detected in qPCR analysis, which has a much lower threshold in respect to absolute RNA-concentrations. Additionally, in the microarray only RNAs can be detected that are intact in the 5'-end due to technical reasons, so RNAs that have a fast turnover are hardly detectable by this method.

In regard to Myc expression the microarray data suggest a feedback regulation of Myc. Target genes of the Myc-associated zink-finger protein MAZ for example, which binds in the promoter region of Myc regulating transcription initiation as well as the termination (Bossone et al., 1992), were upregulated in the A549 J5-1 cells. Furthermore, the downregulation of genes containing a binding site for Myc in the A549 J5-1 cells suggests a negative feedback regulation of Myc-target genes upon their induction by Myc. Additionally, the microRNAs miR-24 and Let-7, which both target Myc-RNA (Lal et al. 2009)(Sampson et al., 2007), were

upregulated in the A549 J5-1 cells, supporting a negative feedback regulation of Myc upon its expression.

In several analysis of the microarray data obtained for A549 and A549 J5-1 cells revealed the oncogenic potential of Myc. For example the upregulation of genes of the Myc-oncogenic-signature, the downregulation of the breast cancer associated tumour suppressor gene *BRCA1* and the downregulation of the tumour suppressor microRNAs miR-15 and -16 in the A549 J5-1 cells clearly reflect the oncogenic potential of Myc. Upon c-Myc-expression in the A549 cells additionally genes associated with proliferation were upregulated, while genes involved in block of proliferation were downregulated. Not surprisingly, among the identified microRNAs upregulated in the A549 J5-1 cells, there were the microRNA-24 and let-7, which downregulate Myc, suggesting activation of a negative feedback loop in the cells responding to the forced expression of the exogenous c-Myc.

Last but not least, the data analyses of the microarray reflect the proliferative potential of Myc. First of all, the mitogenic cascade seems to be stimulated by c-Myc-expression, since we observed a significant downregulation of the set of genes that was reported to be upregulated after a knockdown of KRas (Sweet-Cordero et al., 2006) in the A549 cells upon c-Myc-expression. Additionally an upregulation of gene sets being targets of the transcription factor ETS, which is regulated by the mitogenic cascade, in the A549 J5-1 cells was seen. Furthermore, the downregulation of a gene set containing a binding site for the transcription factor E4F1, which induces cell cycle arrest as described in the results-section, in the A549 J5-1 cells supports the induction of cell cycle progression genes upon c-Myc-expression. These include the downregulation of the microRNA miR-30, which blocks G(1)/S-transition, in the A549 J5-1 cells.

5 Literature

Addya, S., Keller, M.A., Delgrosso, K., Ponte, C.M., Vadigepalli, R., Gonye, G.E., and Surrey, S. (2004). Erythroid-induced commitment of K562 cells results in clusters of differentially expressed genes enriched for specific transcription regulatory elements. Physiol Genomics *19*, 117-130.

Adhikary, S., and Eilers, M. (2005). Transcriptional regulation and transformation by Myc proteins. Nat Rev Mol Cell Biol *6*, 635-645.

Akiyama, Y., Watkins, N., Suzuki, H., Jair, K.W., van Engeland, M., Esteller, M., Sakai, H., Ren, C.Y., Yuasa, Y., Herman, J.G.*, et al.* (2003). GATA-4 and GATA-5 transcription factor genes and potential downstream antitumor target genes are epigenetically silenced in colorectal and gastric cancer. Mol Cell Biol *23*, 8429-8439.

Albino, A.P., Nanus, D.M., Mentle, I.R., Cordon-Cardo, C., McNutt, N.S., Bressler, J., and Andreeff, M. (1989). Analysis of ras oncogenes in malignant melanoma and precursor lesions: correlation of point mutations with differentiation phenotype. Oncogene *4*, 1363-1374.

Angst, B.D., Marcozzi, C., and Magee, A.I. (2001). The cadherin superfamily: diversity in form and function. J Cell Sci *114*, 629-641.

Arnold, I., and Watt, F.M. (2001). c-Myc activation in transgenic mouse epidermis results in mobilization of stem cells and differentiation of their progeny. Curr Biol *11*, 558-568.

Ashburner, M., Ball, C.A., Blake, J.A., Botstein, D., Butler, H., Cherry, J.M., Davis, A.P., Dolinski, K., Dwight, S.S., Eppig, J.T.*, et al.* (2000). Gene ontology: tool for the unification of biology. The Gene Ontology Consortium. Nat Genet *25*, 25-29.

Askew, D.S., Ihle, J.N., and Cleveland, J.L. (1993). Activation of apoptosis associated with enforced myc expression in myeloid progenitor cells is dominant to the suppression of apoptosis by interleukin-3 or erythropoietin. Blood *82*, 2079-2087.

Avruch, J., Zhang, X.F., and Kyriakis, J.M. (1994). Raf meets Ras: completing the framework of a signal transduction pathway. Trends Biochem Sci *19*, 279-283.

Bahram, F., von der Lehr, N., Cetinkaya, C., and Larsson, L.G. (2000). c-Myc hot spot mutations in lymphomas result in inefficient ubiquitination and decreased proteasome-mediated turnover. Blood *95*, 2104-2110.

Barreto, G., Schafer, A., Marhold, J., Stach, D., Swaminathan, S.K., Handa, V., Doderlein, G., Maltry, N., Wu, W., Lyko, F.*, et al.* (2007). Gadd45a promotes epigenetic gene activation by repair-mediated DNA demethylation. Nature *445*, 671-675.

Baudino, T.A., McKay, C., Pendeville-Samain, H., Nilsson, J.A., Maclean, K.H., White, E.L., Davis, A.C., Ihle, J.N., and Cleveland, J.L. (2002). c-Myc is essential for vasculogenesis and angiogenesis during development and tumor progression. Genes Dev *16*, 2530-2543.

Baylin, S.B. (1990). "APUD" cells fact and fiction. Trends in Endocrinology and Metabolism *1*, 198-204.

Bisaglia, M., Mammi, S., and Bubacco, L. (2009). Structural insights on physiological functions and pathological effects of alpha-synuclein. FASEB J *23*, 329-340.

Blackwell, T.K., Kretzner, L., Blackwood, E.M., Eisenman, R.N., and Weintraub, H. (1990). Sequence-specific DNA binding by the c-Myc protein. Science *250*, 1149-1151.

Blackwood, E.M., Luscher, B., and Eisenman, R.N. (1992). Myc and Max associate in vivo. Genes Dev *6*, 71-80.

Borczuk, A.C., and Powell, C.A. (2007). Expression profiling and lung cancer development. Proc Am Thorac Soc *4*, 127-132.

Bossone, S.A., Asselin, C., Patel, A.J., and Marcu, K.B. (1992). MAZ, a zinc finger protein, binds to c-MYC and C2 gene sequences regulating transcriptional initiation and termination. Proc Natl Acad Sci U S A *89*, 7452-7456.

Bouchard, C., Marquardt, J., Bras, A., Medema, R.H., and Eilers, M. (2004). Myc-induced proliferation and transformation require Akt-mediated phosphorylation of FoxO proteins. EMBO J *23*, 2830-2840.

Bourdon, J.C. (2007). p53 Family isoforms. Curr Pharm Biotechnol *8*, 332-336.

Braig, M., and Schmitt, C.A. (2006). Oncogene-induced senescence: putting the brakes on tumor development. Cancer Res *66*, 2881-2884.

Bruening, W., Giasson, B.I., Klein-Szanto, A.J., Lee, V.M., Trojanowski, J.Q., and Godwin, A.K. (2000). Synucleins are expressed in the majority of breast and ovarian carcinomas and in preneoplastic lesions of the ovary. Cancer *88*, 2154-2163.

Camarero, G., Tyrsin, O.Y., Xiang, C., Pfeiffer, V., Pleiser, S., Wiese, S., Gotz, R., and Rapp, U.R. (2006). Cortical migration defects in mice expressing A-RAF from the B-RAF locus. Mol Cell Biol *26*, 7103-7115.

Cardoso, W.V., and Lu, J. (2006). Regulation of early lung morphogenesis: questions, facts and controversies. Development *133*, 1611-1624.

Chong, H., Lee, J., and Guan, K.L. (2001). Positive and negative regulation of Raf kinase activity and function by phosphorylation. EMBO J *20*, 3716-3727.

Clark, W.H., Jr., Elder, D.E., Guerry, D.t., Epstein, M.N., Greene, M.H., and Van Horn, M. (1984). A study of tumor progression: the precursor lesions of superficial spreading and nodular melanoma. Hum Pathol *15*, 1147-1165.

Cleveland, J.L., Huleihel, M., Bressler, P., Siebenlist, U., Akiyama, L., Eisenman, R.N., and Rapp, U.R. (1988). Negative regulation of c-myc transcription involves myc family proteins. Oncogene Res *3*, 357-375.

Cook, A.L., Donatien, P.D., Smith, A.G., Murphy, M., Jones, M.K., Herlyn, M., Bennett, D.C., Leonard, J.H., and Sturm, R.A. (2003). Human melanoblasts in culture: expression of BRN2 and synergistic regulation by fibroblast growth factor-2, stem cell factor, and endothelin-3. J Invest Dermatol *121*, 1150-1159.

Crawford, E.L., Blomquist, T., Mullins, D.N., Yoon, Y., Hernandez, D.R., Al-Bagdhadi, M., Ruiz, J., Hammersley, J., and Willey, J.C. (2007). CEBPG regulates ERCC5/XPG expression in human bronchial epithelial cells and this regulation is modified by E2F1/YY1 interactions. Carcinogenesis *28*, 2552-2559.

Croce, C.M. (2009). Causes and consequences of microRNA dysregulation in cancer. Nat Rev Genet *10*, 704-714.

Cummins, D.L., Cummins, J.M., Pantle, H., Silverman, M.A., Leonard, A.L., and Chanmugam, A. (2006). Cutaneous malignant melanoma. Mayo Clin Proc *81*, 500-507.

Davies, H., Bignell, G.R., Cox, C., Stephens, P., Edkins, S., Clegg, S., Teague, J., Woffendin, H., Garnett, M.J., Bottomley, W., *et al.* (2002). Mutations of the BRAF gene in human cancer. Nature *417*, 949-954.

De Proost, I., Pintelon, I., Brouns, I., Kroese, A.B., Riccardi, D., Kemp, P.J., Timmermans, J.P., and Adriaensen, D. (2008). Functional live cell imaging of the pulmonary neuroepithelial body microenvironment. Am J Respir Cell Mol Biol *39*, 180-189.

Deuschle, U., Meyer, W.K., and Thiesen, H.J. (1995). Tetracycline-reversible silencing of eukaryotic promoters. Mol Cell Biol *15*, 1907-1914.

Downward, J. (1998). Ras signalling and apoptosis. Curr Opin Genet Dev *8*, 49-54.

Eastman, Q., and Grosschedl, R. (1999). Regulation of LEF-1/TCF transcription factors by Wnt and other signals. Curr Opin Cell Biol *11*, 233-240.

Eischen, C.M., Weber, J.D., Roussel, M.F., Sherr, C.J., and Cleveland, J.L. (1999). Disruption of the ARF-Mdm2-p53 tumor suppressor pathway in Myc-induced lymphomagenesis. Genes Dev *13*, 2658-2669.

Eischen, C.M., Woo, D., Roussel, M.F., and Cleveland, J.L. (2001). Apoptosis triggered by Myc-induced suppression of Bcl-X(L) or Bcl-2 is bypassed during lymphomagenesis. Mol Cell Biol *21*, 5063-5070.

Evan, G.I., Wyllie, A.H., Gilbert, C.S., Littlewood, T.D., Land, H., Brooks, M., Waters, C.M., Penn, L.Z., and Hancock, D.C. (1992). Induction of apoptosis in fibroblasts by c-myc protein. Cell *69*, 119-128.

Evans, P.M., and Liu, C. (2008). Roles of Krupel-like factor 4 in normal homeostasis, cancer and stem cells. Acta Biochim Biophys Sin (Shanghai) *40*, 554-564.

Felsher, D.W., and Bishop, J.M. (1999). Transient excess of MYC activity can elicit genomic instability and tumorigenesis. Proc Natl Acad Sci U S A *96*, 3940-3944.

Fernandez, P.C., Frank, S.R., Wang, L., Schroeder, M., Liu, S., Greene, J., Cocito, A., and Amati, B. (2003). Genomic targets of the human c-Myc protein. Genes Dev *17*, 1115-1129.

Flory, E., Hoffmeyer, A., Smola, U., Rapp, U.R., and Bruder, J.T. (1996). Raf-1 kinase targets GA-binding protein in transcriptional regulation of the human immunodeficiency virus type 1 promoter. J Virol *70*, 2260-2268.

Forster, K., Helbl, V., Lederer, T., Urlinger, S., Wittenburg, N., and Hillen, W. (1999). Tetracycline-inducible expression systems with reduced basal activity in mammalian cells. Nucleic Acids Res *27*, 708-710.

Furth, P.A., St Onge, L., Boger, H., Gruss, P., Gossen, M., Kistner, A., Bujard, H., and Hennighausen, L. (1994). Temporal control of gene expression in transgenic mice by a tetracycline-responsive promoter. Proc Natl Acad Sci U S A *91*, 9302-9306.

Futreal, P.A., Coin, L., Marshall, M., Down, T., Hubbard, T., Wooster, R., Rahman, N., and Stratton, M.R. (2004). A census of human cancer genes. Nat Rev Cancer *4*, 177-183.

Garraway, L.A., Widlund, H.R., Rubin, M.A., Getz, G., Berger, A.J., Ramaswamy, S., Beroukhim, R., Milner, D.A., Granter, S.R., Du, J.*, et al.* (2005). Integrative genomic analyses identify MITF as a lineage survival oncogene amplified in malignant melanoma. Nature *436*, 117-122.

Giangreco, A., Reynolds, S.D., and Stripp, B.R. (2002). Terminal bronchioles harbor a unique airway stem cell population that localizes to the bronchoalveolar duct junction. Am J Pathol *161*, 173-182.

Gibbons, D.L., Lin, W., Creighton, C.J., Rizvi, Z.H., Gregory, P.A., Goodall, G.J., Thilaganathan, N., Du, L., Zhang, Y., Pertsemlidis, A.*, et al.* (2009). Contextual extracellular cues promote tumor cell EMT and metastasis by regulating miR-200 family expression. Genes Dev *23*, 2140-2151.

Goodall, J., Wellbrock, C., Dexter, T.J., Roberts, K., Marais, R., and Goding, C.R. (2004). The Brn-2 transcription factor links activated BRAF to melanoma proliferation. Mol Cell Biol *24*, 2923-2931.

Goodliffe, J.M., Wieschaus, E., and Cole, M.D. (2005). Polycomb mediates Myc autorepression and its transcriptional control of many loci in Drosophila. Genes Dev *19*, 2941-2946.

Gossen, M., and Bujard, H. (1992). Tight control of gene expression in mammalian cells by tetracycline-responsive promoters. Proc Natl Acad Sci U S A *89*, 5547-5551.

Gossen, M., Freundlieb, S., Bender, G., Muller, G., Hillen, W., and Bujard, H. (1995). Transcriptional activation by tetracyclines in mammalian cells. Science *268*, 1766-1769.

Gray-Schopfer, V., Wellbrock, C., and Marais, R. (2007). Melanoma biology and new targeted therapy. Nature *445*, 851-857.

Gschwind, A., Fischer, O.M., and Ullrich, A. (2004). The discovery of receptor tyrosine kinases: targets for cancer therapy. Nat Rev Cancer *4*, 361-370.

Guo, L.M., Pu, Y., Han, Z., Liu, T., Li, Y.X., Liu, M., Li, X., and Tang, H. (2009). MicroRNA-9 inhibits ovarian cancer cell growth through regulation of NF-kappaB1. FEBS J *276*, 5537-5546.

Guo, M., Akiyama, Y., House, M.G., Hooker, C.M., Heath, E., Gabrielson, E., Yang, S.C., Han, Y., Baylin, S.B., Herman, J.G.*, et al.* (2004). Hypermethylation of the GATA genes in lung cancer. Clin Cancer Res *10*, 7917-7924.

Guo, M., House, M.G., Akiyama, Y., Qi, Y., Capagna, D., Harmon, J., Baylin, S.B., Brock, M.V., and Herman, J.G. (2006). Hypermethylation of the GATA gene family in esophageal cancer. Int J Cancer *119*, 2078-2083.

Guyonneau, L., Murisier, F., Rossier, A., Moulin, A., and Beermann, F. (2004). Melanocytes and pigmentation are affected in dopachrome tautomerase knockout mice. Mol Cell Biol *24*, 3396-3403.

Haass, N.K., Smalley, K.S., Li, L., and Herlyn, M. (2005). Adhesion, migration and communication in melanocytes and melanoma. Pigment Cell Res *18*, 150-159.

Haenlin, M., Cubadda, Y., Blondeau, F., Heitzler, P., Lutz, Y., Simpson, P., and Ramain, P. (1997). Transcriptional activity of pannier is regulated negatively by heterodimerization of the GATA DNA-binding domain with a cofactor encoded by the u-shaped gene of Drosophila. Genes Dev *11*, 3096-3108.

Hagemann, C., and Rapp, U.R. (1999). Isotype-specific functions of Raf kinases. Exp Cell Res *253*, 34-46.

Hanahan, D., and Weinberg, R.A. (2000). The hallmarks of cancer. Cell *100*, 57-70.

Harris, M.L., and Erickson, C.A. (2007). Lineage specification in neural crest cell pathfinding. Dev Dyn *236*, 1-19.

Henion, P.D., and Weston, J.A. (1997). Timing and pattern of cell fate restrictions in the neural crest lineage. Development *124*, 4351-4359.

Herbst, A., Hemann, M.T., Tworkowski, K.A., Salghetti, S.E., Lowe, S.W., and Tansey, W.P. (2005). A conserved element in Myc that negatively regulates its proapoptotic activity. EMBO Rep *6*, 177-183.

Hodgkinson, C.A., Moore, K.J., Nakayama, A., Steingrimsson, E., Copeland, N.G., Jenkins, N.A., and Arnheiter, H. (1993). Mutations at the mouse microphthalmia locus are associated with defects in a gene encoding a novel basic-helix-loop-helix-zipper protein. Cell *74*, 395-404.

Hoek, K., Rimm, D.L., Williams, K.R., Zhao, H., Ariyan, S., Lin, A., Kluger, H.M., Berger, A.J., Cheng, E., Trombetta, E.S.*, et al.* (2004). Expression profiling reveals novel pathways in the transformation of melanocytes to melanomas. Cancer Res *64*, 5270-5282.

Hong, J.S., Kim, S.W., and Koo, J.S. (2008). Sp1 up-regulates cAMP-response-element-binding protein expression during retinoic acid-induced mucous differentiation of normal human bronchial epithelial cells. Biochem J *410*, 49-61.

Horn, L., and Sandler, A.B. (2009). Angiogenesis in the treatment of non-small cell lung cancer. Proc Am Thorac Soc *6*, 206-217.

Ito, T., Udaka, N., Yazawa, T., Okudela, K., Hayashi, H., Sudo, T., Guillemot, F., Kageyama, R., and Kitamura, H. (2000). Basic helix-loop-helix transcription factors regulate the neuroendocrine differentiation of fetal mouse pulmonary epithelium. Development *127*, 3913-3921.

Ji, J., Yamashita, T., Budhu, A., Forgues, M., Jia, H.L., Li, C., Deng, C., Wauthier, E., Reid, L.M., Ye, Q.H.*, et al.* (2009). Identification of microRNA-181 by genome-wide screening as a critical player in EpCAM-positive hepatic cancer stem cells. Hepatology *50*, 472-480.

Johnston, L.A., Prober, D.A., Edgar, B.A., Eisenman, R.N., and Gallant, P. (1999). Drosophila myc regulates cellular growth during development. Cell *98*, 779-790.

Jontes, J.D., Emond, M.R., and Smith, S.J. (2004). In vivo trafficking and targeting of N-cadherin to nascent presynaptic terminals. J Neurosci *24*, 9027-9034.

Karreman, C. (2002). AiO, combining DNA/protein programs and oligo-management. Bioinformatics *18*, 884-885.

Karreth, F.A., and Tuveson, D.A. (2009). Modelling oncogenic Ras/Raf signalling in the mouse. Current Opinion in Genetics & Development *19*, 4-11.

Kerkhoff, E., Fedorov, L.M., Siefken, R., Walter, A.O., Papadopoulos, T., and Rapp, U.R. (2000). Lung-targeted expression of the c-Raf-1 kinase in transgenic mice exposes a novel oncogenic character of the wild-type protein. Cell Growth Differ *11*, 185-190.

Kim, C.F., Jackson, E.L., Woolfenden, A.E., Lawrence, S., Babar, I., Vogel, S., Crowley, D., Bronson, R.T., and Jacks, T. (2005). Identification of bronchioalveolar stem cells in normal lung and lung cancer. Cell *121*, 823-835.

Kim, N.W., Piatyszek, M.A., Prowse, K.R., Harley, C.B., West, M.D., Ho, P.L., Coviello, G.M., Wright, W.E., Weinrich, S.L., and Shay, J.W. (1994). Specific association of human telomerase activity with immortal cells and cancer. Science *266*, 2011-2015.

King, K.A., Torday, J.S., and Sunday, M.E. (1995). Bombesin and [Leu8]phyllolitorin promote fetal mouse lung branching morphogenesis via a receptor-mediated mechanism. Proc Natl Acad Sci U S A *92*, 4357-4361.

Kleber, M., Lee, H.Y., Wurdak, H., Buchstaller, J., Riccomagno, M.M., Ittner, L.M., Suter, U., Epstein, D.J., and Sommer, L. (2005). Neural crest stem cell maintenance by combinatorial Wnt and BMP signaling. J Cell Biol *169*, 309-320.

Knies-Bamforth, U.E., Fox, S.B., Poulsom, R., Evan, G.I., and Harris, A.L. (2004). c-Myc interacts with hypoxia to induce angiogenesis in vivo by a vascular endothelial growth factor-dependent mechanism. Cancer Res *64*, 6563-6570.

Kobayashi, Y., Furukawa-Hibi, Y., Chen, C., Horio, Y., Isobe, K., Ikeda, K., and Motoyama, N. (2005). SIRT1 is critical regulator of FOXO-mediated transcription in response to oxidative stress. Int J Mol Med *16*, 237-243.

Kolch, W., Kotwaliwale, A., Vass, K., and Janosch, P. (2002). The role of Raf kinases in malignant transformation. Expert Rev Mol Med *4*, 1-18.

Kulesa, P.M., Kasemeier-Kulesa, J.C., Teddy, J.M., Margaryan, N.V., Seftor, E.A., Seftor, R.E., and Hendrix, M.J. (2006). Reprogramming metastatic melanoma cells to assume a neural crest cell-like phenotype in an embryonic microenvironment. Proc Natl Acad Sci U S A *103*, 3752-3757.

Kulkarni, R.M., Greenberg, J.M., and Akeson, A.L. (2009). NFATc1 regulates lymphatic endothelial development. Mech Dev *126*, 350-365.

Kurie, J.M., Morse, H.C., 3rd, Principato, M.A., Wax, J.S., Troppmair, J., Rapp, U.R., Potter, M., and Mushinski, J.F. (1990). v-myc and v-raf act synergistically to induce B-cell tumors in pristane-primed adult BALBC mice. Oncogene *5*, 577-582.

Kuwabara, T., Hsieh, J., Muotri, A., Yeo, G., Warashina, M., Lie, D.C., Moore, L., Nakashima, K., Asashima, M., and Gage, F.H. (2009). Wnt-mediated activation of NeuroD1 and retro-elements during adult neurogenesis. Nat Neurosci *12*, 1097-1105.

Lai, J.F., Cheng, H.Y., Cheng, T.L., Lin, Y.Y., Chen, L.C., Lin, M.T., and Jou, T.S. (2004). Doxycycline- and tetracycline-regulated transcriptional silencer enhance the expression level and transactivating performance of rtTA. J Gene Med *6*, 1403-1413.

Lal, A., Navarro, F., Maher, C.A., Maliszewski, L.E., Yan, N., O'Day, E., Chowdhury, D., Dykxhoorn, D.M., Tsai, P., Hofmann, O.*, et al.* (2009). miR-24 Inhibits cell proliferation by targeting E2F2, MYC, and other cell-cycle genes via binding to "seedless" 3'UTR microRNA recognition elements. Mol Cell *35*, 610-625.

Lauweryns, J.M., and Peuskens, J.C. (1972). Neuro-epithelial bodies (neuroreceptor or secretory organs?) in human infant bronchial and bronchiolar epithelium. Anat Rec *172*, 471-481.

Le Cam, L., Linares, L.K., Paul, C., Julien, E., Lacroix, M., Hatchi, E., Triboulet, R., Bossis, G., Shmueli, A., Rodriguez, M.S.*, et al.* (2006). E4F1 is an atypical ubiquitin ligase that modulates p53 effector functions independently of degradation. Cell *127*, 775-788.

Le Douarin, N.M., Dupin, E. (2003). Multipotentiality of the neural crest. Curr Opin Genet Dev *13*, 529-536.

Levy, C., Khaled, M., and Fisher, D.E. (2006). MITF: master regulator of melanocyte development and melanoma oncogene. Trends Mol Med *12*, 406-414.

Linnoila, R.I. (2006). Functional facets of the pulmonary neuroendocrine system. Lab Invest *86*, 425-444.

Linnoila, R.I., Mulshine, J.L., Steinberg, S.M., Funa, K., Matthews, M.J., Cotelingam, J.D., and Gazdar, A.F. (1988). Neuroendocrine differentiation in endocrine and nonendocrine lung carcinomas. Am J Clin Pathol *90*, 641-652.

Liu, C., Glasser, S.W., Wan, H., and Whitsett, J.A. (2002). GATA-6 and thyroid transcription factor-1 directly interact and regulate surfactant protein-C gene expression. J Biol Chem *277*, 4519-4525.

Liu, Z., Li, T., Liu, Y., Jia, Z., Li, Y., Zhang, C., Chen, P., Ma, K., Affara, N., and Zhou, C. (2009). WNT signaling promotes Nkx2.5 expression and early cardiomyogenesis via downregulation of Hdac1. Biochim Biophys Acta *1793*, 300-311.

Loercher, A.E., Tank, E.M., Delston, R.B., and Harbour, J.W. (2005). MITF links differentiation with cell cycle arrest in melanocytes by transcriptional activation of INK4A. J Cell Biol *168*, 35-40.

Luckett, J.C., Huser, M.B., Giagtzoglou, N., Brown, J.E., and Pritchard, C.A. (2000). Expression of the A-raf proto-oncogene in the normal adult and embryonic mouse. Cell Growth Differ *11*, 163-171.

Manni, I., Artuso, S., Careccia, S., Rizzo, M.G., Baserga, R., Piaggio, G., and Sacchi, A. (2009). The microRNA miR-92 increases proliferation of myeloid cells and by targeting p63 modulates the abundance of its isoforms. FASEB J.

Mao, D.Y., Watson, J.D., Yan, P.S., Barsyte-Lovejoy, D., Khosravi, F., Wong, W.W., Farnham, P.J., Huang, T.H., and Penn, L.Z. (2003). Analysis of Myc bound loci identified by CpG island arrays shows that Max is essential for Myc-dependent repression. Curr Biol *13*, 882-886.

Marshall, C.J. (1999). Small GTPases and cell cycle regulation. Biochem Soc Trans *27*, 363-370.

McCormick, F. (1993). Signal transduction. How receptors turn Ras on. Nature *363*, 15-16.

McGill, G.G., Horstmann, M., Widlund, H.R., Du, J., Motyckova, G., Nishimura, E.K., Lin, Y.L., Ramaswamy, S., Avery, W., Ding, H.F.*, et al.* (2002). Bcl2 regulation by the melanocyte master regulator Mitf modulates lineage survival and melanoma cell viability. Cell *109*, 707-718.

Mercer, K., Giblett, S., Green, S., Lloyd, D., DaRocha Dias, S., Plumb, M., Marais, R., and Pritchard, C. (2005). Expression of endogenous oncogenic V600EB-raf induces proliferation and developmental defects in mice and transformation of primary fibroblasts. Cancer Res *65*, 11493-11500.

Meuwissen, R., and Berns, A. (2005). Mouse models for human lung cancer. Genes Dev *19*, 643-664.

Miller, A.J., and Mihm, M.C., Jr. (2006). Melanoma. N Engl J Med *355*, 51-65.

Mountain, C.F. (1997). Revisions in the International System for Staging Lung Cancer. Chest *111*, 1710-1717.

Murphy, D.J., Junttila, M.R., Pouyet, L., Karnezis, A., Shchors, K., Bui, D.A., Brown-Swigart, L., Johnson, L., and Evan, G.I. (2008). Distinct thresholds govern Myc's biological output in vivo. Cancer Cell *14*, 447-457.

Nguyen, D.X., Chiang, A.C., Zhang, X.H., Kim, J.Y., Kris, M.G., Ladanyi, M., Gerald, W.L., and Massague, J. (2009). WNT/TCF signaling through LEF1 and HOXB9 mediates lung adenocarcinoma metastasis. Cell *138*, 51-62.

Nguyen, D.X., and Massague, J. (2007). Genetic determinants of cancer metastasis. Nat Rev Genet *8*, 341-352.

Patel, J.H., Loboda, A.P., Showe, M.K., Showe, L.C., and McMahon, S.B. (2004). Analysis of genomic targets reveals complex functions of MYC. Nat Rev Cancer *4*, 562-568.

Peake, J.L., Reynolds, S.D., Stripp, B.R., Stephens, K.E., and Pinkerton, K.E. (2000). Alteration of pulmonary neuroendocrine cells during epithelial repair of naphthalene-induced airway injury. Am J Pathol *156*, 279-286.

Perl, A.K., Kist, R., Shan, Z., Scherer, G., and Whitsett, J.A. (2005). Normal lung development and function after Sox9 inactivation in the respiratory epithelium. Genesis *41*, 23-32.

Perl, A.K., Tichelaar, J.W., and Whitsett, J.A. (2002a). Conditional gene expression in the respiratory epithelium of the mouse. Transgenic Res *11*, 21-29.

Perl, A.K., Wert, S.E., Nagy, A., Lobe, C.G., and Whitsett, J.A. (2002b). Early restriction of peripheral and proximal cell lineages during formation of the lung. Proc Natl Acad Sci U S A *99*, 10482-10487.

Peter, M.E. (2009). Let-7 and miR-200 microRNAs: guardians against pluripotency and cancer progression. Cell Cycle *8*, 843-852.

Pollock, P.M., Harper, U.L., Hansen, K.S., Yudt, L.M., Stark, M., Robbins, C.M., Moses, T.Y., Hostetter, G., Wagner, U., Kakareka, J*., et al.* (2003). High frequency of BRAF mutations in nevi. Nat Genet *33*, 19-20.

Pollock, P.M., and Meltzer, P.S. (2002). A genome-based strategy uncovers frequent BRAF mutations in melanoma. Cancer Cell *2*, 5-7.

Poulsen, T.T., Naizhen, X., Poulsen, H.S., and Linnoila, R.I. (2008). Acute damage by naphthalene triggers expression of the neuroendocrine marker PGP9.5 in airway epithelial cells. Toxicol Lett *181*, 67-74.

Principato, M., Klinken, S.P., Cleveland, J.L., Rapp, U.R., Holmes, K.L., Pierce, J.H., and Morse, H.C., 3rd (1988). In vitro transformation of murine bone marrow cells with a v-raf/v-myc retrovirus yields clonally related mature B cells and macrophages. Curr Top Microbiol Immunol *141*, 31-41.

Pritchard, C.A., Bolin, L., Slattery, R., Murray, R., and McMahon, M. (1996). Post-natal lethality and neurological and gastrointestinal defects in mice with targeted disruption of the A-Raf protein kinase gene. Curr Biol *6*, 614-617.

Prochownik, E.V., and Li, Y. (2007). The ever expanding role for c-Myc in promoting genomic instability. Cell Cycle *6*, 1024-1029.

Rapp, U.R. (2007). Metastasis as a faulty recapitulation of ontogeny. In natureprecedings.

Rapp, U.R., Cleveland, J.L., Brightman, K., Scott, A., and Ihle, J.N. (1985). Abrogation of IL-3 and IL-2 dependence by recombinant murine retroviruses expressing v-myc oncogenes. Nature *317*, 434-438.

Rapp, U.R., Fensterle, J., Albert, S., and Gotz, R. (2003). Raf kinases in lung tumor development. Adv Enzyme Regul *43*, 183-195.

Rapp, U.R., Korn, C., Ceteci, F., Karreman, C., Luetkenhaus, K., Serafin, V., Zanucco, E., Castro, I., and Potapenko, T. (2009). MYC is a metastasis gene for non-small-cell lung cancer. PLoS One *4*, e6029.

Rawlins, E.L., Okubo, T., Xue, Y., Brass, D.M., Auten, R.L., Hasegawa, H., Wang, F., and Hogan, B.L. (2009). The role of Scgb1a1+ Clara cells in the long-term maintenance and repair of lung airway, but not alveolar, epithelium. Cell Stem Cell *4*, 525-534.

Robbins, D.J., Zhen, E., Cheng, M., Xu, S., Ebert, D., and Cobb, M.H. (1994). MAP kinases ERK1 and ERK2: pleiotropic enzymes in a ubiquitous signaling network. Adv Cancer Res *63*, 93-116.

Sampson, V.B., Rong, N.H., Han, J., Yang, Q., Aris, V., Soteropoulos, P., Petrelli, N.J., Dunn, S.P., and Krueger, L.J. (2007). MicroRNA let-7a down-regulates MYC and reverts MYC-induced growth in Burkitt lymphoma cells. Cancer Res *67*, 9762-9770.

Schreck, R., and Rapp, U.R. (2006). Raf kinases: oncogenesis and drug discovery. Int J Cancer *119*, 2261-2271.

Sears, R., Nuckolls, F., Haura, E., Taya, Y., Tamai, K., and Nevins, J.R. (2000). Multiple Ras-dependent phosphorylation pathways regulate Myc protein stability. Genes Dev *14*, 2501-2514.

Seftor, E.A., Brown, K.M., Chin, L., Kirschmann, D.A., Wheaton, W.W., Protopopov, A., Feng, B., Balagurunathan, Y., Trent, J.M., Nickoloff, B.J.*, et al.* (2005). Epigenetic transdifferentiation of normal melanocytes by a metastatic melanoma microenvironment. Cancer Res *65*, 10164-10169.

Servitja, J.M., Pignatelli, M., Maestro, M.A., Cardalda, C., Boj, S.F., Lozano, J., Blanco, E., Lafuente, A., McCarthy, M.I., Sumoy, L.*, et al.* (2009). Hnf1alpha (MODY3) controls tissue-specific transcriptional programs and exerts opposed effects on cell growth in pancreatic islets and liver. Mol Cell Biol *29*, 2945-2959.

Shah, U., Sharpless, N.E., and Hayes, D.N. (2008). LKB1 and lung cancer: more than the usual suspects. Cancer Res *68*, 3562-3565.

Sharma, S.V., Bell, D.W., Settleman, J., and Haber, D.A. (2007). Epidermal growth factor receptor mutations in lung cancer. Nat Rev Cancer *7*, 169-181.

Sharpless, E., and Chin, L. (2003). The INK4a/ARF locus and melanoma. Oncogene *22*, 3092-3098.

Sholl, L.M., Long, K.B., and Hornick, J.L. (2009). Sox2 Expression in Pulmonary Non-small Cell and Neuroendocrine Carcinomas. Appl Immunohistochem Mol Morphol.

Slominski, A., Tobin, D.J., Shibahara, S., and Wortsman, J. (2004). Melanin pigmentation in mammalian skin and its hormonal regulation. Physiol Rev *84*, 1155-1228.

Smith, M.L., and Seo, Y.R. (2002). p53 regulation of DNA excision repair pathways. Mutagenesis *17*, 149-156.

Song, Y., Wu, J., Oyesanya, R.A., Lee, Z., Mukherjee, A., and Fang, X. (2009). Sp-1 and c-Myc mediate lysophosphatidic acid-induced expression of vascular endothelial growth factor in ovarian cancer cells via a hypoxia-inducible factor-1-independent mechanism. Clin Cancer Res *15*, 492-501.

Stone, J., de Lange, T., Ramsay, G., Jakobovits, E., Bishop, J.M., Varmus, H., and Lee, W. (1987). Definition of regions in human c-myc that are involved in transformation and nuclear localization. Mol Cell Biol *7*, 1697-1709.

Storm, S.M., Cleveland, J.L., and Rapp, U.R. (1990). Expression of raf family proto-oncogenes in normal mouse tissues. Oncogene *5*, 345-351.

Storm, S.M., and Rapp, U.R. (1993). Oncogene activation: c-raf-1 gene mutations in experimental and naturally occurring tumors. Toxicol Lett *67*, 201-210.

Subramanian, A., Tamayo, P., Mootha, V.K., Mukherjee, S., Ebert, B.L., Gillette, M.A., Paulovich, A., Pomeroy, S.L., Golub, T.R., Lander, E.S.*, et al.* (2005). Gene set enrichment analysis: a knowledge-based approach for interpreting genome-wide expression profiles. Proc Natl Acad Sci U S A *102*, 15545-15550.

Sweet-Cordero, A., Tseng, G.C., You, H., Douglass, M., Huey, B., Albertson, D., and Jacks, T. (2006). Comparison of gene expression and DNA copy number changes in a murine model of lung cancer. Genes Chromosomes Cancer *45*, 338-348.

Takahashi, K., and Yamanaka, S. (2006). Induction of pluripotent stem cells from mouse embryonic and adult fibroblast cultures by defined factors. Cell *126*, 663-676.

Tarasov, K.V., Testa, G., Tarasova, Y.S., Kania, G., Riordon, D.R., Volkova, M., Anisimov, S.V., Wobus, A.M., and Boheler, K.R. (2008). Linkage of pluripotent stem cell-associated transcripts to regulatory gene networks. Cells Tissues Organs *188*, 31-45.

Tebar, M., Destree, O., de Vree, W.J., and Ten Have-Opbroek, A.A. (2001). Expression of Tcf/Lef and sFrp and localization of beta-catenin in the developing mouse lung. Mech Dev *109*, 437-440.

Thomas, A.J., and Erickson, C.A. (2008). The making of a melanocyte: the specification of melanoblasts from the neural crest. Pigment Cell Melanoma Res *21*, 598-610.

Thompson, J.F., Scolyer, R.A., and Kefford, R.F. (2005). Cutaneous melanoma. Lancet *365*, 687-701.

Travis, W.D., Brambilla, E., Müller-Hermelink, H.K., and Harris, C.C. (2004). Pathology and Genetics of Tumours of the Lung, Pleura, Thymus and Heart (Lyon, IARC Press).

Troppmair, J., and Rapp, U.R. (2003). Raf and the road to cell survival: a tale of bad spells, ring bearers and detours. Biochem Pharmacol *66*, 1341-1345.

van der Sluis, M., Melis, M.H., Jonckheere, N., Ducourouble, M.P., Buller, H.A., Renes, I., Einerhand, A.W., and Van Seuningen, I. (2004). The murine Muc2 mucin gene is transcriptionally regulated by the zinc-finger GATA-4 transcription factor in intestinal cells. Biochem Biophys Res Commun *325*, 952-960.

Wakana, K., Akiyama, Y., Aso, T., and Yuasa, Y. (2006). Involvement of GATA-4/-5 transcription factors in ovarian carcinogenesis. Cancer Lett *241*, 281-288.

Wan, P.T., Garnett, M.J., Roe, S.M., Lee, S., Niculescu-Duvaz, D., Good, V.M., Jones, C.M., Marshall, C.J., Springer, C.J., Barford, D.*, et al.* (2004). Mechanism of activation of the RAF-ERK signaling pathway by oncogenic mutations of B-RAF. Cell *116*, 855-867.

Wang, J., Xie, L.Y., Allan, S., Beach, D., and Hannon, G.J. (1998). Myc activates telomerase. Genes Dev *12*, 1769-1774.

Weir, B.A., Woo, M.S., Getz, G., Perner, S., Ding, L., Beroukhim, R., Lin, W.M., Province, M.A., Kraja, A., Johnson, L.A., *et al.* (2007). Characterizing the cancer genome in lung adenocarcinoma. Nature *450*, 893-898.

Weiss, L. (2000). Metastasis of cancer: a conceptual history from antiquity to the 1990s. Cancer Metastasis Rev *19*, I-XI, 193-383.

Wellbrock, C., Karasarides, M., and Marais, R. (2004). The RAF proteins take centre stage. Nat Rev Mol Cell Biol *5*, 875-885.

Wellbrock, C., Rana, S., Paterson, H., Pickersgill, H., Brummelkamp, T., and Marais, R. (2008). Oncogenic BRAF regulates melanoma proliferation through the lineage specific factor MITF. PLoS One *3*, e2734.

Wojnowski, L., Stancato, L.F., Zimmer, A.M., Hahn, H., Beck, T.W., Larner, A.C., Rapp, U.R., and Zimmer, A. (1998). Craf-1 protein kinase is essential for mouse development. Mech Dev *76*, 141-149.

Wojnowski, L., Zimmer, A.M., Beck, T.W., Hahn, H., Bernal, R., Rapp, U.R., and Zimmer, A. (1997). Endothelial apoptosis in Braf-deficient mice. Nat Genet *16*, 293-297.

Wu, F., Zhu, S., Ding, Y., Beck, W.T., and Mo, Y.Y. (2009). MicroRNA-mediated regulation of Ubc9 expression in cancer cells. Clin Cancer Res *15*, 1550-1557.

Wu, H., Goel, V., and Haluska, F.G. (2003). PTEN signaling pathways in melanoma. Oncogene *22*, 3113-3122.

Xie, K., Zhang, J., Xiang, Y., Feng, Q., Han, B., Chu, Z., Wang, S., Zhang, Q., and Xiong, L. (2005). Isolation and annotation of 10828 putative full length cDNAs from indica rice. Sci China C Life Sci *48*, 445-451.

Xu, T., Zhu, Y., Xiong, Y., Ge, Y.Y., Yun, J.P., and Zhuang, S.M. (2009). MicroRNA-195 suppresses tumorigenicity and regulates G1/S transition of human hepatocellular carcinoma cells. Hepatology *50*, 113-121.

Yordy, J.S., and Muise-Helmericks, R.C. (2000). Signal transduction and the Ets family of transcription factors. Oncogene *19*, 6503-6513.

You, M.J., Castrillon, D.H., Bastian, B.C., O'Hagan, R.C., Bosenberg, M.W., Parsons, R., Chin, L., and DePinho, R.A. (2002). Genetic analysis of Pten and Ink4a/Arf interactions in the suppression of tumorigenesis in mice. Proc Natl Acad Sci U S A *99*, 1455-1460.

Zhang, Y., Goss, A.M., Cohen, E.D., Kadzik, R., Lepore, J.J., Muthukumaraswamy, K., Yang, J., DeMayo, F.J., Whitsett, J.A., Parmacek, M.S., *et al.* (2008). A Gata6-Wnt pathway required for epithelial stem cell development and airway regeneration. Nat Genet *40*, 862-870.

Zhong, D., Liu, X., Khuri, F.R., Sun, S.Y., Vertino, P.M., and Zhou, W. (2008). LKB1 is necessary for Akt-mediated phosphorylation of proapoptotic proteins. Cancer Res *68*, 7270-7277.

Zhu, Z., Zheng, T., Lee, C.G., Homer, R.J., and Elias, J.A. (2002). Tetracycline-controlled transcriptional regulation systems: advances and application in transgenic animal modeling. Semin Cell Dev Biol *13*, 121-128.

Zochbauer-Muller, S., Gazdar, A.F., and Minna, J.D. (2002). Molecular pathogenesis of lung cancer. Annu Rev Physiol *64*, 681-708.

Curriculum Vitae

Personal Information
Name: Katharina Elisabeth Lütkenhaus
Date and place of birth: 09th of June 1980 in Regensburg
Nationality: German
Marriage status: single

Professions/PhD-Thesis
since 04/2005   PhD-thesis at the Institut für Medizinische Strahlenkunde
                                und Zellforschung, University of Würzburg (Titel: "Tumor
                                development in Raf-driven cancer mouse models")
since 04/2009   Continuation of the PhD thesis at the Institute of
                                Microbiology, University of Würzburg

Education
10/1999 – 02/2005   Studies in Biology at the Bayerische-Julius-Maximilans
                                University, Würzburg
05/2004-02/2005   Diploma thesis at the Institut für Medizinische
                                Strahlenkunde und Zellforschung, Würzburg (Titel:
                                "Bacterial tumour therapy against melanoma"
                                (outstanding))
09/1990-06/1999   Katharinen-Gymnasium, Ingolstadt

Stay Abroad
08/2002-06/2003   Stay abroad at the State University of New York, Albany,
                                Department of Biology (Group of Prof. Dr. R.Zitomer)

Publications
Poster:
"Bacterial immunotherapy against melanoma." Katharina Luetkenhaus, Ulf R. Rapp and
Joachim Fensterle. Presentation at "Advances in Immunotherapy" Symposium in München,
2005.
Paper:
"Combinatorial Repression of the Hypoxic Genes of Saccharomyces Cerevisiae by DNA
binding proteins Rox1 and Mot3." Lee G. Klinkenberg, Thomas A. Manella, Katharina
Luetkenhaus and Richard S. Zitomer. Eukaryotic Cell, April 2005.
"Polycomb group protein Bmi1 is required for growth of RAF-driven non-small-cell lung
cancer." Matthias Becker, Christian Korn, Arnold R. Sienerth, R Voswinckel, Katharina
Luetkenhaus and Ulf R. Rapp. PLoS ONE, April 2009.
"Myc is a Metastasis Gene for Non-Small-Cell Lung Cancer." Ulf R. Rapp, Christian Korn,
Fatih Ceteci, Christiaan Karreman, Katharina Luetkenhaus, Valentina Serafin, Emanuele
Zanucco, Ines Castro and Tamara Potapenko. PLoS ONE,June 2009
"Epigenetic switch to intestinal fate by Myc in Non-Small-Cell Lung Cancer involves
demethylation and self-sustaining expression of GATA4." Katharina Luetkenhaus and Achim
Breiling (equally contributed) et al., in preparation.

Katharina Lütkenhaus